PhD PROCEEDINGS

ANNUAL ISSUES OF THE DOCTORAL SCHOOL

FACULTY OF INFORMATION TECHNOLOGY & BIONICS

2017

PhD PROCEEDINGS

ANNUAL ISSUES OF THE DOCTORAL SCHOOL

FACULTY OF INFORMATION TECHNOLOGY & BIONICS
PÁZMÁNY PÉTER CATHOLIC UNIVERSITY

PhD PROCEEDINGS

ANNUAL ISSUES OF THE DOCTORAL SCHOOL

FACULTY OF INFORMATION TECHNOLOGY & BIONICS

2017

PÁZMÁNY UNIVERSITY *e*PRESS
BUDAPEST, 2017

HU ISSN 2064-7271

Kiadja a Pázmány Egyetem eKiadó
Budapest, 2017

Felelős kiadó
Ft. Dr. Szuromi Szabolcs Anzelm O. Praem.
a Pázmány Péter Katolikus Egyetem rektora

Támogató: Emberi Erőforrások Minisztériuma
Támogatáskezelő: Emberi Erőforrás Támogatáskezelő
NTP-FKT-M-16-0004

Contents

Introduction

It is our pleasure to publish this Annual Proceedings again to demonstrate the genuine interdisciplinary research done at the Jedlik Laboratories by young talents working in the Roska Tamás Doctoral School of Sciences and Technology of the Faculty of Information Technology and Bionics at Pázmány Péter Catholic University. The scientific results of our PhD students show the main recent research directions in which our faculty is engaged. Thanks are also due to the supervisors and consultants, as well as to the five collaborating National Research Laboratories of the Hungarian Academy of Sciences, the Semmelweis Medical School and the University of Pannonia. The collaborative work with the partner universities, especially, Katolieke Universiteit Leuven, Politecnico di Torino, Technische Universität München, University of California at Berkeley, University of Notre Dame, Universidad de Sevilla, Universita di Catania, Université de Bordeaux, Universidad Autonoma de Madrid is gratefully acknowledged.

As an important development of this special collaboration, we were able to jointly accredit a new undergraduate curriculum on Molecular Bionics with the Semmelweis Medical School, the first of this kind in Europe.

We acknowledge the many sponsors of the research reported here. Namely,

- the Hungarian National Research Fund (OTKA),
- the Hungarian Academy of Sciences (MTA),
- the National Research, Development and Innovation Office (NKFIH),
- the Gedeon Richter Co.,
- the Office of Naval Research (ONR) of the US,
- NVIDIA Ltd.,
- Verizon Computer Vision Group (Eutecus), Berkeley, CA,
- MorphoLogic Ltd., Budapest,
- Analogic Computers Ltd., Budapest,
- AnaFocus Ltd., Seville,

and some other companies and individuals.

Needless to say, the resources and support of the Pázmány Péter Catholic University is gratefully acknowledged.

Budapest, June 2017.

GÁBOR PRÓSZÉKY

Chairman of the Board of the Doctoral School

PÉTER SZOLGAY

Head of the Doctoral School
Head of the Jedlik Laboratory

PROGRAM 1
BIONICS, BIO-INSPIRED WAVE COMPUTERS, NEUROMORPHIC MODELS

Heads: Tamás FREUND, György KARMOS, Zsolt LIPOSITS, Sándor PONGOR

Glucagon-like peptide-1 activates gonadotropin-releasing hormone neurons via endocannabinoid and nitric oxide pathways

Flóra Bálint
(Supervisor: Dr. Imre Farkas, Prof. Zsolt Liposits)
Pázmány Péter Catholic University, Faculty of Information Technology and Bionics
50/a Práter street, 1083 Budapest, Hungary
balint.flora@itk.ppke.hu

Glucagon-like peptide-1 (GLP-1) is one of the metabolic signal molecules which regulates reproduction. This gut hormone is secreted by the intestinal L-cells and it has multiple functions such as reduces food intake, inhibits gastric emptying and increases glucose-stimulated insulin secretion. GLP-1 and GLP-1 receptor (GLP-1R) agonists can cross the blood-brain barrier, suggesting an ability to reach various control centers of homeostasis.

GLP-1 is also produced in neurons of the lower brain stem, clustering in the nucleus of the solitary tract and the reticular nucleus of the medulla oblongata. GLP-1 immunoreactive (IR) fibers and terminals were observed in the hypothalamus, thalamus, septal regions, cortex and hindbrain. GLP-1R is widely expressed in the human and rodent brains: neurons of the circumventricular organs, amygdala, hypothalamic nuclei, NST, thalamic paraventricular nucleus, hippocampus and cortex, in various loci for hypothalamic regulation of glucose homeostasis and parabrachial nucleus, one of the regulatory centers of feeding behavior.
In addition to modulating energy homeostasis, GLP-1 is a potent regulator of reproduction. Since gonadotropin-releasing hormone (GnRH) neurons are the key regulators of the reproduction, any GLP-1-induced modulation of the GnRH neuronal system itself has a major impact on various events of reproductive physiology. Although some of the intracellular elements of the GLP-1 signaling has already been identified, the involved molecular mechanisms have not been elucidated, yet.
Therefore, the present study was aimed at revealing the putative direct effects of GLP-1 upon electric activity of GnRH neurons in male mice.
Loose patch-clamp recordings revealed that the GLP-1 analog Exendin-4 (100 *nM*-5 μM) dose-dependently elevated firing rate in GnRH neurons of male mice via activation of GLP-1R. Whole-cell patch-clamp measurements demonstrated increased excitatory GABAergic miniature postsynaptic currents (mPSCs) frequency after Exendin-4 administration, which was eliminated by the GLP-1R antagonist Exendin-3(9-39) (1 μM). Intracellular application of the G-protein inhibitor GDP-β-S (2 *mM*) blocked the action of Exendin-4 on

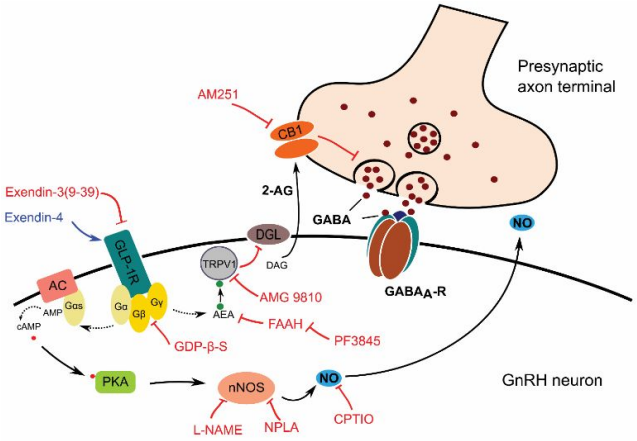

Fig. 1: Schematic illustration of GLP-1 receptor signaling on GnRH neurons.

mPSCs, suggesting direct excitatory action of GLP-1 on GnRH neurons. Blockade of nitric-oxide (NO) synthesis by L-NAME (100 μM) or NPLA (1 μM) or intracellular scavenging of NO by CPTIO (1 *mM*) partially attenuated the excitatory effect of Exendin-4. Similar partial inhibition was achieved by hindering endocannabinoid pathway using the CB1 inverse-agonist AM251 (1 μM).
Blockade of NO and endocannabinoid signaling mechanisms simultaneously eliminated action of Exendin-4 suggesting involvement of both retrograde machineries. Intracellular application of the TRPV1-antagonist AMG9810 (10 μM) or the FAAH-inhibitor PF3845 (5 μM) impeded the GLP-1-triggered endocannabinoid pathway indicating an anandamide-TRPV1-sensitive control of 2-AG production in GnRH neurons.

Our electrophysiological results indicate that GLP-1 exerts direct actions via GLP-1R on GnRH neurons and modulates NO and 2-AG retrograde signaling mechanisms to regulate the presynaptic excitatory GABAergic inputs to GnRH neurons.

F. BÁLINT, "Glucagon-like peptide-1 activates gonadotropin-releasing hormone neurons via endocannabinoid and nitric oxide pathways" in *PhD Proceedings Annual Issues of the Doctoral School, Faculty of Information Technology and Bionics, Pázmány Péter Catholic University 2017.* G. Prószéky, P. Szolgay Eds. Budapest: Pázmány University ePress, 2017, pp 10– 10.

Cross-frequency coupling in the human hippocampus

Virág BOKODI
(Supervisor: Dániel FABÓ, István ULBERT)
Pázmány Péter Catholic University, Faculty of Information Technology and Bionics
50/a Práter street, 1083 Budapest, Hungary
National Institute of Clinical Neurosciences
57 Amerikai street, 1145 Budapest, Hungary
bokodi.virag@itk.ppke.hu

I. Introduction

Neuronal oscillations of different frequencies can interact with one another, which in different bands is commonly called "cross-frequency coupling" (CFC). In one type of these interaction known as phase-amplitude coupling (PAC) or nesting, when the amplitude of high-frequency oscillations is modulated by the phase of low-frequency rhythms.[1][2] Phase – amplitude coupling between neuronal oscillations has been receiving interest. Perhaps the best-known example of this type of CFC occurs in the hippocampus, where the theta (5–10 Hz) phase modulates the gamma (30–100 Hz). This phenomenon has been well described in rat under REM sleep, awake state and different tasks [3][4][5], furthermore in human intracranial recording [6]. In spite of recent progress, little is known about the evaluation of CFC characteristics in human hippocampal sub-regions in vivo. So, our aims was to characterize the general patterns of PAC in sub-regions of the human hippocampus (Hc), in vivo, under general anaesthesia in 8 temporal lobe epilepsy patients during stimulus-evoked potentials.

II. Methods

We used laminar multi-electrodes [7] to record local field potential (LFP) by cortical electrical stimulation (0.2 ms; 5-15 mA; 0.5 Hz). Hippocampal regions were reconstructed based on histological assessment of the removed hippocampus, and sub-regions were determined: Cornu Ammonis 2-3 (CA2-3), Dentate Gyrus (DG), Subiculum (Sub) and HCDG, which is the area at the junction of the end of DG granule cell blades and CA3 apical dendrites. The severity of the hippocampal sclerosis (HS) was categorized into mild, and severe HS which may correspond to HS ILEA Type 2 and 1. [8] To assess phase-amplitude coupling, we used modulation index (MI) described in detail in Tort et al. [2] PAC values were calculated from the complex Morlet wavelet of the -1000 – 1000 ms data around every stimulation from one session. Due to the relatively short epochs statistical control analysis was performed for a single MI value to infer whether the observed value differs from what would be expected from chance. We worked with a distribution of 200 surrogate MI values achieved by applying the MI measure to trial shuffled composite time series. The resulting MI matrices are collected according to sub-regions of Hc and severity of hippocampal sclerosis.

III. Results

We analysed the interaction of frequencies between 10 to 1000 Hz grouped by CA2-3, DG, subiculum and HCDG. The five regions show similar coupling pattern during evoked events. The most significant modulating frequencies appear between 10-30 Hz in every case while the most modulated frequencies usually occur between 30-60 Hz and 60-120 Hz, except subiculum, where the modulated frequencies are shifted to higher range (120-240 Hz). Statistical analysis showed significant ($p<0.001$) increase in modulation differences between active and background activity in CA3 (between 70-90 Hz), DG (between 35-50 Hz and 60-120 Hz) and subiculum (60-85 Hz and 120-240 Hz).

IV. Discussion

Our results demonstrate that phase-amplitude coupling is a prominent feature of the oscillatory LFP in epileptic hippocampus. As a result, we found two gamma bands (slow gamma, 30-60 Hz and high gamma, 60-120 Hz) modulated by beta frequency (10-30 Hz) which is similar to recent findings from human hippocampus. The phase-amplitude coupling pattern between different frequency ranges may represent different activity. Therefore, these events were detectable only by means of CFC analyses.

Acknowledgements

This study was supported by the Hungarian Brain Research Program (KTIA_NAP_13-1-2013_0001). We are grateful to Lucia Wittner and Zsófia Maglóczky for providing help with histology and to Loránd Erőss and László Entz for surgery.

References

[1] Voytek et al, *A method for event-related phase-amplitude coupling*, NeuroImage, pp. 416-424, 2013.
[2] Tort et al, *Measuring Phase-Amplitude Coupling Between Neuronal Oscillations*, J Neurophysiol, vol.104, pp.1195-1210, 2010.
[3] Tort et al, *Dynamic cross-frequency couplings of local field potential oscillations in rat striatum and hippocampus during performance of a T-maze task*, PNAS, vol. 105, pp. 20517-20522, 2008.
[4] Schomburg et al, *Theta Phase Segregation of Input-Specific Gamma Patterns in Entorhinal-Hippocampal Networks*, Neuron, vol. 84, pp.470-485, 2014.
[5] Scheffer-Teixeira et al, *Theta Phase Modulates Multiple Layer-Specific Oscillations in the CA1 Region*, Cerebral Cortex, vol. 51, pp. 2289-2296, 2010.
[6] Zhang et al, *Traveling Theta Waves in the Human Hippocampus*, J. Neuroscience, vol 36, pp. 12477-12487, 2015.
[7] Ulbert et al, *Multiple microelectrode-recording system for human intracortical applications*, J Neurosci Methods, vol 106, pp. 69-79, 2001.
[8] Blumcke et al, *Molecular neuropathology of human mesial temporal lobe epilepsy*, Epilepsy Research, vol.36, pp. 205-223, 1999.

V. BOKODI, "Cross-frequency coupling in the human hippocampus" in *PhD Proceedings Annual Issues of the Doctoral School, Faculty of Information Technology and Bionics, Pázmány Péter Catholic University 2017.* G. Prószéky, P. Szolgay Eds. Budapest: Pázmány University ePress, 2017, pp 11– 11.

Investigation of age-related functional changes and membrane transporter interactions at the blood-brain barrier in rats

Luca Anna BORS
(Supervisor: Franciska ERDŐ)
Pázmány Péter Catholic University, Faculty of Information Technology and Bionics
50/a Práter street, 1083 Budapest, Hungary
bors.luca.anna@itk.ppke.hu

SUMMARY

The blood-brain barrier (BBB) has a very important role in the defensive system of the brain; without its function, the altered environment could inflict serious damage to the sensitive neurons. However, this barrier can decline with age and let through neurotoxic substances causing diseases like Alzheimer's disease and other types of dementia. [1]- [3]

Efflux transporters of the BBB, like Multi-drug Resistance (MDR) proteins, are working continuously to clear their substrates out of the brain. Studies have shown that if this function decreases in time and it can responsible for different types of neurodegeneration at old age. [1] - [9] However this theory has not been proved in vivo yet.

The efficiency of the P-glycoprotein (or MDR1); a transporter in the BBB, can be examined with the help of its substrate, quinidine (QND) by measuring the QND concentration in blood and brain after intravenous administration. Using dual- and triple

probe microdialysis experiments in rats can be a possible way to prove in vivo, that the aging can cause impairment of the protective barrier of the brain.

Microdialysis (MD) is a minimally invasive technique. Sampling can be done directly from the extracellular space of the striatum (in aging rats also from the lateral ventricles) and from the jugular vein lumen. [10] Sampling with MD for 5 hours can result one pharmacokinetic curve per rat. The animals were anesthetized and were treated according to the animal welfare laws.

It was observed how the advanced age and p-gp inhibition alter the function of the BBB. 4 groups of rats were studied: 1) aged treated with QND, 2) aged treated with QND and inhibitor PSC-833, 3) young adult treated with QND and 4) young adult treated with QND and PSC. The samples were collected with microdialysis method. The efficiency of the P-gp can be determined from AUCStriatum/AUCBlood ratio.

REFERENCES

[1] R. J. Boado, Y. Zhang, C.F. Xia, W. M Pardridge, "Fusion antibody for Alzheimer's disease with bidirectional transport across the blood-brain barrier and abeta fibril disaggregation.", *Bioconjug Chem.*, vol. 18, no. 2, pp. 447-55, 2007.

[2] C. Chiu, M. C. Miller, R. Monahan, D. P. Osgood, E. G. Stopa and G. D. Silverberg, "P-glycoprotein expression and amyloid accumulation in human aging and Alzheimer's disease: preliminary observations.," Neurobiol Aging., vol. 36, no. 9, pp. 2475-82, 2015.

[3] R. Deane and B. V. Zlokovic. "Role of the blood-brain barrier in the pathogenesis of Alzheimer's disease.," *Curr Alzheimer Res.*, vol. 4, no. 2, pp. 191-7, 2007.

[4] E. Beéry, Z. Rajnai, T. Abonyi, I. Makai, S. Bánsághi, F. Erdő, I. Sziráki, K. Herédi-Szabó, E. Kis, M. Jani, J. Márki-Zay, G. K. Tóth and P. Krajcsi, "ABCG2 modulates chlorothiazide permeability–in vitro-characterization of its interactions.," *Drug Metab Pharmacokinet.*, vol. 27, no. 3, pp. 349-53, 2012.

[5] J. R. Cirrito, R. Deane, A. M. Fagan, M. L. Spinner, M. Parsadanian, M. B. Finn, H. Jiang, J. L. Prior, A. Sagare , K. R. Bales, S. M. Paul, B. V. Zlokovic, D. Piwnica-Worms and D. M. Holtzman, "P-glycoprotein deficiency at the blood-brain barrier increases amyloid-beta deposition in an Alzheimer disease mouse model.," *J Clin Invest.*, vol. 115, no. 11, pp. 3285-90, 2005.

[6] P. Ballabh, A. Braun and M. Nedergaard, "The blood-brain barrier: an overview: structure, regulation, and clinical implications.," *Neurobiol Dis.*, vol. 16, no. 1, pp. 1-13, 2004.

[7] G. D. Silverberg, M. C. Miller, A. A. Messier, S. Majmudar, J. T. Machan, J. E. Donahue, E. G. Stopa and C. E. Johanson, "Amyloid deposition and influx transporter expression at the blood-brain barrier increase in normal aging.," *J Neuropathol Exp Neurol.*, vol. 69, no. 1, pp. 98-108, 2010.

[8] S. Syvõnen and J. Eriksson, "Advances in PET imaging of P-glycoprotein function at the blood-brain barrier.," *ACS Chem Neurosci.*, vol. 4, no. 2, pp. 225-37, 2013.

[9] F. Erdő, L. Denes and E. de Lange, "Age-associated physiological and pathological changes at the blood-brain barrier: A review.," *J Cereb Blood Flow Metab.*, vol. 37, no. 1, pp. 4-24, 2016.

[10] T. S. Shippenberg and T. A. C, "Overview of microdialysis.," *Current protocols in neuroscience*, unit 7.1, 2001.

L. BORS, "Investigation of age-related functional changes and membrane transporter interactions at the blood-brain barrier in rodents" in *PhD Proceedings Annual Issues of the Doctoral School, Faculty of Information Technology and Bionics, Pázmány Péter Catholic University 2017.* G. Prószéky, P. Szolgay Eds. Budapest: Pázmány University ePress, 2017, pp 12– 12.

Perceived Quality of Interpolated Images on Light Field Displays

Aron CSERKASZKY
(Supervisor: Dr. Peter SZOLGAY)
Pázmány Péter Catholic University, Faculty of Information Technology and Bionics
50/a Práter street, 1083 Budapest, Hungary
cserkaszky.aron@itk.ppke.hu

I. Introduction

Interpolation is a technique where new data is constructed from the available data. This construction can be considered an estimation, as we do not possess the necessary information regarding the unavailable data, but we still would like to know about it – even if it is not as precise as possible. A very basic way to visualize this is to select data points on a plot, and then draw lines connecting these points. The chosen, consistent way we connect the points are different methods of interpolation (e.g., linear, polynomial etc.).

In multimedia, a common form of interpolation uses the existing video frames to create new ones. Lets say that we have a video clip with a duration t, consists of f frames and plays at a frame rate of r. If we created a total of f' frames based on the available f frames, we could i.e. keep the same duration t and play the video at a higher frame rate of r', or we could turn the clip into a so-called "slow-motion video", by keeping the original value of rate r and extend the duration to t'.

In the 3D object visualizations on light field displays, the source content can be imagined as a series of images which capture the object from different angles. For the sake of simplicity, let us restrict this concept to horizontal parallax. The number of existing images that are to be displayed in the given field of view determines the angular resolution of the visualization; the more images there are in the fixed field of view, the higher the angular resolution is. The reason why it's important to have a sufficiently high angular resolution is to enable a good 3D visual experience via a smooth horizontal motion parallax. Based on the previous examples, it is effortless to think of a benefit of interpolation for such visualization techniques: by interpolating the existing views of the object, the number of views and thus the angular resolution can be increased. However, as stated earlier, interpolation is an estimation, which may result in inaccuracies (e.g., reduced visual quality).

II. Observations Regarding Quality

We began testing the perceived quality of selected interpolation techniques on four rendered models in front of a plain background. Two of these models were complex mathematical bodies (a polyhedron with 972 faces and a structure of 120 regular dodecahedra) and the other two were laser-scanned statues. The models were rendered with different angular resolutions in a fixed spatial resolution.

The first major interpolation challenge we encountered was with the polyhedron. Due to the construction of the model, the back of the grid can only be observed through the frontal grid. As the back of the grid have occluded areas from the virtual cameras' point of view, it cannot be precisely interpolated. For a scene like this, a 3D reconstructing method is required, which takes into account all available camera views and with the help of continuity assumptions, reconstructs the 3D model of the scene. From this reconstructed scene, we then can render virtual views.

In case of the dodecahedra structure, we observed that even the sweeping planes based approach introduced artifacts. This degradation of quality is due to the complexity of the model, and in this investigated example, the cameras viewing the model were relatively far away from each other.

After interpolating the first statue, we encountered an issue with the disparity based interpolation. The source of the problem was that finding row-wise color correspondences is challenging in the parts of the scene that lay in extreme depths compared to the rest of the scene. This is due to the higher relative angle with respect to this part of the scene.

The second statue had suffered no noticeable visual degradation when it was interpolated with the simple disparity based interpolation, as the cameras were close enough (1.5 degrees difference). However, it became burdened with many row-wise blurring artifacts when the disparity was not defined properly between the far views of the two cameras.

In the investigated examples, the visual quality of the outputs of the interpolation techniques was degraded in several cases – at least to a noticeable extent – however, as the interpolation increased the number of views, the horizontal motion parallax became smoother and thus improved this aspect of the perceived quality. While testing specific parameter combinations, we came across interpolation results visualized on light field displays where the trade-off between the quality of the interpolated images and the smoothness of the parallax effect was not obvious at all. Note that below a degree of angular resolution – depending on the attributes of the model – visualization also suffered the crosstalk effect, during which neighboring views overlap each other in a semi-transparent manner. Discrete image borders also appeared, which also caused so-called "jumps" between views. One of the most potential topics of future studies on the perceived quality of interpolation for light field displays is the investigation of this trade-off, where test participants choose their preference in a subjective quality assessment experiment.

Acknowledgment

This research is done as a part of ETN-FPI training network (project number 676401), which is funded under the H2020-MSCA-ITN-2015 call and is part of the Marie Sklodowska-Curie Actions Innovative Training Networks (ITN) funding scheme.

Á. CSERKASZKY, "Subjective Assessment of Interpolation Performance on a Light Field Display" in *PhD Proceedings Annual Issues of the Doctoral School, Faculty of Information Technology and Bionics, Pázmány Péter Catholic University 2017.* G. Prószéky, P. Szolgay Eds. Budapest: Pázmány University ePress, 2017, pp 13– 13.

Towards defining functionally relevant motions in proteins by ensemble selection based on experimental parameters

Dániel DUDOLA
(Supervisor: Dr. Zoltán GÁSPÁRI)
dudola.daniel@itk.ppke.hu

***Abstract*—Internal dynamics of proteins plays an important role in governing their function like protein-protein and protein-ligand interactions. The most powerful tool to yield detailed information on internal dynamics, but even this method reveals only a fraction of details of the assumed internal motions. To obtain a more complete picture on these motions, experiments can be combined with computational calculations, in which the parameters from the experiments – if they have a satisfactory spatial resolution – can be used as restraints in molecular dynamics.**

Conventional models protein structures based on experimental data only yield structural information as they correspond to a single conformer or a limited number of similar conformers. In ensemble-based representations, the compliance to the experimental data is interpreted and expected on the whole ensemble, since a single structure can not hold dynamic information.

The results of these simulations provide the base data set for testing the new and the existing features of our CoNSEnsX [1] service under development, which can back-calculate the NMR parameters from simulation outputs specifically for ensemble-based models.

An important aspect of further development is the inclusion of a selection feature that can be used in further evaluation of the ensembles.

***Keywords*-protein dynamics; protein ensembles; ensemble selection**

Currently there are two main approaches for the generation of ensemble-based representations of protein internal dynamics: restrained molecular dynamics simulations and sub-ensemble selection from a conformer pool. Both of these approaches has its merit and its use, depending on the protein – globular or intrinsically disordered – and the extent of conformational diversity to be described [2].

CoNSEnsX was designed as a standardized evaluation tool for structural ensembles reflecting dynamics. The service can back-calculated various parameters from the input ensemble such as chemical shifts, order parameters as well as scalar and residual dipolar couplings. Because of the highly variable amount of experimental data available for different proteins, the server does not report a single measure of compliance but provides correlation, RMSD and – for RDCs – Q-value for each parameter set.

To improve our service, we are testing the incorporation of a selection feature capable of generating a sub-ensemble with correspondence to selected experimental parameters. Our working hypothesis is that a small ensemble close to the minimal set required for compliance with the measurements might reveal the most important aspects of structural diversity of the different states of the molecule provided [3].

Currently the CoNSEnsX software is available as a web service (http://consensx.itk.ppke.hu/), neither installation nor registration needed. Since the software is in use for more than a year, several suggestions arrived from users and reviewers of the service. Based on these suggestions, several other enhancements will be implemented, such as:

- tooltips on the client side of the web service, clarifying the meaning of each input field
- serving calculation result sheets from the database with a permanent link
- only enable q-value based selection on S^2 parameters
- bulk selection for parameter types on the selection form

REFERENCES

[1] A. F. Ángyán, B. Szappanos, A. Perczel, and Z. Gáspári, "Consensx: an ensemble view of protein structures and nmr-derived experimental data," *BMC Structural Biology*, vol. 10:39, 2010.

[2] A. F. Angyan and Z. Gaspari, "Ensemble-based interpretations of NMR structural data to describe protein internal dynamics," *Molecules*, vol. 18, pp. 10548–10567, Aug 2013.

[3] A. Fizil, Z. Gaspari, T. Barna, F. Marx, and G. Batta, ""Invisible" conformers of an antifungal disulfide protein revealed by constrained cold and heat unfolding, CEST-NMR experiments, and molecular dynamics calculations," *Chemistry*, vol. 21, pp. 5136–5144, Mar 2015.

D. DUDOLA, "Towards defining functionally relevant motions in proteins by ensemble selection based on experimental parameters" in *PhD Proceedings Annual Issues of the Doctoral School, Faculty of Information Technology and Bionics, Pázmány Péter Catholic University 2017.* G. Prószéky, P. Szolgay Eds. Budapest: Pázmány University ePress, 2017, pp 14– 14.

Age-related alterations in the resting state effective connectivity

Bálint FILE
(Supervisor: Dániel FABÓ, István ULBERT)
Pázmány Péter Catholic University, Faculty of Information Technology and Bionics
50/a Práter street, 1083 Budapest, Hungary
file.balint@itk.ppke.hu

I. Introduction

The recent challenge of the cognitive neuroscience models of aging is to understand the brain mechanism that may underlie the cognitive deficits in aging. Long range connections, especially between the posterior and anterior brain regions seems extremely vulnerable. These functional and structural connections were linked to many psychological deficit of aging such as working memory or autobiographical memory scores [1]. In this study, age-related changes of the EEG resting-state brain interactions investigated with a novel directed (effective) connectivity measure [2]. We applied Phase Transfer Entropy (PTE), which is based on Granger's definition on causality, in which the effect of X signal on Y signal is measured by the improvement of predictability of the future value of Y signal caused by including not only its own past values for the prediction, but the past values of X too. The effective connectivity analysis of the two age groups was performed between the reconstructed source signals of the eyes closed resting-state EEG. We were interested in the age-related changes of the anterior-posterior information flow.

II. Methods

Healthy, right-handed young (mean age= 22.4 $\pm$ 3.1; N = 22;) and elderly (mean age= 66.3 $\pm$ 3.9 ; N = 19; 12 women) took part in the study. The participants were seated in an acoustically attenuated and electrically shielded room. The EEG was recorded by 64 Ag/AgCl electrodes placed according to the international 10-20 system using Neuroscan software and amplifiers (Scan 4.3., Nuamps, 45 Hz low-pass filter with 24dB/octave roll off, sampling rate: 1000 Hz). The 4 min of spontaneous EEG data of subjects were recorded in eyes-closed resting state condition. The time series of the cortical surface were reconstructed using sLORETA. The time signal of the cortical surface points (with the orientation perpendicular to the cortical surface) were reconstructed, and then averaged to 62 cortical regions. Signal was filtered to 4 distinct frequency band: theta (4-8 Hz), low alpha (8-10 Hz), high alpha (10-13 Hz) and beta (13-30 Hz) bands. dPTE is a normalized measure of PTE, where each bidirectional pair of PTE was normalized between 0 and 1 [3].

III. Results

We have found altered anterior-posterior information flow between the two age group. In healthy young subjects, the frontal brain regions sending information towards posterior areas in lower frequency bands, while in higher frequency bands parieto-occipital regions become the senders to frontal regions. In elderly subject the dominant information flow showed a posterior to anterior direction in all frequency bands. In the elderly, the most prominent decrease in the posterior to anterior information flow were observed in high alpha band.

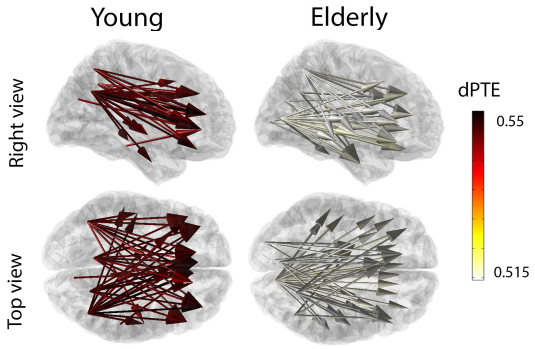

Fig. 1. Dominant information flow between the 62 cortical regions in the young and elderly group separately in high alpha band. For an overview the 50 highest PTE values were in a template brain viewed from the top and right direction. dPTE values indicating causal relations between brain regions in the direction of the arrow. Color of the edges indicate the dPTE values on the same scale for the young and elderly.

IV. Discussion

Presents results provide an evidence for the frequency dependent directional information flow in resting brain with advanced age. These finding are in line with previous results indicating the long-range structural and functional disconnection in the elderly [4]. From a network perspective the connections of hub regions decrease, while the importance of peripheral brain regions increase, which can be also interpret as the loss of posterior and increase of the frontal connectedness [5].

References

[1] R. Sala-Llonch, D. Bartrés-Faz, and C. Junqué, *Reorganization of brain networks in aging: a review of functional connectivity studies*, Front. Psychol., vol 6, pp. 663, 2015.

[2] Lobier, Muriel and Siebenhühner, Felix and Palva, Satu and Palva, J Matias, *Phase transfer entropy: a novel phase-based measure for directed connectivity in networks coupled by oscillatory interactions*, Neuroimage, vol 85, pp. 853-872, 2014.

[3] Hillebrand, Arjan and Tewarie, Prejaas and van Dellen, Edwin and Yu, Meichen and Carbo, Ellen WS and Douw, Linda and Gouw, Alida A and van Straaten, Elisabeth CW and Stam, Cornelis J, *Direction of information flow in large-scale resting-state networks is frequency-dependent*, Proceedings of the National Academy of Sciences, vol 113, pp. 3867-3872, 2016.

[4] Knyazev, Gennady G and Volf, Nina V and Belousova, Ludmila V, *Age-related differences in electroencephalogram connectivity and network topology*, Neurobiology of aging, vol 36, pp. 1849-1859, 2015.

[5] Andrews-Hanna, Jessica R and Snyder, Abraham Z and Vincent, Justin L and Lustig, Cindy and Head, Denise and Raichle, Marcus E and Buckner, Randy L, *Disruption of large-scale brain systems in advanced aging*, Neuron, vol 56, pp. 924-935, 2007.

B. FILE, "Age-related alterations in the resting state effective connectivity" in *PhD Proceedings Annual Issues of the Doctoral School, Faculty of Information Technology and Bionics, Pázmány Péter Catholic University 2017.* G. Prószéky, P. Szolgay Eds. Budapest: Pázmány University ePress, 2017, pp 15– 15.

Planning a safe and customizable measurement environment to the Neuro-Bit memristor chip

András GELENCSÉR
(Supervisor: Péter SZOLGAY)
Pázmány Péter Catholic University, Faculty of Information Technology and Bionics
50/a Práter street, 1083 Budapest, Hungary
gelencser.andras@itk.ppke.hu

***Abstract*—My research focuses on the bioinspired applicability of memristive devices, based on simulations. Using Neuro-Bit memristor chip and its breakout board, I can move forward to the real implementation of basic image processing tasks. In this article I make a brief summary of the available hardware elements and present the basic implementation of the planned measurement environment, preparing hardware and software components, which are essential to the behavior analysis of the memristor in a more complex circuit.**

***Keywords*-memristor; measurement**

I. Introduction

Over the past few years the memristive phenomenon was deeply discussed between the researchers working on the field of micro and nano electonics [1], [2], [3], [4]. This is a new emerging technology, which maybe able to improve or replace the existing electronic devices for digital and analog circuit applications including neuromorphic networks.

II. The hardware elements

A. The memristor chip

The Bio Inspired Technologies produced a memristor called Neuro-Bit. These memristors are available in multiple forms of packing. I use 44-Pin PLCC version, which is the biggest available including 20 memristor. This is a chalcogenide based ion-conducting memristor, which has biologically inspired synapse-like properties through the use of a metallic dendrite according to the product description [5].

B. The ESD protection board

The chance is high for accidentally overloading the Neuro-Bit chip, due to noise or mistakes. To ensure the protection of the chip, a protection board was designed and produced at the PPKE ITK Robotic's Lab, which can be connected to the manufacturers original breakout board.

III. The measurement environment

Due to the physical limitations of the memristor technology it is important to study the chip's behaviour to ensure the characteristics correspond with its data sheet. Measurement should validate the responds to write/read operations, noise of the output signal, etc.
If I want accurate picture of the memristors' state, I have to know their exact resistance. According to the device's user guide measurement of the memristor resistance with a multi-meter is prohibited, because it would damage the device due to high open-circuit voltage. Without multi-meter resistance can be determined indirectly with Ohm's law, given the current which flows through the memristor, and the applied voltage. With the ELVIS platform the measurement of voltage is straightforward, but measuring the current meets difficulties, which I solved with a built-in current-voltage converter. As the passive current-voltage converter has many limitations, I chose a Transresistance Amplifier Circuit (or Transimpedance Amplifier), which will also be more beneficial in case of small currents. Figure 5 shows the complete initial measurement environment.

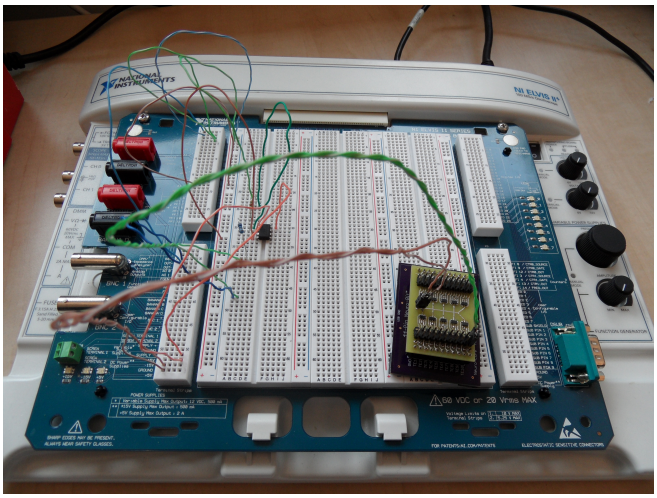

Fig. 1: The initial measurement set up

IV. Future plans

The measurement environment is ready, the Labview code to maintain a continuous data acquisition from the memristor and some supplementary MatLab code for input bias generation and output data analyzation are currently developed.
These will be connected to the boards to measure the memristor, and to design a memristive circuit with simple image processing functions.

References

[1] Chua LO, *Memristor - the missing circuit element*, IEEE Trans. Circuit Theory, 1971., vol. ct18, 507–591.
[2] Chua LO, Kang SM, *Memristive devices and systems*, Proc. IEEE, 1976., vol. 64, 209–223.
[3] Strukov DB, Snider GS, Stewart DR, Stanley Williams R, *The missing memristor found*, Nature, 2008, vol. 453, 80–83.
[4] Prodromakis T, Toumazou C, Chua LO, *Two centuries of memristors*, Nat. Mater., 2007, vol. 6, 824–832.
[5] Bio Inspired Technologies, *Neuro-Bit Memristo*, Rev. 2, Jun 2015.

A. GELENCSÉR, "Planning a safe and customizable measurement environment to the Neuro-Bit memristor chip" in *PhD Proceedings Annual Issues of the Doctoral School, Faculty of Information Technology and Bionics, Pázmány Péter Catholic University 2017.* G. Prószéky, P. Szolgay Eds. Budapest: Pázmány University ePress, 2017, pp 16– 16.

An Acoustic Approach to Study Fetal Biophysical Profile

Márton Áron GODA
(Supervisor: Ferenc KOVÁCS)
Pázmány Péter Catholic University, Faculty of Information Technology and Bionics
50/a Práter street, 1083 Budapest, Hungary
goda.marton.aron@itk.ppke.hu

***Abstract*—The principal objective of this study is to determine the fetal breathing movement by phonocardiography. Nowadays, the Doppler-based ultrasonic monitoring is a routine medical examination. While this technique is capable of determining several fetal degenerations, it can offer only a clinical investigation and requires special expertise.**

The assessment of fetal breathing movement can describe fetal well-being. From the third trimester, the fetal breathing movement is well detectable, and it is related to the functionality of autonomic nervous system of the fetus. Phonocardiogram is a commercially available, cheap device, It offers a harmless, easy-to-use, replicable method for 24 hour tele-monitoring fetal breathing. The assessment of breathing motion is based on time-frequency domain analysis. Our findings suggest, that it can offer a reliable real-time data processing, and easy assessment not only for doctors, but also pregnant mothers.

We have used phonocardiography based on Fetaphon2000™ with own method. The device looks like a cardiotocograph (CTG), but it is a totally passive measurement for fetal heart sound analysis. This device has been regularly used in some countries.

***Keywords*-keyword; fetal breathing movement, phonocardiography, time-frequency domain analysis**

Statement of originality: This report describes the work of the doctoral student during the academic year 2016/2017. Parts of this work might be under submission to scientific conferences and journals.

I. Introduction

Every fetus is different; therefore, their movement patterns are also different. The modulated acoustic signals of the FBM are hardly uniformisable. Disturbing factors could be the separation of specific fetal movements e.g. shoulder, chest, torso and limb movements, hiccups, but the gastroenteric sounds also pose a problem [3].

The FBM has a specific movement pattern, which is detectable from the 12th gestation week. However, the relevance of FBM is only after the third trimester. The BPP protocol [1] prescribes that there must be at least one FBM longer than 30 seconds within 30 minutes. The detection of these is not only difficult, it is also time-consuming with ultrasound monitoring. If BPP parameters are low, the test must be repeated within 24 hours, because the fetus's life might be in danger.

II. Methods and data processing

Although the fetus is not breathing, i.e. the oxygen uptake is done through the placenta, FBM is continuously developing during the gestation age. The activity depends largely on the fetal wellbeing. The average FBM is around 50 breaths per minute in active state, but it is not detectable all the time.

A database of more than 3,000 recordings with FBM helps us to develop our test method [4]. The dataset is large enough to use a machine learning algorithm [5]. The most important first step in this process is not only the removal of mother's breathing [2], heart and gastroenteric sounds, but also the additional analysis of the frequency components in order to separate fetal breathing movements from fetal hiccups, limb and torso movements.

The BPP test examines at least 20-30-second-long fetal breathing movements. Therefore, we identified and cut out such sequences from the measurement results, and grouped them for comparison. After the detection of some unique movement patterns, we developed a self-learning algorithm, based on the previously recorded records (more than 3,000). This algorithm will probably be more accurate if the number of analysed samples is increased. This higher specificity is a prerequisite for BPP assessment.

III. Results

Fetal breathing movement is one of the parameters required for the BPP. It has been determined by ultrasound devices. An easier way to detect fetal breathing movement was found with our previously developed phonocardiography based method.

Our future aim is to develop a more sophisticated selflearning algorithm, which is capable of detecting fetal breathing movements real time more accurately than earlier ultrasound-based methods.

Acknowledgements

I would like to offer my sincere thanks to my supervisors to Ferenc KOVÁCS - Lecturer of Pázmány Péter Catholic University Faculty of Information Technology and Bionics - for his valuable information and guidance.

I would like to express a deep sense of gratitude to Éva Tokics (sonographer), Nándor Tűzkő (obstetrician gynecologist) and Ferenc Katona (neonatologist) for the valuable information and guidance, which helped us in completing our current research.

References

[1] F. A. Manning, N. Bondaji, C. R. Harman, *Fetal assessment based on fetal biophysical profile scoring: VIII. The incidence of cerebral palsy in tested and untested perinates*, American Journal of Obstetrics and Gynecology 178, pp. 696–706., 1988

[2] F. Kovács, M. Torok, I. Habermajer, *A rule-based phonocardiographic method for longterm fetal heart rate monitoring*, IEEE Transactions on Biomedical Engineering, pp.124–130., 2000

[3] A. Jiménez-González, C. J. James, *Time-Structure Based Reconstruction of Physiological Independent Sources Extracted From Noisy Abdominal Phonograms*, IEEE Transactions on Biomedical Engineering 57, pp. 2322-2330, 2010

[4] F. Kovacs, H. Csaba, Á . T. Balogh, *Extended Noninvasive Fetal Monitoring by Detailed Analysis of Data Measured With Phonocardiography*, IEEE Transactions on Biomedical Engineering 58, pp.64-70., 2011

[5] M. Á. Goda, P. Hajas, *Morphological Determination of Pathological PCG Signals by Time and Frequency Domain Analysis*, Computing in Cardiology - Vancouver, pp. 1133-1136, 2016.

M. GODA, "An Acoustic Approach to Study Fetal Biophysical Profile" in *PhD Proceedings Annual Issues of the Doctoral School, Faculty of Information Technology and Bionics, Pázmány Péter Catholic University 2017.* G. Prószéky, P. Szolgay Eds. Budapest: Pázmány University ePress, 2017, pp 17– 17.

Ensemble-based assessment of the internal dynamics of small antifungal proteins

Máté HANDBAUER
(Supervisor: Zoltán GÁSPÁRI)
Pázmány Péter Catholic University, Faculty of Information Technology and Bionics
50/a Práter street, 1083 Budapest, Hungary
handbauer.mate@itk.ppke.hu

I. Introduction

The filamentous fungus Penicillium chrysogenum secretes PAF (Penicillium Antifungal Protein) which is small, basic cationic and cysteine rich molecule. The protein exhibits antimicrobial and antimycotic activity towards a variety of filamentous fungi, e.g. the often lethal Aspergillus infections that occur in humans (Aspergillus niger, A. fumigatus) and plant pathogenic molds (Botrytis cinerea) without toxic effects on mammalian cells. Therefore it may represent a considerable drug candidate against the aforementioned pathogens. The pathogenesis of PAF on sensitive fungi involves G-protein coupled signaling followed by apoptosis.[1] By creating a structural ensemble of PAF that represents the experimentally observed motions of the protein and using computational methods such as molecular dynamics (MD) may help to understand the mechanics behind these functions. I have applied MD simulations combined with experimental data derived from NMR measurements.

MD is a computer simulation method to study the behavior and interactions of atoms and molecules. In the case of proteins MD is able to sample the conformational space of a given molecule and provide information about the energy landscape. The dynamic behavior of a system is investigated for a given time frame usually at an order of a few to several hundred nanoseconds, depending on available computational resources. Interactions between atoms are calculated by taking into account the bonded (atomic bonds and angles) and non-bonded (electrostatic and Van der Waals) interactions that are described by an energy function known as a force field. [2] Solvent is also a crucial factor when dealing with biomolecules, most often water is used as a solvent either in an implicit (no actual atoms involved) or explicit (represented by H_2O molecules) form.

In order to accurately describe and understand key molecular mechanisms such as enzymatic catalysis or molecular recognition, conformational heterogeneity has to be taken into account. [3] This flexibility can be represented by using several structures in different conformations that show the -presumably- most important changes in the structure at a given timescale. The collection of these structures is the structural ensemble of a protein. During structure determination by NMR spectroscopy a penalty is applied to a molecular simulation if it does not adhere to experimental restraints. Most often these distance restraints derived form Nuclear Overhauser Effect (NOE). [4] Structures produced by this method fulfill all experimental restrains, however NMR measurements are derived as averages from an ensemble of molecules over time. [5] Thus it has to be stated that this average structure does not necessarily represent the conformational flexibility of a protein. This can be a problem if a protein adopts multiple conformers during structural fluctuations. MD simulations that integrate experimental data about the dynamics of proteins have been used in the past to produce conformational ensembles of proteins. Using MD simulations the NMR restraints can be applied as averages over several copies or replicas of the protein. [6] The generation of such ensembles can be achieved by ensemble-restrained molecular dynamics simulations, an example for which is the so-called MUMO protocol (minimal under-restraining minimal over-restraining) [6], or by selecting a sub-ensemble from a conformer library with structures representing extensive conformational sampling. Methods for the generation of such libraries for well-folded proteins include replica-exchange [7] and the AMD (accelerated molecular dynamics) scheme [8].

II. Results

I performed initial calculations to explore the structural diversity of the disulfide-rich antifungal protein called sf-PAFB, a homolog of PAF. I have used restrained molecular dynamics simulations and also started exploratory calculations with methods capable more efficient conformational sampling. Optimization of the parameters of the calculations based on the comparison of the obtained ensembles with available structures of related proteins and experimental data is currently in progress.

References

[1] G. Batta, T. Barna, Z. Gáspári, S. Sándor, K. E. Kövér, U. Binder, B. Sarg, L. Kaiserer, A. K. Chhillar, A. Eigentler, É. Leiter, N. Hegedüs, I. Pócsi, H. Lindner, and F. Marx, "Functional aspects of the solution structure and dynamics of PAF - A highly-stable antifungal protein from Penicillium chrysogenum," *FEBS Journal*, vol. 276, no. 10, pp. 2875–2890, 2009.

[2] P. J. M. D. van der Spoel, E. Lindahl, B. Hess, A. R. van Buuren, E. Apol, R. v. D. D. P. Tieleman, A. L. T. M. Sijbers, K. A. Feenstra, H. J. C., and Berendsen, *Gromacs User Manual version 4.5.6*. 2010.

[3] A. F. Ángyán and Z. Gáspári, "Ensemble-based interpretations of NMR structural data to describe protein internal dynamics," *Molecules*, vol. 18, no. 9, pp. 10548–10567, 2013.

[4] N. E. Jacobsen, *NMR Spectroscopy Explained: Simplified Theory, Applications and Examples for Organic Chemistry and Structural Biology*. Wiley-Interscience, 2007.

[5] I. Bertini, K. S. McGreevy, G. Parigi, and Wiley InterScience, *NMR of biomolecules : towards mechanistic systems biology*, vol. 38. 1989.

[6] B. Richter, J. Gsponer, P. Várnai, X. Salvatella, and M. Vendruscolo, "The MUMO (minimal under-restraining minimal over-restraining) method for the determination of native state ensembles of proteins," *Journal of Biomolecular NMR*, vol. 37, no. 2, pp. 117–135, 2007.

[7] Y. Sugita and Y. Okamoto, "Replica-exchange molecular dynamics method for protein folding," *Chemical Physics Letters*, vol. 314, no. 1-2, pp. 141–151, 1999.

[8] D. Hamelberg, J. Mongan, and J. A. McCammon, "Accelerated molecular dynamics: A promising and efficient simulation method for biomolecules," *Journal of Chemical Physics*, vol. 120, pp. 11919–11929, jun 2004.

M. HANDBAUER, "Ensemble-based assessment of the internal dynamics of small antifungal proteins" in *PhD Proceedings Annual Issues of the Doctoral School, Faculty of Information Technology and Bionics, Pázmány Péter Catholic University 2017.* G. Prószéky, P. Szolgay Eds. Budapest: Pázmány University ePress, 2017, pp 18– 18.

Generation and analysis of dynamic structural ensembles of human gastrotropin

Zita HARMAT
(Supervisor: Zoltán GÁSPÁRI)
Pázmány Péter Catholic University, Faculty of Information Technology and Bionics
50/a Práter street, 1083 Budapest, Hungary
harmat.zita@itk.ppke.hu

The protein named gastrotropin (FABP6) stems from the family of intracellular lipid binding proteins [1] and binds bile salts in the cytoplasm of the cells in the small intestine and hence taking part in the transportation of bile salts from the liver to the small intestine and from the small intestine back to the liver [2]. This is called the enterohepatic circulation of bile salts and the process is very important, because this ensures, that only a small fraction of bile salts has to be synthetised de novo [3].

Glycocholic acid, glycochenodeoxycholic acid [4], [5] and taurocholic acid (cholyltaurine) are bile salts bound by this protein [2]. The binding of glycocholic acid and glycochenodeoxycholic acid to gastrotropin has been shown take place in a site selective and cooperative manner mediated by allosteric communication [4], [6]. It is also capable of binding of fatty acids [1].

This protein has been extensively studied by solution NMR measurements, producing structures for the free form (PDB ID: 1O1U [2]), the single liganded form (PDB ID: 1O1V [2]) and a doubly ligated form (PDB ID: 2MM3 [7]). As for its structure, it forms a beta clam structure composed of two beta sheets having 5 beta strands termed with letters A-E and F-J respectively and two alpha helices termed with Roman numbers I-II capping the barrel-like structure [2]. It is also stated, that gastrotropin in the apo form is in a slow exchange with such a conformation, which is quite similar to the holo form [6], [7].

One approach to represent the dynamics of a protein is to generate ensembles and to handle the experimental parameters as ensemble-averaged values instead of forcing all of the structures to correspond to all the parameters [8]. According to our preliminary results, ensembles generated by restrained molecular dynamics simulatins reflect the dynamics of the protein in terms of experimental parametes slightly better than the conformers deposited in the PDB database [9].

S^2 order parameters describe the ps-ns timescale dynamics of the N-H bonds of the proteins. They are defined in the range of 0 and 1 with 1 meaning completely rigid, 0 meaning completely dynamic bonds [10], [11]. Nuclear Overhauser Effect (NOE) distances tell us about the relations of the H atoms in a protein and they can be converted into distance ranges between H atoms [10], [11].

Our objective is to understand the dynamics of ligand-binding and especially to know where the ligands enter the protein, all of this in an atomic level description. We investigate this question by generating an emsemble of protein structures to reflect the dynamics of the protein.

We performed molecular dynamics simulations with an in-house modified version of Gromacs 4.5.5 [12], [13] (available at users.itk.ppke.hu/ gaszo) with S^2 and NOE restraints based on the NMR experimantal data of Orsolya Tőke, Gergő Horváth et al. [6] to generate the ensembles using the MUMO (minimal under-restraining minimal over-restraining) method [10] for 8 replicas. The resulting structures were analysed by Principal Component Analysis and the correspondence to the experimental parameters were determined with the CoNSEnsX webserver [14].

References

[1] C. Lücke, F. Zhang, H. Rüterjans, J. A. Hamilton, and J. C. Sacchettini, "Flexibility is a likely determinant of binding specificity in the case of ileal lipid binding protein," *Structure (London, England: 1993)*, vol. 4, pp. 785–800, July 1996.

[2] M. Kurz, V. Brachvogel, H. Matter, S. Stengelin, H. Thüring, and W. Kramer, "Insights into the bile acid transportation system: the human ileal lipid-binding protein-cholyltaurine complex and its comparison with homologous structures," *Proteins*, vol. 50, pp. 312–328, Feb. 2003.

[3] S. M. Houten, M. Watanabe, and J. Auwerx, "Endocrine functions of bile acids," *The EMBO journal*, vol. 25, pp. 1419–1425, Apr. 2006.

[4] G. P. Tochtrop, G. T. DeKoster, D. F. Covey, and D. P. Cistola, "A single hydroxyl group governs ligand site selectivity in human ileal bile acid binding protein," *Journal of the American Chemical Society*, vol. 126, no. 35, pp. 11024–11029, 2004. PMID: 15339188.

[5] G. Horváth, P. Király, G. Tárkányi, and O. Toke, "Internal motions and exchange processes in human ileal bile acid binding protein as studied by backbone (15)N nuclear magnetic resonance spectroscopy," *Biochemistry*, vol. 51, pp. 1848–1861, Mar. 2012.

[6] G. Horváth, O. Egyed, and O. Toke, "Temperature dependence of backbone dynamics in human ileal bile acid-binding protein: implications for the mechanism of ligand binding," *Biochemistry*, vol. 53, pp. 5186–5198, Aug. 2014.

[7] G. Horváth, Bencsura, Simon, G. P. Tochtrop, G. T. DeKoster, D. F. Covey, D. P. Cistola, and O. Toke, "Structural determinants of ligand binding in the ternary complex of human ileal bile acid binding protein with glycocholate and glycochenodeoxycholate obtained from solution NMR," *The FEBS journal*, vol. 283, pp. 541–555, Feb. 2016.

[8] A. F. Ángyán and Z. Gáspári, "Ensemble-based interpretations of NMR structural data to describe protein internal dynamics," *Molecules (Basel, Switzerland)*, vol. 18, no. 9, pp. 10548–10567, 2013.

[9] H. M. Berman, J. Westbrook, Z. Feng, G. Gilliland, T. N. Bhat, H. Weissig, I. N. Shindyalov, and P. E. Bourne, "The Protein Data Bank," *Nucleic Acids Research*, vol. 28, pp. 235–242, Jan. 2000.

[10] B. Richter, J. Gsponer, P. Várnai, X. Salvatella, and M. Vendruscolo, "The MUMO (minimal under-restraining minimal over-restraining) method for the determination of native state ensembles of proteins," *Journal of biomolecular NMR*, vol. 37, pp. 117–135, Feb. 2007.

[11] I. R. Kleckner and M. P. Foster, "An introduction to NMR-based approaches for measuring protein dynamics," *Biochimica Et Biophysica Acta*, vol. 1814, pp. 942–968, Aug. 2011.

[12] D. Van Der Spoel, E. Lindahl, B. Hess, G. Groenhof, A. E. Mark, and H. J. C. Berendsen, "GROMACS: fast, flexible, and free," *Journal of Computational Chemistry*, vol. 26, pp. 1701–1718, Dec. 2005.

[13] S. Pronk, S. Páll, R. Schulz, P. Larsson, P. Bjelkmar, R. Apostolov, M. R. Shirts, J. C. Smith, P. M. Kasson, D. van der Spoel, B. Hess, and E. Lindahl, "GROMACS 4.5: a high-throughput and highly parallel open source molecular simulation toolkit," *Bioinformatics (Oxford, England)*, vol. 29, pp. 845–854, Apr. 2013.

[14] A. F. Angyán, B. Szappanos, A. Perczel, and Z. Gáspári, "CoNSEnsX: an ensemble view of protein structures and NMR-derived experimental data," *BMC structural biology*, vol. 10, p. 39, 2010.

Z. HARMAT, "Generation and analysis of dynamic structural ensembles of human gastrotropin" in *PhD Proceedings Annual Issues of the Doctoral School, Faculty of Information Technology and Bionics, Pázmány Péter Catholic University 2017.* G. Prószéky, P. Szolgay Eds. Budapest: Pázmány University ePress, 2017, pp 19– 19.

Optimization of isothermal DNA amplification methods in different microfluidic environments Summary

Márton HARTDÉGEN
(Supervisor: Kristóf IVÁN PhD)
Pázmány Péter Catholic University, Faculty of Information Technology and Bionics
50/a Práter street, 1083 Budapest, Hungary
hartdegen.marton@itk.ppke.hu

I. Review

Giardia duodenalis is a cosmopolitan enteric parasite with a very wide host range, including domestic and wild animals as well as human beings [1]. It causes *giardiasis*, what is one of the most common parasitic gastrointestinal diseases in humans worldwide, and it is considered a neglected tropical disease [2]. The parasite has at least seven morphologically identical genetic assemblages (named A to G), and the assemblages are currently distinguished by polymerase chain reaction (PCR) and different kind of DNA amplification methods [3].

In 2000 Notomi et al. [4] developed a novel, loop-mediated isothermal amplification method, which is an isotherm reaction with higher sensitivity and specificity compared with the standard PCR methods. This method relies on an auto-cycling strand displacement DNA synthesis that is performed by a DNA polymerase with high displacement activity and a set of two inner and two outer primers [5]. Another beneficial feature of the LAMP method that during the DNA amplification process a by-product, pyrophosphate ion is produced, yielding white precipitate of magnesium pyrophosphate in the reaction mixture [6]. This by-product eventuated to the possibility of real-time monitoring of the LAMP reaction, and Y. Mori et al. [7] published an apparatus capable of measuring the turbidity of multiple samples simultaneously while maintaining constant temperature to conduct real-time measurements of the changes in the turbidity of LAMP reactions. Following this different kind of LAMP methods and primer sets were employed to increase the sensitivity and specificity of the LAMP reactions (e.g.: Touchdown LAMP) [8].

In 2009 Plutzer et al. [9] developed a rapid identification method of two human-pathogenic *Giardia duodenalis* assemblages A and B in faecal and water samples by loop-mediated isothermal amplification. The presented method was reproducible, rapid, specific and has lower cost compared to the other molecular assays. In 2013 a new primer set for the DNA amplification of *Giardia lamblia* has been reported by Jie Li [10]. Their measurements showed that specific amplification products were obtained only with *Giardia lamblia*, while no amplification products were detected with DNA of other related protozoans. The new method was 10 times more sensitive than PCR. The genetic detection of parasites and pathogens at the point of care has become an increasingly important role in the world [11]. The combination of different kind of microfluidic systems with loop-mediated isothermal amplification opened a new opportunity in the clinical testing and evaluation. Microfluidic Electrochemical Quantitative LAMP system was designed for rapid, sensitive and quantitative detection of pathogenic DNA and automatic assays for targeted ribonucleic acid (RNA) extraction [12] and one-step reverse transcription LAMP process for rapid detection of viruses from tissue samples [13].

The aim of our work in the Pázmány Péter Catholic University Biomicrofluidics Laboratory is to optimize the standard LAMP protocol for reduced measurement time and reagents and to construct a microfluidic system for LAMP measurements.

References

[1] Appelbee AJ, Thompson RC, Olson ME., *Gardia and Cryptosporidium in mammalian wildlife-current status and future needs*, Trends Parasitol, 21:370-376, 2005.
[2] C. Minetti, K. Lamden, Jonathan M. Wastling, *Determination of Giardia duodenalis assemblages and multi-locus genotypes in patients with sporadic giardiasis from England*, Parasites and Vectors, 2015.
[3] Y. Feng, L. Xiao, et al., *Zoonotic potential and molecular epidemiology of Giardia species and giardiasis*, Clin. Microbiol Rev., 24(1):110-40, 2011.
[4] Notomi, Tsugunori, et al. *Loop-mediated isothermal amplification of DNA* Nucleic acids research 28.12 e63-e63 2000.
[5] Tang, Meng-Jun, et al., *Rapid and sensitive detection of Listeria monocytogenes by loop-mediated isothermal amplification*, Current microbiology, 63.6, 511-516, 2011.
[6] Y. Mori, K. Nagamine, N. Tomita and T. Notomi, *Detection of Loop-Mediated Isothermal Amplification Reaction by Turbidity Derived from Magnesium Pyrophosphate Formation*, Biochemical and Biophysical Research Communications, 150-154, 2001.
[7] Y. Mori, M. Kitao, N. Tomita and T. Notomi, *Real-time turbidimetry of LAMP reaction for quantifying template DNA*, Elsevier, 145-157, 2003.
[8] D. Wang, J. D. Brewster, P. M. Tomasula, *Two Methods for Increased Specificity and Sensitivity in Loop-Mediated Isothermal Amplification*, Molecules, 6048-6059, 2015.
[9] J. Plutzer, P. Karanis, *Rapid identification of Giardia duodenalis by loop-mediated- isothermal-amplification (LAMP) from faecal and environmental samples and comparative findings by PCR and real-time PCR methods*, Parasitology research, 104.6, 1527-1533, 2009.
[10] Jie Li, Peiyuan Wang, Aiguo Zhang, Guoqing Li, *Sensitive and Rapid Detection of Giardia lamblia Infection in Pet Dogs using Loop-Mediated Isothermal Amplification*, Korean J Parasitol, 2013.
[11] S. Derveaux, et al., *Analytical and bioanalytical chemistry*, Anal. Bioanal Chem, 2008.
[12] K. Hsieh, A. Patterson, B. Ferguson, K. W. Plaxco and H. T. Soh, *Rapid, Sensitive, and Quantitative Detection of Pathogenic DNA at the Point of Care via Microfluidics Electrochemical Quantitative Loop-Mediated Isothermal Amplification (MEQ-LAMP)*, National Institutes of Health, Angew Chem Int Ed, 2012.
[13] C. Wang, K. Lien, T. Wang and G. Lee, *An integrated microfluidic loop-mediated-isothermal-amplification system for rapid sample pre-treatment and detection of viruses*, Biosensors and Bioelectronics, 2010.
[14] Qiagen, *QIAamp DNA Mini and Blood Mini Handbook*, Fifth Edition, 2016.

M. HARTDÉGEN, "Optimization of isothermal DNA amplification methods in different microfluidic environments" in *PhD Proceedings Annual Issues of the Doctoral School, Faculty of Information Technology and Bionics, Pázmány Péter Catholic University 2017.* G. Prószéky, P. Szolgay Eds. Budapest: Pázmány University ePress, 2017, pp 20– 20.

Ligand-binding of the 3rd PDZ domain of PSD95 studied by ensemble-based structural models

Anett HINSENKAMP
(Supervisor: Zoltán GÁSPÁRI PhD)
Pázmány Péter Catholic University, Faculty of Information Technology and Bionics
50/a Práter street, 1083 Budapest, Hungary
anett.hinsenkamp@itk.ppke.hu

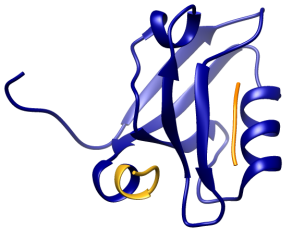

Fig. 1. The full form of the third PDZ domain of PSD-95 in complex with CRIPT peptide (partial).

I. Introduction

Synaptic signal transduction is an elaborate process that not only provides the means of transmitting the excited state of one neuron to another but also plays an important role in basic phenomena underlying neural development, learning and memory.[1] The postsynaptic density (PSD) is a characteristic part of excitatory chemical synapses. It is composed of a dense, dynamic network of proteins.[2] This highly organized molecular system of proteins provide a complex link between the intracellular part of membrane receptors, adhesion molecules and the cytoskeleton. PDZ domain containing scaffold proteins have key role in organizing the PSD network. PDZ domains (named for three proteins in which they were identified, PSD-95, Discs-large, ZO-1) are 80-100 residues long, adopt a globular structure of five to six beta sheets forming a half barrel and two alpha helices on each side. The secondary structure creates a protein binding groove typically for C-terminal tail of partner proteins, although alternative forms of interactions are known as well.[3], [4], [5], [6] One of the most abundant protein of the PSD network is PSD-95. It consists of three PDZ, one SH3 and one GK domain. The third PDZ domain (PDZ3) of PSD-95 contains an additional (third) alpha helix at its carboxy terminus besides the secondary structure elements characteristic of PDZ domains in general. Andrew Lee and his coworkers showed that removal of the extra helix leads to over twenty fold decrease in the binding affinity of the CRIPT peptide to PSD-95 even though the binding site is reasonably far from the helix. The changes in the binding affinity were attributed to the presence of entropic contributions resulting from an intramolecular allostery involving the additional helix and the ligand binding pocket.[7] The aim of this study was to generate detailed atomic-level structural models that reflect the experimentally determined mobility of the free and ligand bound states of PDZ3 variants. These models can help in establishing the mechanistic details behind the allosteric behaviour of the domain.

II. Methods

Multiple ensembles of the PDZ3 domain of PSD-95 were generated using ensemble restrained molecular dynamics simulations with a modified version of the open source GROMACS.4.5.5. package.[8] Calculations were performed in explicit water and the AMBER99SB-ILDN force field. Published backbone and side-chain S2 order parameters (obtained from NMR spin relaxation experiments)[7] were added as restraints in different combinations. The resulting ensembles were evaluated using the CoNSEnsX method [10] for correspondence with experimental parameters, both included and not included in the calculations as restraints. Free, complexed, full and truncated forms of PDZ3 were analyzed and compared to each other in terms of the conformational space covered by the different ensembles. Exploratory calculations of conformational entropy difference upon binding were carried out using multiple different methods available in the literature.[x,y,z] Ensembles obtained from longer production runs will be further analyzed in detail primarily focusing on the conformational entropy difference of PDZ3-CRIPT upon binding.

References

[1] Rudy JW., 'The neurobiology of learning and memory', Sinauer Associates, Sunderland, MA, USA, 2008
[2] Carlin RK, 'Isolation and characterization of postsynaptic densities from various brain regions:enrichment of different types of postsynaptic densities', J Cell Biol, 86, 831–845, 1980.
[3] Wei Feng and Mingjie Zhang, 'Organization and dynamics of PDZ domain related supramodules int he postsynaptic density', Nature Reviews Neuroscience, Volume 10, Pages 87-99, 2009.
[4] Eunjoon Kim and Morgan Sheng, 'PDZ domain proteins os synapses' Nature Reviews Neuroscience, Volume 5, Pages 771-781, 2004.
[5] Alan S. Fanning and James Melvin Anderson, 'Protein-protein interactions: PDZ domain networks', Current Biology, Volume 6, Number 11,Pages 1385-1388, 1996.
[6] Harold D. MacGillavry, Yu Song, Sridhar Raghavachari, Thomas A. Blanpied, 'Nanoscale scaffolding domains within the postsynaptic density concentrate synaptic AMPA receptors', Neuron, Volume 78, Pages 615-622, 2013.
[7] Chad M. Petit, Jun Zhang, Paul J. Sapienza, Ernesto J. Fuentes and Andrew L. Lee, 'Hidden dynamic allostery in a PDZ domain', PNAS, Valume 106, Number 43, Pages 18249-18254, 2009.
[8] B. Hess, C. Kutzner, D. van der Spoel, and E. Lindahl, 'Gromacs 4: algorithms for highly efficient, load-balanced, and scalable molecular simulation', Journal of Chemical Theory and Computation, Volume 4,Pages 435-447, 2008.
[9] A.F.Ángyán, B. Szappanos, A. Perczel and Z. Gáspári, 'Consensx: an ensemble view of protein structures and nmr-derived experimental data', BMC Structural Biology, Volume 10 2010.

A. HINSENKAMP, "Ligand-binding of the 3rd PDZ domain of PSD95 studied by ensemble-based structural models" in *PhD Proceedings Annual Issues of the Doctoral School, Faculty of Information Technology and Bionics, Pázmány Péter Catholic University 2017.* G. Prószéky, P. Szolgay Eds. Budapest: Pázmány University ePress, 2017, pp 21– 21.

Modeling moderate quorum sensing parasites in microbial communities

János JUHÁSZ
(Supervisor: Dr. Sándor PONGOR)
Pázmány Péter Catholic University, Faculty of Information Technology and Bionics
50/a Práter street, 1083 Budapest, Hungary
juhasz.janos@itk.ppke.hu

***Abstract*—The composition of multispecies microbial communities can be stable even though the members of these communities use the same environmental resources. Molecular signaling networks could have an important role in stabilizing complex bacterial communities. Bacteria can moderate themselves, i.e. they do not use all the resources they could. The aim of this study is to demonstrate with *in silico* simulations that moderation could have beneficial effects on the stability of microbial communities. The experiments were performed in a hybrid computational model which is able to simulate the *quorum sensing* mediated swarming behavior of bacteria. The bacterial cells are represented as discrete agents and the chemical signals, factors and nutrients are considered as diffusible gradients in the model. The results with partial wild type mutants showed that moderation via public good production threshold modification enables these cells to form stable communities with wild type cells. These results highlight that studying different methods of self-restraint could be important in understanding the dynamics of complex microbiomes.**

***Keywords*-microbiome stability; quorum sensing; multispecies communities; moderation; partial parasite; agent-based model**

I. Introduction

Bacteria are the most widespread life forms on Earth, although they are unicellular and of micrometer size. They populate every habitat, including the surfaces of the human body, which holds more prokaryotes than human cells. In most cases bacterial cells form communities that consist of many species. Members of complex microbial communities, for example human gut flora, interact with each other. One way of inter-cellular bacterial cooperation is quorum sensing, where cells start to produce chemical compounds (so-called factors) that act only in a concentration that can be achieved with the contribution of a given number of cells [1][2]. An important concept in studying interactions in diverse systems is moderation or self-restraint, when members do not use all available resources. Rather, they make trade-offs between individual benefits and sustainability [3]. It is not completely understood how this behavior evolved, which parameters of the cells are crucial to maintain it and how does the help formation of diverse microbial communities.

II. The model

For studying the effects of moderation, our research group used a previously developed model of quorum sensing (QS) mediated swarming [1][4][5]. The bacterial cells are represented as discrete agents and the chemical signals, factors and nutrients are considered as diffusible gradients in the model. Swarming cells can extend the colony boundaries and populate fields of a longitudinal 2D track with high nutrient concentration, while cells that move slower starve and become eliminated in the nutrient depleted environment. This modeling setup is a simplified representation of a dendrite growing from a bacterial colony (e.g. *Pseudomonas aeruginosa*) placed on an agar plate. My goal was to improve the modeling concept. I defined partial mutants or parasites, which produced less QS public goods and compensated their higher fitness with a higher signal threshold. Community stability and invasiveness were studied in the simulations. I measured the change in the ratio of different cell types during the simulations and recorded the speed of the communities derived from the location of the swarming zone.

III. Results

The achieved stable and diverse populations have characteristic parasite/WT ratio defined by the severity of mutation and the rate of moderation. The key of this coexistence is at least partial separation in the active zone between the different cell types. The swarming of parasites was less efficient than swarming of the WT cells. Parasites needed higher population number to achieve their QS signal threshold, and their active zone propagated slower in the track than the WT active zone. In mixed populations, the faster WT cell in the front of the swarming zone defined the speed of the entire community. This phenomenon can be interpreted as a division of tasks between population members. The WT cells maintain the swarming, and the parasites consume the leftover nutrients.

IV. Discussion

My research objective was defining partial wild type mutants, which produce public goods in a smaller amount than the WT cells. This indicates that they can swarm alone, allowing us to identify a range of signal threshold type self-restraint. These partial mutant cells can form a stable coexistence with the normal WT cells, and swarm using their speed. This new class of cells can live and swarm alone, but they are able to take benefits, faster swarming in our case, from others without eliminating them. The significance of these results is that the described scenario of partial mutants which are viable alone but can invade and populate WT colonies and can permanently gain an advantage from them is more similar to the dynamics of natural microbial communities than our previous model experiments. My results highlight that studying different methods of self-restraint could be important in understanding different aspects of interactions in complex microbiomes.

Acknowledgements

This project was developed in the Faculty of Information Technology and Bionics, Pázmány Péter Catholic University, Budapest. Thanks are due to my supervisor, Prof. Sándor

J. JUHÁSZ, "Modeling moderate quorum sensing parasites in microbial communities" in *PhD Proceedings Annual Issues of the Doctoral School, Faculty of Information Technology and Bionics, Pázmány Péter Catholic University 2017.* G. Prószéky, P. Szolgay Eds. Budapest: Pázmány University ePress, 2017, pp 22– 23.

Pongor as well as Dóra Bihary and Ádám Kerényi, who were the previous developers of the quorum sensing model. Furthermore, I would like to thank Dr. Nóra Wenszky and Ms. Hanni Thoma for their remarks about the language and style of this paper.

REFERENCES

[1] S. Netotea, I. Bertani, L. Steindler, V. Venturi, S. Pongor, and A. Kerenyi, "A simple model for the early events of quorum sensing in Pseudomonas aeruginosa: modeling bacterial swarming as the movement of an "activation zone"," *Biol Direct*, vol. 4, p. 6, 2008.

[2] L. Steindler, I. Bertani, L. De Sordi, S. Schwager, L. Eberl, and V. Venturi, "LasI/R and RhlI/R quorum sensing in an environmental strain of Pseudomonas aeruginosa," *submitted*, vol. 75, pp. 5131–5140, 2009.

[3] A. Ross-Gillespie, A. Gardner, A. Buckling, S. A. West, and A. S. Griffin, "Density Dependence and Cooperation: Theory and a Test With Bacteria," *Evolution*, vol. 63, no. 9, pp. 2315–2325, 2009.

[4] V. Venturi, I. Bertani, A. Kerenyi, S. Netotea, and S. Pongor, "Co-swarming and local collapse: quorum sensing conveys resilience to bacterial communities by localizing cheater mutants in Pseudomonas aeruginosa," *PLoS ONE*, vol. 5, p. e9998, 2010.

[5] Á. Kerényi, D. Bihary, V. Venturi, and S. Pongor, "Stability of Multi-species Bacterial Communities: Signaling Networks May Stabilize Microbiomes," *PLoS ONE*, vol. 8, p. e57947, mar 2013.

Electrophysiological analysis of synchronization applying bicuculline in human neocortex in vitro

Ágnes KANDRÁCS
(Supervisor: Lucia WITTNER)
Pázmány Péter Catholic University, Faculty of Information Technology and Bionics
50/a Práter street, 1083 Budapest, Hungary
kandracs.agnes@itk.ppke.hu

The generally accepted definition of epilepsy has been formed by the International League Against Epilepsy (ILAE) and the International Bureau for Epilepsy (IBE) in 2005. Most importantly, they have specified the chief differences between epileptic seizures and epilepsy, as a disease. The former is a transient sign or symptom. It is the result of excessive or synchronous, but definitely abnormal neuronal activity in the brain. However, epilepsy refers to disorders of the brain. It is characterized by a permanent tendency to produce epileptic seizures. Furthermore, it may have neurological, cognitive, psychological and social consequences [1], [2].

Neurons of the cortex have two major groups. The principal cells (pyramidal and spiny stellate cells) are responsible for excitation, while diverse groups of interneurons are responsible for inhibition. The complex and intricate network of these neurons makes possible the proper functioning of the brain. According to the most common hypothesis, if the proportion of these components shifts to the direction of excitation and reaches a certain level, a seizure will be generated. Distinct intrinsic (e.g. biochemical modification of receptors) and extrinsic (e. g. synaptic reorganisation) factors can be responsible for the abnormal behavior of neurons [1], [2], [3].

Postoperative neocortical tissue is able to generate spontaneous synchronous population activity (SPA) in vitro. These synchronous population bursts consist of rhythmically recurring extracellular local field potential (LFP) deflections associated with high frequency oscillations and an increased neuronal firing. This phenomenon is considered to be the result of excitatory and inhibitory network mechanisms. Our preliminary data shows that not only epileptic neocortical tissue is capable of generating SPAs, but non-epileptic tissue as well [4], [5].

The major inhibitory neurotransmitter is the gamma-aminobutyric acid (GABA). The postsynaptic $GABA_A$ receptor regulates the flow of chloride (Cl^-) ions across cell membranes. The inflow of negatively charged ions hyperpolarize the cell, thus inhibiting the generation of action potentials. $GABA_A$ receptor antagonist Bicuculline is widely used to induce epileptiform activity in animal cortical tissue. The presence of massive recurrent excitatory connections in the neocortex is thought to be a crucial factor in the generation of the large, synchronized bursts of activity underlying these seizures. By using this agent, we investigate the effect of the blockade of GABAergic inhibition in human neocortical tissue [2], [3], [5], [6], [7].

Postoperative neocortical tissue resected from epileptic and tumour patients have been investigated. Slices of 500 μm thickness were cut, and then LFPg recordings were obtained by 24 channel laminar multielectrode in oxygenated artificial cerebrospinal fluid (ACSF). On active slices 20 μM Bicuculline bath was applied. Population activity detection was performed, then LFPg, MUA and power-source density (CSD) were analysed. Single cells were detected by their action potentials and classified by their properties. As a control, we used neocortical tissue obtained from patients with tumor. The samples used in this experiment was not affected by the tumor. In case of tumour patients, the abscence of epilepsy has been tested by scalp EEG recordings. Tumour patients with epileptic seizure(s) were excluded from this study [2], [4], [5], [9].

The estimated number of patients suffering from epilepsy worldwide is about 65 million. 0.3-0.6% of the Hungarian population are affected. If the medical treatment fails, the removal of the epileptogenic zone can provide a solution. Epilepsy surgery is currently at the stage of development. An important element is to enhance the efficiency of the seizure onset zone's detection. Understanding the pathological neuronal properties and behavior can help in this intention. Our goal is to compare the electrophysiological characteristics of postoperative neocortical slices derived from patients with epilepsy and patients with tumour but without epilepsy in vitro [2], [10], [11], [8].

REFERENCES

[1] R. S. Fisher W. van Emde Boas, W. Blume, C. Elger, P. Genton, P. Lee and J. Engel., "Epileptic seizures and epilepsy: definitions proposed by the International League Against Epilepsy (ILAE) and the International Bureau for Epilepsy (IBE)," *Epilepsia*, vol. 46, pp. 470–472, 2005.

[2] Á. Kandrács, "The effect of $GABA_A$ receptor antagonist Bicuculline on human neocortex in vitro" in PhD Proceedings Annual Issues of the Doctoral School, Faculty of Information Technology and Bionics, Pázmány Péter Catholic University, 2016

[3] E. B. Bromfield, J. Cavazos, J. Sirven, (2006). *An Introduction to Epilepsy* [Online]. Available: http://www.ncbi.nlm.nih.gov/books/NBK2510/

[4] R. Köhling, A. Lücke, H. Straub, E. J. Speckmann, I. Tuxhorn, P. Wolf, H. Pannek, and F. Oppel, "Spontaneous sharp waves in human neocortical slices excised from epileptic patients," *Brain*, vol. 121, pp. 1073-1087, 1998.

[5] Á. Kandrács, "Investigation of the role of GABAergic inhibition in epileptic human neocortex" in PhD Proceedings Annual Issues of the Doctoral School, Faculty of Information Technology and Bionics, Pázmány Péter Catholic University, pp. 57–60, 2015

[6] A. Bragin, I. Mody, C. Wilson and J. Engel, "Local Generation of Fast Ripples in Epileptic Brain, " *The Journal of Neuroscience*, vol. 22, no. 5, pp. 2012-2021, March 2002

[7] D. McKormick and D. Contreras, "On the cellular and network bases of epileptic seizures., " Annu. Rev. Physiol, vol. 63, pp. 815–46, 2001.

[8] B. Mikudina et al., "Epilepszia betegségteher felmérés Magyarországon," *Gondolatok közös javainkról. Válság az oktatásban? Oktatás a válságban!*, Budapest, 2010, pp. 179–188.

[9] I. Ulbert, E. Halgren, G. Heit, and G. Karmos, "Multiple microelectrode-recording system for human intracortical applications.," J. Neurosci. Methods, vol. 106, pp. 69–79, 2001.

[10] J. Janszky and A. Szűcs, "Az epilepsziás rohamok diagnózisa és kezelése, " *Hippocrate: Neurológia*, pp. 104-109, March-April, 2002.

[11] D. Thurman et al., "Standards for epidemiologic studies and surveillance of epilepsy," *Epilepsia*, vol. 52, pp. 2–26, 2011

Á. KANDRÁCS, "Electrophysiological analysis of synchronization applying bicuculline in human neocortex in vitro" in *PhD Proceedings Annual Issues of the Doctoral School, Faculty of Information Technology and Bionics, Pázmány Péter Catholic University 2017.* G. Prószéky, P. Szolgay Eds. Budapest: Pázmány University ePress, 2017, pp 24– 24.

Features of intrinsic disorder in pre- and postsynaptic proteins

Annamária KISS-TÓTH
(Supervisor: Zoltán GÁSPÁRI)
Pázmány Péter Catholic University, Faculty of Information Technology and Bionics
50/a Práter street, 1083 Budapest, Hungary
kiss-toth.annamaria@itk.ppke.hu

Intrinsically disordered proteins have been shown to participate in a number of important biological processes where they make use of their unique partner binding properties. My work focused on a comprehensive analysis of structural disorder in pre- and postsynaptic proteins with emphasis on comparing the obtained features with reference protein sets representing multidomain proteins, signal transduction-associated proteins and the entire human proteome.

The human brain contains more than a 100 billion neurons which communicate with each other through chemical synapses. Most proteins in the central nervous system are located in the synapses. They are essential to proper brain function and may be a source of dysfunction underlying many neurological disorders such as Parkinson's disease and Alzheimer's disease [1]. This makes the synapse an excellent candidate for for large-scale proteomic study. SynaptomeDB contains a set of proteins located in synapses [2]. Immunome database contains proteins involved in the human immune system [3]. Signalink contains proteins participating in signaling networks [4]. Orthologs are created by speciation and possess the same function [5].

Synaptic proteins were selected from the Synaptome Database for computational analysis and a list of 1873 proteins was created. Multiple prediction methods were used for both intrinsic disorder tendency prediction and coiled-coil structure prediction. This yields more reliable results in both cases.

Intrinsic disorder prediction was performed with three different methods: IUPred, VSL2B and RONN [6-9]. Coiled-coil prediction was performed with two different methods: COILS and PairCoil [10, 11]. Consensus was also calculated. Genuine disorder was determined by eliminating the overlap of disordered regions and coiled-coil structures from the sequences predicted as disordered. The minimum length of disordered regions was initially set to 30 consecutive amino acids and the window size of the coiled-coil structures was set to 21. After some consideration, the minimum length of disordered regions was first lowered to 20 and then 10 amino acids in order to identify shorter disordered sequences.

Many of these synaptic proteins are not specific to synapses. Therefore GO term filtering was applied and the proteins participating in synaptic transmission were selected. This way a list of 161 proteins was created.

Orthologous proteins from three primates (Western lowland gorilla, Sumatran orangutan, common chimpanzee) were added. Two different ortholog databases were considered: OMA and EggNOG. They give slightly different results and a consensus of the two was used. An exhaustive computational analysis was performed.

The structural preferences of reference set proteins were also analyzed with the same methods. Reference sets include the entire human proteome, immunome proteins and Signalink proteins. The results were compared to the structural preferences of the synaptic proteins.

My preliminary results reveal that intrinsic disorder is not a general feature in synaptic proteins and in the specific reference sets used. Detailed analysis of the regions detected and the proteins with most disordered regions is under way. An important aspect is the role of the disordered regions, whether they form interaction sites or can be regarded as structural elements (linkers) between ordered domains. The data will be further dissected in terms of protein localization in the pre- and postsynaptic regions and whether this localization is exclusive or not. The orthologs investigated so far also do not reveal striking differences to their human counterparts. We believe that our approach focusing on 'genuine disorder' will be fruitful in obtaining a functionally relevant census of disordered regions in the synaptome.

References

[1] Van Spronsen M, Hoogenraad CC. Synapse pathology in psychiatric and neurologic disease. Current Neurology and Neuroscience Reports 10(3):207-214 (2010).
[2] Pirooznia M, Wang T, Avramopoulos D, Valle D, Thomas G, Huganir RL, Goes FS, Potash JB, Zandi PP. SynaptomeDB: an ontology-based knowledgebase for synaptic genes. Bioinformatics (2012).
[3] Ortutay C, Vihinen M. Immunome: a reference set of genes and proteins for systems biology of the human immune system. Cell Immunol. 244(2):87-9 (2006).
[4] Fazekas D, Koltai M, Türei D, Módos D, Pálfy M, Dúl Z, Zsákai L, Szalay-Bek M, Lenti K, Farkas IJ, Vellai T, Csermely P, Korcsmáros T. SignaLink 2 – a signaling pathway resource with multi-layered regulatory networks. BMC Systems Biology 7(1):7 (2013).
[5] Jensen, Roy A. "Orthologs and paralogs - We need to get it right." Genome Biology 2.8 (2001).
[6] Zsuzsanna Dosztányi, Veronika Csizmók, Péter Tompa and István Simon. IUPred: web server for the prediction of intrinsically unstructured regions of proteins based on estimated energy content. Bioinformatics 21, 3433-3434 (2005).
[7] Yang, ZR, Thomson, R, McNeil, P, and Esnouf. RONN: the bio-basis function neural network technique applied to the detection of natively disordered regions in proteins. RM (2005).
[8] Peng K., Radivojac P., Vucetic S., Dunker A.K., and Obradovic Z. Length-dependent prediction of protein intrinsic disorder. BMC Bioinformatics 7:208 (2006).
[9] Obradovic Z., Peng K., Vucetic S., Radivojac P., and Dunker A.K., Exploiting heterogeneous sequence properties improves prediction of protein disorder. Proteins 61(S7):176-182 (2005).
[10] Lupas, A., Van Dyke, M., and Stock, J. Predicting coiled-coils from protein sequences. Science 252:1162-1164 (1991).
[11] Bonnie Berger, David B. Wilson, Ethan Wolf, Theodore Tonchev, Mari Milla, and Peter S. Kim. Predicting coiled-coils by use of pairwise residue correlations. Proceedings of the National Academy of Science USA, vol 92, pp. 8259-8263 (1995).

A. KISS-TÓTH, "Features of intrinsic disorder in pre- and postsynaptic proteins" in *PhD Proceedings Annual Issues of the Doctoral School, Faculty of Information Technology and Bionics, Pázmány Péter Catholic University 2017.* G. Prószéky, P. Szolgay Eds. Budapest: Pázmány University ePress, 2017, pp 25– 25.

Towards a unified model of regulation in parvulin-type PPIases

Bertalan KOVÁCS
(Supervisor: Dr. Zoltán GÁSPÁRI)
Pázmány Péter Catholic University, Faculty of Information Technology and Bionics
50/a Práter street, 1083 Budapest, Hungary
kovacs.bertalan@itk.ppke.hu

I. Introduction

Rotamases or peptidyl-prolyl isomerases (PPIase) catalyze the cis-trans isomerization of a pre-proline peptide bond. They play key roles in a number of different biological processes such as cell-cycle regulation, apoptosis and chromatin remodeling [1].

Two main types of parvulins can be distinguished: Pin1-type and non-Pin1-type ones. For the first group the isomerization reaction is phosphorylation-dependent, therefore they contain a phosphate binding-loop in the catalytic domain as well as an N-terminal WW domain responsible for ligand recognition. On the other hand, the catalysis of non-Pin1-type parvulin enzymes do not depend on phosphorylation, therefore they also lack the phosphate-binding loop as well as the WW domain.

There has been no consensus achieved on the exact mechanism of parvulins so far, however it is generally accepted that there is no breaking and reforming of the peptide bond. The two highly conserved histidines as well as 5 residues composing a hydrogen-bonding network in the large lobe next to the ligand-binding cleft were speculated to be crucial for the catalysis in parvulins.

In order to get further insight into the dynamics and mechanism of parvulins, three distinct parvulin types have been investigated: SaParsA from *Staphylococcus aureus* (id: 2JZV) [2], TbPin1 from *Trypanosoma brucei* (id: 2LJ4) [3] and CsPinA from *Cenarchaeum symbiosum* (id: 2RQS) [4]. The structures were selected on the basis of available dynamic NMR experimental data, specifically backbone S^2 order parameters. They were submitted to externally restrained molecular dynamic simulations to later analyze their main motional modes as well as how their internal dynamics is influenced by the hydrogen-bonding network and the interaction with the WW domain.

Results of the described research have been presented and discussed in detail in our recent paper [5].

II. Results and discussion

In the generated dynamic structural ensembles good compliance with the experimental S^2 was achieved without compromising the correlation with the Cα and Hα chemical shifts. The resulting ensembles are more diverse than the original ones in the Protein Data Bank, as they cover a larger part of the conformational space.

PCA analysis of the restrained ensembles reveals that the main internal motion of the molecules corresponds to the opening and closing of the two lobes surrounding the ligand-binding cleft ('breathing motion'). The three different ensembles occupy different regions along this PCA coordinate, thus they represent different state of openness.

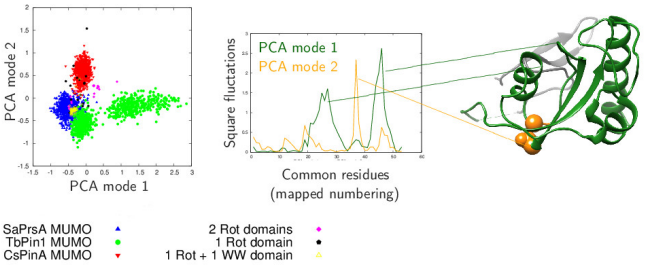

Fig. 1. PCA analysis of the consensus sequence of 100 rotamase domains. The first PCA mode corresponds to the opening and closing of the binding cleft ('breathing motion'), whereas the second mode coincides with the displacement of the hinge region at the bottom of the large and small lobes. The Figure was published in Czajlik et al. 2017 2017 [5].

Comparison of the restrained ensembles to 100 rotamase domains shows that next to the 'breathing motion', the second most predominant internal dynamics is the displacement of the hinge region near the bottom of the two lobes (Figure 1). These residues are in direct contact with the WW domain, if present, of the parvulin molecule in question.

Analysis of the conformation of two conserved histidines in the large lobe next to the ligand binding cleft revealed that different protonation states correlate with the distribution along the first PCA coordinate.

Based on the presented results we propose a general model for parvulin regulation. Dynamics of the ligand binding cleft might be modulated both by the protonation state of the histidines and the interaction with the WW domain, which, eventually, can also account for ligand specificity.

References

[1] S. D. Hanes, "Prolyl isomerases in gene transcription.," *Biochimica et biophysica acta*, vol. 1850, pp. 2017–34, oct 2015.

[2] O. Heikkinen, R. Seppala, H. Tossavainen, S. Heikkinen, H. Koskela, P. Permi, and I. Kilpeläinen, "Solution structure of the parvulin-type PPIase domain of Staphylococcus aureus PrsA–implications for the catalytic mechanism of parvulins.," *BMC Structural Biology*, vol. 9, no. 1, p. 17, 2009.

[3] L. Sun, X. Wu, Y. Peng, J. Y. Goh, Y.-C. C. Liou, D. Lin, and Y. Zhao, "Solution structural analysis of the single-domain parvulin TbPin1," *PLoS ONE*, vol. 7, no. 8, p. e43017, 2012.

[4] Ł. Jaremko, M. Jaremko, I. Elfaki, J. W. Mueller, A. Ejchart, P. Bayer, and I. Zhukov, "Structure and dynamics of the first archaeal parvulin reveal a new functionally important loop in parvulin-type prolyl isomerases," *Journal of Biological Chemistry*, vol. 286, pp. 6554–6565, feb 2011.

[5] A. Czajlik, B. Kovács, P. Permi, and Z. Gáspári, "Fine-tuning the extent and dynamics of binding cleft opening as a potential general regulatory mechanism in parvulin-type peptidyl prolyl isomerases," *Scientific Reports*, vol. 7, p. 44504, mar 2017.

B. KOVÁCS, "Towards a unified model of regulation in parvulin-type PPIases" in *PhD Proceedings Annual Issues of the Doctoral School, Faculty of Information Technology and Bionics, Pázmány Péter Catholic University 2017.* G. Prószéky, P. Szolgay Eds. Budapest: Pázmány University ePress, 2017, pp 26– 26.

Towards a better understanding of intra- and extracellular neural signals and their relationships

Domokos MESZÉNA
(Supervisor: István ULBERT, MD, D.Sc.)
Pázmány Péter Catholic University, Faculty of Information Technology and Bionics
50/a Práter street, 1083 Budapest, Hungary
meszena.domokos@itk.ppke.hu

***Abstract*—In spite of the widespread use of multi-channel extracellular electrodes, very limited knowledge is available about the intracellular validation of these signals. In this study, a novel experimental method is presented for simultaneous recording of extra- and intracellular activity in rat hippocampal slices. Electrophysiological measurements were completed with subsequent histological analysis. Our method allows the investigation of single cell contribution on the extracellularly recorded signals. These simultaneous, multi-modal signals recorded with our system can yield additional information for various model-based calculations of neuronal dynamics.**

***Keywords*-Extracellular Recordings; Patch-Clamp; Electrode development; two-photon microscopy;**

I. Introduction

It has long been known, that neurons communicate via bioelectric signals, which are systematic alterations of the membrane potential. There are numerous ways for studying these bioelectric phenomena. Recently, multi-electrode arrays were developed (from 16 up to 1024 channels) and automatic spike sorting algorithms were implemented to separate hundreds of neurons simultaneously in one experiment [2]. Despite the technological advances, several aspects of extracellular potential generation remain poorly understood.

Our study attempts to assemble a panoramic view of the neural signal integration using intra- and extracellular recordings, Ca^{2+} dynamics and morphological information. These investigations can significantly help us to understand single-cell dynamics better.

II. Background and Methods

A. Targeted simultaneous electrophysiology

Patch-clamp recordings are made by glass microelectrodes (5-9 $M\Omega$) filled with special intracellular solution. Extracellular recordings are carried out with a commercially available, sixteen-shank silicon probes with 50 μm separation distance between the shanks (A16x1-2mm-50-177-A16, Neuronexus Technologies, Ann Arbor, MI, USA).

During the off-line processing, slices could be investigated using light or electron microscopy or with other histological techniques (Please see B. Kerekes et al. for more details [3]).

III. Results

Extracellular recordings and intracellular Patch-Clamp were executed simultaneously, under the two-photon microscope. During the Z-stack projection, numerous surface scans are merged together into one 3-D like picture. The approximated cell-electrode distances from the first and the second contact points can be indicated. Please note that Patch-Clamp method is capable of filling the neuron with *byiocitin* tracer molecule, thus reconstructing the complete cell morphology.

IV. Conclusion

This study addresses several questions related to extracellularly recorded potentials of the underlying neural activity. We have designed a new, integrative method for multi-modal investigation of in vitro slices. We had already tested the complex methodology on pre-experiments. Finally, we can conclude that these investigations can help us to understand neural communication dynamics better. Thus in the future, they would have a good contribution even for the therapy of neural diseases.

Statement of originality

This PhD report describes the work of the doctoral student during the academic year 2016/2017. Parts of this work might be under submission to scientific conferences and journals.

Acknowledgement

The author would express deep gratitude to his supervisor, István Ulbert, MD, DSc for the promotion of the doctoral research work. In addition, the author wish to express thanks to Zoltán Somogyvári, PhD, "Soma", for his excellent advices, to Gergely Márton for developing the novel electrode, and to Viktor Oláh, Bálint Kerekes and Ildikó Pál, for their technical assistances and their encouragements. This research has been funded by the EU FP7 Grant No. 600925 NeuroSeeker and the Hungarian Brain Research Program - Grant No. KTIA-13-NAP-A-IV/1,2,3,4,6.

References

[1] Pettersen, K. H., Lindén, H., Dale, A. M., and Einevoll, G. T. (2012). Extracellular spikes and CSD. *Handbook of Neural Activity Measurement*, 92-135.

[2] Gold, C., Henze, D. A., Koch, C., and Buzsáki, G. (2006). On the origin of the extracellular action potential waveform: a modeling study. *Journal of neurophysiology*, 95(5), 3113-3128.

[3] Kerekes, B. P., Tóth, K., Kaszás, A., Chiovini, B., Szadai, Z., Szalay, G., ... and Wittner, L. (2014). Combined two-photon imaging, electrophysiological, and anatomical investigation of the human neocortex in vitro. *Neurophotonics*, 1(1), 011013-011013.

[4] Katona, G., Szalay, G., Maák, P., Kaszás, A., Veress, M., Hillier, D., ... and Rózsa, B. (2012). Fast two-photon in vivo imaging with three-dimensional random-access scanning in large tissue volumes. *Nature methods*, 9(2), 201-208.

[5] Somogyvári, Z., Cserpán, D., Ulbert, I., and Érdi, P. (2012). Localization of single cell current sources based on extracellular potential patterns: the spike CSD method. *European Journal of Neuroscience*, 36(10), 3299-3313.

[6] Pettersen, K. H., Devor, A., Ulbert, I., Dale, A. M., and Einevoll, G. T. (2006). Current-source density estimation based on inversion of electrostatic forward solution: effects of finite extent of neuronal activity and conductivity discontinuities. *Journal of neuroscience methods*, 154(1), 116-133.

D. MESZÉNA, "Towards a better understanding of intra- and extracellular neural signals and their relationships" in *PhD Proceedings Annual Issues of the Doctoral School, Faculty of Information Technology and Bionics, Pázmány Péter Catholic University 2017.* G. Prószéky, P. Szolgay Eds. Budapest: Pázmány University ePress, 2017, pp 27– 27.

Novel analysis tools for correlated confocal and super-resolution microscopy

Vivien MICZÁN
(Supervisors: Dr. István KATONA, Dr. András HORVÁTH)
Pázmány Péter Catholic University, Faculty of Information Technology and Bionics
50/a Práter utca, 1083 Budapest, Hungary,
Institute of Experimental Medicine of the Hungarian Academy of Sciences
43 Szigony utca, 1083 Budapest, Hungary
miczan.vivien@itk.ppke.hu

***Abstract*—Single-molecule localization microscopy can visualize the nanoscale molecular composition of brain networks with a comparable localization precision of target proteins to immunogold electron microscopy. Moreover, its capability of imaging multiple proteins simultaneously with higher immunolabeling density after a faster tissue processing protocol represents potential major advantages over electron microscopy in several neuroscience applications. Considering the complex nature of brain circuits and the lacking investigation tools our aim was to develop an efficient approach for cell and cell-type specific nanoscale molecular imaging in the brain.**

We have developed an immunostaining and imaging protocol optimized for correlated confocal and super-resolution microscopy [1] and since the analysis of the coordinate-based SMLM data needs special tools we developed an open-source visualization and analysis software named VividSTORM. Indeed, we have recently shown that combining Stochastic Optical Reconstruction Microscopy (STORM) with confocal microscopy allows rapid and efficient nanoscale molecular imaging within morphologically and neurochemically defined cellular and subcellular context in intact brain circuits [2]. The original workflow includes i) simultaneous visualization and analysis of both pixel-intensity-based (e.g. confocal, widefield, TIRF, STED, SIM) and single-molecule localization-based (e.g. STORM, PALM) microscopy data ii) alignment and overlay of the pixel-intensity-based image and the molecular localization coordinates; iii) delineation of the labeled target cell or subcellular structure as region-of-interest (ROI); iv) selection of those specific single molecule localization points, which belong to the identified target profile; v) coordinate-based analysis of the super-resolution data.

To further facilitate the correlated visualization and data analysis of super-resolution and confocal images, we have recently implemented multiple new features not yet available in any other microscopy software packages. VividSTORM is equipped with a graphical user interface, this way the steps of the analysis process can be easily performed. We implemented several novel tools in the software. Manual and automatic, fiducial-marker-based or image-based alignment methods allow for the registration of the two imaging modalities. For the fiducial-marker-based method we used fluorescent beads to enrich the sample. Then affine transformation is performed on all channels of the confocal image based on the landmarks set up manually, resulting in good alignment between the corresponding channels in both modalities across the field of view. For automatic image-based registration the STORM coordinate list was converted to pixel-intensity-based image with density-based sampling and Gaussian blur. ORB [3] algorithm was carried out searching for similar features of the STORM and confocal image, then random consensus and sampling (RANSAC) [4] algorithm was used to select the correct keypoints and omit incorrect ones. Optimal transformation including translation, rotation and scaling was carried out on the confocal image to match the STORM image resulting in a good fit.

An unbiased ROI selection feature by automated 2D or 3D segmentation of the pixelated image using a modified Morphological Active Contours Without Edges (MACWE) algorithm [5] is also available. The first time it is possible to capture and analyse 3D stacks of STORM images and confocal stacks together. This way bigger structures with a broader z-range can be targeted.

The analysis of molecular clustering is also a key feature of VividSTORM. Previously we used the Density-based Spatial Clustering of Applications with Noise [6] which is a powerful method for finding clusters in the sample with a predefined size and also for eliminating the nonspecific noise. One of the major drawbacks of this method is that it is highly dependent on user-specified parameters, so we wanted to implement a more unbiased approach. A new method for quantifying the clustering of single-molecule microscopy data using Bayesian statistics was published recently [7] and we implemented it in Python and integrated it in VividSTORM. We validated the method using mitochondrial staining with known cluster sizes and found that this method is a powerful tool for selecting optimal clustering parameters for localization points. The batch analysis of pre-selected ROIs is also supported to allow for the flexible and user-friendly usage of the software.

The latest VividSTORM version available at: http://katonalab.hu/vividstorm2/ . These new features together further facilitate high-throughput correlated confocal and super-resolution data analysis and functional interpretation of quantitative molecular observations within identified cellular and subcellular structures in the brain.

REFERENCES

[1] B. Dudok, L. Barna, M. Ledri, S. I. Szabó, E. Szabadits, B. Pintér, S. G. Woodhams, C. M. Henstridge, G. Y. Balla, R. Nyilas, C. Varga, S.-H. Lee, M. Matolcsi, J. Cervenak, I. Kacskovics, M. Watanabe, C. Sagheddu, M. Melis, M. Pistis, I. Soltesz, and I. Katona, "Cell-specific STORM super-resolution imaging reveals nanoscale organization of cannabinoid signaling," *Nature Neuroscience*, vol. 18, pp. 75–86, dec 2014.

[2] L. Barna, B. Dudok, V. Miczán, A. Horváth, Z. I. László, and I. Katona, "Correlated confocal and super-resolution imaging by VividSTORM," *Nat Protoc*, vol. 11, pp. 163–183, dec 2015.

[3] E. Rublee, V. Rabaud, K. Konolige, and G. Bradski, "Orb: an efficient alternative to sift or surf," *IEEE Int Conf on Comp Vis*, 2011.

[4] M. Fischler and R. Bolles, "Random sample consensus: A paradigm for model fitting with applications to image analysis and automated cartography," *Communications of the ACM*, vol. 6, pp. 381—395, 1981.

[5] P. Marquez-Neila, L. Baumela, and L. Alvarez, "A morphological approach to curvature-based evolution of curves and surfaces," *IEEE Transactions on Pattern Analysis and Machine Intelligence*, vol. 36, pp. 2–17, jan 2014.

[6] M. Ester, H.-P. Kriegel, J. Sander, and X. Xu, "A density-based algorithm for discovering clusters in large spatial databases with noise," pp. 226–231, 1996.

[7] P. Rubin-Delanchy, G. L. Burn, J. Griffié, D. J. Williamson, N. A. Heard, A. P. Cope, and D. M. Owen, "Bayesian cluster identification in single-molecule localization microscopy data," *Nat Methods*, no. 12, pp. 1072–6, 2015.

V. MICZÁN, "Novel analysis tools for correlated confocal and super-resolution microscopy" in *PhD Proceedings Annual Issues of the Doctoral School, Faculty of Information Technology and Bionics, Pázmány Péter Catholic University 2017.* G. Prószéky, P. Szolgay Eds. Budapest: Pázmány University ePress, 2017, pp 28– 28.

Estimation of Hawkes Processes in Modeling the Self-Exciting Nature of Epilepsy

György PERCZEL
(Supervisors: Loránd ERŐSS, László GERENCSÉR, Zsuzsanna VÁGÓ)
Pázmány Péter Catholic University, Faculty of Information Technology and Bionics
50/a Práter street, 1083 Budapest, Hungary
National Institute of Clinical Neurosciences, Department of Functional Neurosurgery
57. Amerikai street, 1145 Budapest, Hungary
perczel.gyorgy.miklos@itk.ppke.hu

Statement of originality:
This report describes the work of the doctoral student during the academic year 2016/2017. Parts of this work might be under submission to scientific conferences and journals.

I. Introduction

Hawkes process represents the basic model of self-excitation in the field of stochastic point processes: previous events influence the future evolution of the process and this interaction of microscopic events may lead to formation of macroscopically observable clusters[1]. Though it has first been introduced in the field of seismology, later, based on the similarities in the mathematical concepts describing the brain and the upper crust of the Earth [2], it has been proposed to model neural interactions regarding spikes as events [3], [4]. Is has been shown that spike trains of single unit activity (SUA) fit better to Hawkes processes than to (in)homogeneous Poisson processes [5]. So conceptually, the 'Hawkes representation' of neural data should be interesting, especially in the context of epilepsy.

II. Background and Methods

To implement and evaluate a parameter estimating system that would enable us to fit such a model to experimental data, we first simulated Hawkes processes using its dynamical representation. Estimation was carried out via maximum likelihood estimation (MLE). We used the general form of the log-likelihood function of Hawkes processes that was previously given by T. Ozaki in [6]. Suiting this to our parametrization, we could express both the negative log-likelihood function (NLL) of the process and its gradient in a closed form. As a measure of the precision of our optimization algorithm, we defined the error of estimation (EE) as the Euclidean norm of the normalized distances of each parameters original and estimated values. We screened a wide range of the parameter space by simulating multiple time series using combinations of parameters along a low-resolution grid. Initial values for the estimation were acquired using a $\pm 50\%$ perturbation on every parameter.

III. Results and Discussion

Low values of EE corresponding to precise estimation occurred in a large region. However in some regions high EE-values were observed. To better understand the cause of this inaccuracy, we visualized the cross sections of the cost function and noticed that in regions with low EE-values it depended primarily on one parameter. We interpret these parts as degenerate regions of the model, where the parameters that are responsible for the self-excitation of the model are so small, that the model converges to the simple case of a Poisson-like process with one parameter. It is important to highlight, that this latter parameter is estimated with high precision throughout the observed regions.

IV. Conclusion

Hawkes processes as a simple stochastic model of self-excitation can be a useful tool in the field of neuroscience and especially in that of epilepsy to analyze e.g. SUA. To implement and evaluate a parameter estimating system that would enable us to fit such a model to experimental data, we first simulated Hawkes processes using its dynamical representation and showed that our method works on a wide range of parameters. Estimation was carried out via MLE. We demonstrate, that our method is able to estimate the parameters of the model with high fidelity in large regions of the parameter space. Though MLE was inaccurate with respect to every single parameter in some regions, we demonstrated, that in these regions our model tends to become a one parametered Poisson-like process and that the one parameter having a large effect on the model is well-estimated.

References

[1] A. G. Hawkes, "Spectra of some self-exciting and mutually exciting point processes," *Biometrika*, vol. 58, no. 1, pp. 83–90, apr 1971. [Online]. Available: http://biomet.oxfordjournals.org/content/58/1/83.abstract
[2] D. Sornette and I. Osorio, "Prediction," in *Epilepsy*. CRC Press, may 2011, pp. 203–237. [Online]. Available: http://dx.doi.org/10.1201/b10866-17 http://arxiv.org/abs/1007.2420
[3] D. H. Johnson, "Point process models of single-neuron discharge," *J. Comp. Neurosci.*, vol. 3, pp. 275–299, 1996.
[4] P. Reynaud-Bouret and S. Schbath, "Adaptive estimation for hawkes processes; Application to genome analysis," *Annals of Statistics*, vol. 38, no. 5, pp. 2781–2822, 2010.
[5] P. Reynaud-Bouret, C. Tuleau-Malot, V. Rivoirard, and F. Grammont, "Spike trains as (in) homogeneous Poisson processes or Hawkes processes: non-parametric adaptive estimation and goodness-of-fit tests," *Journal of Mathematical Neuroscience*, 2013.
[6] T. Ozaki, "Maximum likelihood estimation of Hawkes' self-exciting point processes," *Annals of the Institute of Statistical Mathematics*, vol. 31, no. 1, pp. 145–155, 1979. [Online]. Available: http://dx.doi.org/10.1007/BF02480272

Gy. PERCZEL, "Estimation of Hawkes Processes in Modeling the Self-Exciting Nature of Epilepsy" in *PhD Proceedings Annual Issues of the Doctoral School, Faculty of Information Technology and Bionics, Pázmány Péter Catholic University 2017.* G. Prószéky, P. Szolgay Eds. Budapest: Pázmány University ePress, 2017, pp 29– 29.

Developing a general software framework for the automatized testing of neural models

Sára SÁRAY
(Supervisors: Szabolcs KÁLI, Tamás FREUND)
Pázmány Péter Catholic University, Faculty of Information Technology and Bionics
50/a Práter street, 1083 Budapest, Hungary
Institute of Experimental Medicine of the Hungarian Academy of Sciences
43 Szigony street, 1083 Budapest, Hungary
saray.sara@itk.ppke.hu

***Keywords*-model validation, CA1 pyramidal cell, python, jupyter notebook**

Performing simulations on anatomically and biophysically detailed computational neural models can often be a useful method to understand the function and behavior of the different types of neurons in different situations, but it is still a complex and difficult task to tune the unknown parameters, when the goal is to make the model be able to reproduce the real cell's behavior in as many aspects as possible.

To explore the changes in the model's behavior during the parameter tuning process and to compare models that were developed using different methods and for different purposes, we are developing an automatized python test suite called Hippounit. This job is also part of a larger scale work in the European Human Brain Project (HBP).

Hippounit is based on NeuronUnit [1] which is a SciUnit [2] repository for testing neuronal models. The tests of the test suite automatically perform simulations that mimic experimental protocols on detailed hippocampal CA1 pyramidal cell models built in the NEURON simulator [3].

The test suite initially contained three different tests: the *Somatic Features Test*, the *Depolarization Block Test* and the *Oblique Integration Test*. We recently extended Hippounit by implementing the *Trunk Integration Test*, which investigates the integrational properties of the main apical dendrite (trunk) of hippocampal CA1 pyramidal cell models based on the experimental results of Gasparini and Magee 2006 [4].

The first version of the test suite imposed strong constraints on the model, so further developing the test suite the main goal was to make it as general as possible so that it fits the larger-scale workflow in the HBP, and to allow the testing of certain types of models with minimal effort. For this we made the *model class* - that contains functions that define and execute the stimuli on the models and load the model files - more general. In this new version the user is not needed to modify the *model class* inside its python file, because every important parameter is available from outside this file after the *model class* is instantiated. The initialize function of the *model class*, whose main task is to load the model, is now able to handle hoc templates as well, that are the output of the BluePyOpt [5], the model optimization framework used in the HBP.

Another significant improvement which decreases the effort needed to run the *Oblique Integration Test*, is that a new function of the *model class* now automatically chooses the appropriate oblique dendrites that meet the following criteria: its distance from the soma on the trunk should be at most 120 microns, it originates directly from the trunk, it has no branches (child). The proximal and distal stimulation locations on the obliques are also automatically chosen according to the experimental protocol [6]. The only constraint is that the model needs to include section lists containing the sections of the trunk and the oblique dendrites, which is a much more reasonable constraint than expecting the user to choose the obliques that are in the proper distance from the soma, and also measuring the distances on the dendrite to choose the proper proximal and distal locations for stimulation.

To integrate the test suite into the Brain Simulation Platform [7] of the Human Brain Project we created interactive Jupyter notebooks in our collab page (CA1 pyramidal cell validation) that shows the usage of the different tests step-by-step, and makes it possible to run the tests on different models online on the platform.

In the future we plan to extend the test suite by adding more tests regarding the behavior of CA1 pyramidal cell models. We also would like to further generalize the test suite by expanding its usage to other cell types of the hippocampus.

ACKNOWLEDGEMENTS

Grants from the European Human Brain Project are gratefully acknowledged. I thank Szabolcs Káli, Christian Rössert, Michele Migliore, Carmen Lupascu for their help.

REFERENCES

[1] R. C. Gerkin and C. Omar, "Neuronunit: Validation tests for neuroscience models," *Frontiers in Neuroinformatics*, no. 13, 2013. [Online]. Available: http://www.frontiersin.org/neuroinformatics/10.3389/conf.fninf.2013.09.00013/full

[2] C. Omar and R. Gerkin, "Sciunit: A test-driven framework for formally validating scientific models against data," 2014, last accesed on: 28th April 2017. [Online]. Available: https://github.com/scidash/sciunit

[3] N. T. Carnevale and M. L. Hines, *The NEURON Book*, 1st ed. New York, NY, USA: Cambridge University Press, 2009.

[4] S. Gasparini and J. C. Magee, "State-dependent dendritic computation in hippocampal ca1 pyramidal neurons," *Journal of Neuroscience*, vol. 26, no. 7, pp. 2088–2100, 2006. [Online]. Available: http://www.jneurosci.org/content/26/7/2088

[5] W. Van Geit, M. Gevaert, G. Chindemi, C. Rössert, J.-D. Courcol, E. B. Muller, F. Schürmann, I. Segev, and H. Markram, "Bluepyopt: Leveraging open source software and cloud infrastructure to optimise model parameters in neuroscience," *Frontiers in Neuroinformatics*, vol. 10, no. 17, 2016. [Online]. Available: http://www.frontiersin.org/neuroinformatics/10.3389/fninf.2016.00017/abstract

[6] A. Losonczy and J. C. Magee, "Integrative properties of radial oblique dendrites in hippocampal ca1 pyramidal neurons," *Neuron*, vol. 50, no. 2, pp. 291 – 307, 2006. [Online]. Available: http://www.sciencedirect.com/science/article/pii/S0896627306002133

[7] F. Schürmann, E. Muller, and I. Segev, "Hbp brain simulation platform (bsp) march 30th 2016 demo (v2)," Youtube, last accessed on: 29th April 2017. [Online]. Available: https://www.youtube.com/watch?v=C3bU_U3vx68

S. SÁRAY, "Developing a general software framework for the automatized testing of neural models" in *PhD Proceedings Annual Issues of the Doctoral School, Faculty of Information Technology and Bionics, Pázmány Péter Catholic University 2017.* G. Prószéky, P. Szolgay Eds. Budapest: Pázmány University ePress, 2017, pp 30– 30.

Pattern detection in computational models of auditory scene analysis

Beáta Tünde SZABÓ
(Supervisor: István WINKLER, István ULBERT)
Pázmány Péter Catholic University, Faculty of Information Technology and Bionics
50/a Práter street, 1083 Budapest, Hungary
szabo.beata.tunde@itk.ppke.hu

SUMMARY

Auditory scene analysis (ASA) refers to the brain function of parsing the complex acoustic input into auditory perceptual objects, which can represent physical sources, or temporal sound patterns. In this study, we summarize a theoretically motivated review of the recently published computational models. Based on the summary we investigate the possible directions for a computational model that can detect auditory patterns, as this ability is crucial for any method aiming to segregate sound sources. We summarize the non-parametric Bayesian Indian Buffet Process as a possible modelling approach for this purpose.

In everyday life, the acoustic scene contains an unknown number of active sources. To parse the resulting complex mixture of sound and determine the sources that produce the incoming auditory signal, our auditory system needs to parse the acoustic scene into auditory objects. This process has been termed auditory scene analysis (ASA) in Bregman's seminal book (1990). The difficulty lies in the fact that ASA is an ill-posed problem, i.e. the incoming acoustic information does not fully specify the sources. However, our experience tells us that we can reliably decompose auditory scenes. This means that our auditory perception is rarely chaotic or misleading in natural environments. Nevertheless, the neural mechanisms by which our brain solves ASA are still unknown.

We know that for any mechanism that aims to solve this task, needs to explore the relations across simultaneous and successive sounds. We also know, that during solving the ASA problem, the human auditory system processes sound patterns (sequences of acoustic events) very effectively. Acoustic patterns stand for temporally structured, spectrally coherent sound-sequence, that can be segregated from other patterns or from the background noise. When modelling auditory processing (including ASA), explaining the detection and representation of sound patterns is an essential step. The human auditory system is highly sensitive to sound patterns, detecting them very quickly with performance approaching that of an ideal observer (Barascud et al. 2016). Modelling the processing of sound patterns is also because most of what we have learned about the human auditory system up to now has been inferred from experiments presenting isolated sounds (i.e., in the absence of concurrent sounds and using very simple stimuli, such as repeating tones).

We summarize the recent computational models of auditory scene analysis. In our summary, the main questions regarding the models are: how they achieve the grouping and separation of sound elements (theoretical basis); whether they implement some form of competition between alternative interpretations of the sound input; to what extent do they rely on predictive mechanisms. We also investigate their pattern-detection ability through representative examples of the model groups. Regarding the theoretical basis of the models, basing on the set of models reviewed here, we distinguish three broad classes of principles: Bayesian inference rules, neural processing, and temporal coherence. Note that the term *neural* here refers to the group of models that have been formulated with a view towards neurocomputational processes.

Two main approaches of processing sound patterns can be considered based on the different paths they take to segregate patterns from other patterns, or from background noise. One approach places the main emphasis on the spectral regularities, with spectral features driving sound segregation. The other approach examines the role of temporal regularities in the emergence of a sound pattern. Naturally, the two approaches can't be discussed separately, as a pattern needs to be spectrotemporally defined, but usually only either the spectral or the temporal regularity is thoroughly investigated in the studies. A joint approach would be an experimental setup, where the temporal and spectral pattern-constituents are also complex, e.g. a pattern in noise stimuli as in Tóth et al. (2016), but instead of constant chords, the chords could change in time. Similarly, stimuli as the pure-tone sequences in Barascud et al. (2016) extended for complex tone sequences could result the same experimental direction.

We offer an unsupervised learning algorithm for pattern detection, in the form of a non-parametric Bayesian method. More specifically, we discuss the input representation and the output distribution of the Indian Buffet Process (IBP), which can be used for inferring hidden causes (Wood et al. 2012). In our case, hidden causes are the sources generating the sounds. Bayesian inference is an efficient mechanism for processing hierarchically structured information, and it is in line with human performance in many cases (Barniv and Nelken 2015, Orbán et al. 2008 in the visual modality). The IBP model has the advantage of the ability to infer unconstrained number of hidden causes, i.e. the number of sound sources is not restricted by the model.

The IBP model can be an effective tool for modelling pattern detection, once the proper input representation is found. We discuss possible approaches for constructing the input representations, namely the spectral and temporal feature-representations. Finding the right input representation then could yield a result where patterns are segregated from the noisy environment. Also, multiple patterns could be separated, and with the right setup of the features this could lead to a model of acoustic stream segregation.

B. SZABÓ, "Pattern detection in computational models of auditory scene analysis" in *PhD Proceedings Annual Issues of the Doctoral School, Faculty of Information Technology and Bionics, Pázmány Péter Catholic University 2017.* G. Prószéky, P. Szolgay Eds. Budapest: Pázmány University ePress, 2017, pp 31– 31.

Investigation of the electrophysiological properties of hippocampal synchronous population activity, in vitro

Csilla SZABÓ
(Supervisor: Lucia WITTNER, István ULBERT)
Pázmány Péter Catholic University, Faculty of Information Technology and Bionics
50/a Práter street, 1083 Budapest, Hungary
szabo.csilla@itk.ppke.hu

Population activities like hippocampal sharp wave-ripples (SPW-Rs) and dentate spikes from the dentate gyrus described for freely moving rats occur during slow wave sleep and behavioral immobility and are thought to play a leading role in memory processes. [1] [2] In vitro models of SPW-Rs activity show similarities with SPW-Rs occurring in vivo as both kind of events consist of a field potential gradient, high frequency oscillations and increased neuronal firing. In vitro, these events are initiated in the CA3 and spread to the DG [3].

In vitro studies showed that potentials from the dentate gyrus can be recorded, in vitro. These "dentate waves" composed of depolarizing current and appeared to be locally generated within the granular cell layer. [5] We investigated the cellular and network properties of these activities with simultaneous laminar multielectrode in a rat hippocampal slice model, using physiological bathing medium. Brain slices were prepared from adult Wistar rats (200-600 g), from both sexes. Animals were anaesthetized intraperitoneally with urethane and perfused intracardinally with a solution of 248 mM sucrose, 26 mM $NaHCO_3$, 1 mM KCl, 10 mM $MgCl_2$, 1 mM $CaCl_2$, 10 mM glucose, equilibrated with 5% CO_2– 95% O_2 at 3–5 ^oC. When two-photon imaging was performed as well, animals were anaesthetized with isoflurane. Then animals were decapitated, whole brain dissected and horizontal slices of 500 μm were prepared from ventral hippocampus towards to the dorsal area. Slices were carried to the interface recording chamber and perfused with a soulution of 124 mM NaCl, 26 mM $NaHCO_3$, 4 mM KCl, 2 mM $MgCl_2$, 2 mM $CaCl_2$, 10 mM glucose, equilibrated with 5% CO_2– 95% O_2 at 34–35 ^oC. Slices recuperated in standard oxygenated artificial cerebrospinal fluid (ACSF) for an hour before starting extracellular recording. Local field potential gradient (LFPg) was recorded with laminar multielectrode array (Pt/Ir, 24 channels, 150 μm intercontact distance). The electrode was placed on the surface of the brain slice, perpendicularly to the cell layers of the CA3 region and the dentate gyrus as well. In this way extracellular recordings were made simultaneously from both hippocampal region.

Spontaneous population activities were generated in the dentate gyrus and CA3 region of slices prepared from the temporal hippocampus of young rats, in vitro. These events were characterized by a LFPg transient, increased fast oscillatory activity and increased multiple unit activity (MUA). They were apparently similar to synchronous population bursts previously recorded in rodent hippocampal slices, considered as in vitro models of SPW-Rs. [4] The synchronous population activity recorded in the dentate gyrus was termed dentate wave in rat. CSD analysis, which estimates transmembrane currents in the local neuronal population confirmed that SPW-Rs were locally generated in each of the DG and CA3 region with conserved intrahippocampal connections. CSD heatmaps showed sinks and sources of neuronal populations. Sinks correspond to either an inward current representing active excitation or a passive return current. Sources correspond to an outward active inhibitory current or a passive return current. Simultaneous recordings revealed that the waves were often synchronized in the DG and CA3, even though data showed that propagation was not unidirectional, it proceeded from both the CA3 region and DG as well. This suggests that the information transmission among the CA3 region and the DG consists of multidirectional processes. In the future we would like to examine the role of glutamatergic signaling in the spreading of SPW-Rs and dentate waves applying the type II. metabotropic glutamate receptor (mGluR2) agonist DCG-IV, as it is used to block the glutamate release from mossy fibers, the only direct connection between CA3 and DG.

References

[1] Buzsáki G, Leung LW, Vanderwolf CH. 1983. Cellular bases of hippocampal EEG in the behaving rat. Brain Res 287:139-171
[2] Buzsáki G, 1989. Two-stage model of memory trace formation: A role foor 'noisy' brain states, Neuroscience 31:551-570
[3] Kubota D, Colgin LL, Casale M, BrucherFA, Lynch G. 2003. Endogenous waves in hippocampal slices. J Neurophysiol 89:81-89
[4] Hofer, K. T., Kandrács, Á., Ulbert, I., Pál, I., Szabó, C., Héja, L. and Wittner, L. (2015), The hippocampal CA3 region can generate two distinct types of sharp wave-ripple complexes, in vitro. Hippocampus, 25: 169–186. doi: 10.1002/hipo.22361
[5] Colgin, L. L., Kubota, D., Brucher, F. a, Jia, Y., Branyan, E., Gall, C. M., Lynch, G. (2004). Spontaneous waves in the dentate gyrus of slices from the ventral hippocampus. Journal of Neurophysiology, 92(6), 3385–98. http://doi.org/10.1152/jn.00478.2004

Cs. SZABÓ, "Investigation of the electrophysiological properties of hippocampal synchronous population activity, in vitro" in *PhD Proceedings Annual Issues of the Doctoral School, Faculty of Information Technology and Bionics, Pázmány Péter Catholic University 2017.* G. Prószéky, P. Szolgay Eds. Budapest: Pázmány University ePress, 2017, pp 32– 32.

Analysis of the genetic background of type 2 diabetes mellitus focused on the fat metabolism and the lipase genes

A short summary

Réka SZALKAI-DÉNES
(Supervisors: Zoltán GÁSPÁRI PhD, Zsolt RÓNAI MD, PhD)
Pázmány Péter Catholic University, Faculty of Information Technology and Bionics
50/a Práter street, 1083 Budapest, Hungary
denes.reka@itk.ppke.hu

***Abstract*—Type 2 diabetes is a complex disease, caused by complicated interactions between genetic and environmental factors. Obesity is believed to account for 80–85% of the risk of developing type 2 diabetes. This fact (among others) suggests the investigation of lipases in connection with the disease, as these enzymes play a major role in the fat metabolism. This project is focused on the relationship between the fat metabolism and certain polymorphisms of the lipase genes using traditional and high-throuhgput biological methods as well, such as Sanger sequencing, PCR-RFLP and TaqMan® OpenArray® method.**

***Keywords*-lipase; diabetes mellitus; genetics; sequencing; RFLP; real-time PCR**

Diabetes mellitus is a chronic disease caused by inherited and/or acquired deficiency in production of insulin by the pancreas, or by the ineffectiveness of the insulin produced. Type 2 diabetes results from the body's inability to respond properly to the action of insulin produced by the pancreas [1].

Our research is focused on type 2 diabetes mellitus. Obesity is believed to account for 80–85% of the risk of developing type 2 diabetes, and recent research suggests that obese people are up to 80 times more likely to develop type 2 diabetes than those with a BMI of less than 22.

The aim of this PhD project is to analyze the association between certain genetic factors and type 2 diabetes, using molecular genetic and computational approaches.

Polymorphisms are genetic variants structurally similar to mutations. They can affect just one (SNP – single nucleotide polymorphism) or several (VNTR – variable number of tandem repeats) nucleotides. Their minor allele frequency is usually higher than 5%, and they cause susceptibility to a certain complex disease or property.

This project is focused on the relationship between the fat metabolism and certain polymorphisms of the lipase genes, since malfunctions in fat metabolism can cause serious disorders, such as diabetes mellitus [2].

Lipases are enzymes that break down fats, produced by the liver, pancreas, and other digestive organs. They are part of the family of hydrolases that act on carboxylic ester bonds. The physiologic role of lipases is to hydrolyze triglycerides into diglycerides, monoglycerides, fatty acids and glycerol.

Based on *in silico* data, 32 SNPs were chosen for subsequent genetic study. Buccal DNA samples were collected and purified from 350 diabetic and 450 control people. SNPs were first genotyped using the TaqMan OpenArray genotyping platform.

Genotype call was based on the fluorescence intensity data, using the TaqMan Genotyper Software. Out of the 32 SNPs, we could not evaluate 9 SNPs due to technical reasons, therefore these measurements were excluded from further analyses. The average call rate was 84.6%.

Hardy-Weinberg equilibrium was calculated for each SNP in the control group. Two SNPs showed significant discrepancy from the Hardy-Weinberg model in the control group, therefore two more SNPs were excluded.

Association study was performed by χ^2-test in combination with correction for multiple testing. Several SNPs showed nominally significant difference ($p<0.05$) between the control and the diabetic population, whereas two of these results (LPL rs11570892 and LIPG rs3786248) were still significant after the Bonferroni correction.

During the classification, in case of the LPL 3'UTR SNP (rs11570892) we noticed a fourth group besides the three well separated genotype group. We assumed, that another SNP interferes with our genotype results. We applied PCR-RFLP (restriction fragment length polymorphism) and Sanger sequencing to resolve the problem.

Based on these methods we determined another SNP (rs3208305) 32 base pairs past from the rs11570892 SNP.

The two statistically significant SNPs (LPL rs11570892 and LIPG rs3786248) are both located in the 3' untranslated (UTR) regulatory region of the LPL and LIPG genes, respectively. The 3' UTR contains binding sites for both regulatory proteins and microRNAs. The LPL rs11570892 and LIPG rs3786248 may influence the binding sites of certain miRNAs and thus alter the expression level of the LPL and LIPG genes, respectively.

The aim of our current ongoing work is to investigate the microRNA binding sites and expression of lipase genes using luciferase reporter system. Currently, the plasmid constructs are designed and produced for the measurements.

These results might contribute to the understanding of molecular processes in the background of diabetes mellitus, which could be of clinical significance providing the bases of novel approaches of therapy or secondary prevention.

References

[1] Pickup JC, Crook MA. Is type II diabetes mellitus a disease of the innate immune system? Diabetologia. 1998 Oct;41(10):1241-8. Review. PubMed PMID: 9794114.

[2] Carr MC, Brunzell JD. Abdominal obesity and dyslipidemia in the metabolic syndrome: importance of type 2 diabetes and familial combined hyperlipidemia in coronary artery disease risk. J Clin Endocrinol Metab. 2004 Jun;89(6):2601-7. Review. PubMed PMID: 15181030.

R. SZALKAI-DÉNES, "Analysis of the genetic background of type 2 diabetes mellitus focused on the fat metabolism and the lipase genes" in *PhD Proceedings Annual Issues of the Doctoral School, Faculty of Information Technology and Bionics, Pázmány Péter Catholic University 2017.* G. Prószéky, P. Szolgay Eds. Budapest: Pázmány University ePress, 2017, pp 33– 33.

Investigating Molecular Markers and Regulators of Dermal Stem Cell Function

BALAZS SZEKY
(Supervisor:SAROLTA KARPATI,KRISZTIAN NEMETH)
Pázmány Péter Catholic University, Faculty of Information Technology and Bionics
50/a Práter street, 1083 Budapest, Hungary
szeba@itk.ppke.hu

***Abstract*—Dermal tissue, the connective tissue of mammalian skin harbours fibroblastic cells utilizing multiple functions to ensure regenerative capacity and barrier function. Despite their role in tissue renewal, stem cell populations supporting tissue homeostasis are still incompletely characterized. Here we show, that diverse mesenchymal cell populations can be distinguished based on the expression profiles of perivascular and mesenchymal stem cell markers among dermal and subcutaneous fibroblasts. Moreover, mesenchymal cells of different origin have different capacities for osteoblastic and adipogenic differentiation in vivo. Whereas subcutaneous fibroblasts generate osteocytes and adipocytes, dermal fibroblasts and fibroblasts from melanoma do not differentiate into adipocytes at all. Our results confirms the existence of heterogeneous mesenchymal cell populations, which differentially express stem cell markers and contribute differentially to dermal tissue homeostasis.**

B. SZÉKY, "Investigating Molecular Markers and Regulators of Dermal Stem Cell Function" in *PhD Proceedings Annual Issues of the Doctoral School, Faculty of Information Technology and Bionics, Pázmány Péter Catholic University 2017.* G. Prószéky, P. Szolgay Eds. Budapest: Pázmány University ePress, 2017, pp 34– 34.

Filtration of circulating tumor cells using microfluidic devices

Ádám György Szélig
(Supervisor: Kristóf Iván Ph.D.)
Pázmány Péter Catholic University, Faculty of Information Technology and Bionics
50/a Práter street, 1083 Budapest, Hungary
szelig.adam.gyorgy@itk.ppke.hu

Circulating tumor cells (CTCs) are defined as tumor cells in the circulation. Cancer metastasis occurs when CTCs disassociate from the primary or secondary tumor, enter the circulation, and migrate to distant organs through the peripheral blood stream or lymphatic drainage and is the leading cause of death in patients with cancer. Clinical trials have shown that the presence of CTC is predictive of survival in several types of cancer, including breast, prostate, colon, gastric, small and non-small cell lung carcinoma and melanoma [1]. Identification and characterization of CTCs offers an opportunity to understand the metastatic cascade, help in the selection of the proper cancer treatment and enable the monitoring of treatment progression. In clinical practice, analysis of CTCs can provide a minimally-invasive approach for tumor characterization. An average tumor may release an estimated million cells per day into the bloodstream; however, most of these cancer cells do not survive. The typical CTC concentration is approximately 1 CTC in 1 mL of blood compared to $\sim$5*10^9 red blood cells and $\sim$7*10^6 leukocytes. To capture sufficient numbers of CTCs for reliable diagnosis many novel methods have been developed. Microfluidic technologies are an effective means to isolate and detect CTCs. Parameters in microfluidic devices can be precisely controlled at the cellular scale; this precise control facilitates capture efficiency and isolation purity. Furthermore, isolated CTCs can be manipulated to next-stage analysis or on-chip cell culturing as part of the cell separation process, speeding up the overall CTC characterization process and eliminating the intermediate procedures [2].

A variety of technologies have been developed to improve detection and capture of CTCs from peripheral blood. These technologies use one or more unique properties of CTCs that distinguish them from the surrounding normal blood cells: biological properties (surface protein expression, presence of mutations, expression of specific genes, viability, and invasion capacity) and/or physical properties (size, shape, density, electrical charges, deformability, inertia, optical properties and acoustic features). It is important to note that most of the current technologies that rely on isolating CTCs based on biological properties are based on epithelial cell adhesion molecule (EpCAM). The second most frequent approach is to isolate CTCs using the fact that most but not all of the tumor cells in the circulation are larger than most blood cells. Therefore, finely tuned filters can be manufactured that retain only tumor cells and let most of the blood cells go through.

Four types of filtration have been reported in microfluidic systems: weir-type, pillar, cross-flow, and membrane. In weir-type filtration, a barrier is fabricated to constrict the height of the channel, with a space maintained between the barrier and the ceiling of the channel that allows fluids and small particles to pass through while retaining large particles. In pillar-type filtration, micro-pillars are spaced apart in an array along the micro-channel to filter out particles. Cross-flow filtration is based on the same principle, but the flow is perpendicular to the micro-pillar array. This system has the advantage of being less prone to fouling than the aforementioned systems because the filtered particles will flow perpendicular to the direction of the flow, while the undesired particles along with the waste will flow parallel to the flow direction. Membrane filters contain well-defined pores that separate larger cells from the fluid and from smaller particles. This system is robust and widely used in industrial ares but in case of many particles it can be easily clogged.

A challenge in microfluidic CTC filtration that large sample volumes needs to be analyzed due to the low concentration of CTCs in the blood sample. Typically, a fixed volume of 7.5 mL blood is processed. The volume capacity of a microchannel is typically less than 100 μL, which is too small to process 7.5 mL of blood in a reasonable time. To reduce the required long processing time (several hours), flow rate is usually increased. However, at increased flow rates when the cells enter a channel constriction they can easily deform, which will induce cell membrane stress and damage, and if the operating conditions are not carefully controlled, passage through small openings may cause cell loss. When designing a microfluidic filtration device many important factors have to be taken into consideration like filter material, filter gap, filter width, channel width, density and distribution. Blood dilution, fixation and pressure will also influence the passage of blood through the filters and thereby the effectiveness of CTC isolation.

For my device design cross-flow filtration method was selected for its robustness and its capability of being less prone to clogging. The microfluidic device has a long snake shape channel with long parallel sections. Between the parallel sections chalice like microcapillary structures have been incorporated. This device was successfully used to filter out CTCs with higher than 90% efficiency at low flow rates using EDTA treated blood.

References

[1] F. Coumans, G. van Dalum, M. Beck and L. Terstappen, "Filtration Parameters Influencing Circulating Tumor Cell Enrichment from Whole Blood", *PLoS ONE*, vol. 8, no. 4, p. e61774, 2013.

[2] P. Li, Z. Stratton, M. Dao, J. Ritz and T. Huang, "Probing circulating tumor cells in microfluidics", *Lab on a Chip*, vol. 13, no. 4, p. 602, 2013.

Á. SZÉLIG, "Filtration of circulating tumor cells using microfluidic devices" in *PhD Proceedings Annual Issues of the Doctoral School, Faculty of Information Technology and Bionics, Pázmány Péter Catholic University 2017.* G. Prószéky, P. Szolgay Eds. Budapest: Pázmány University ePress, 2017, pp 35–35.

PROGRAM 2
COMPUTER TECHNOLOGY BASED ON MANY-CORE PROCESSOR CHIPS, VIRTUAL CELLULAR COMPUTERS, SENSORY AND MOTORIC ANALOG COMPUTERS

Head: Péter SZOLGAY

Subjective Assessment Methodologies for Quality of Experience Evaluation on Glasses-free Light Field Displays

Subbareddy DARUKUMALLI
(Supervisor: Peter SZOLGAY)
Pázmány Péter Catholic University, Faculty of Information Technology and Bionics
50/a Práter street, 1083 Budapest, Hungary
darukumalli@itk.ppke.hu

***Abstract*—As an advancement in the 3D technology, apart from the traditional stereoscopic technologies, the auto-stereoscopic technologies are gaining popularity in the consumer market. With the new emerging 3D visualization techniques, one can experience the 3D without any additional hardware support, such as head gears and special glasses. To estimate the user Quality of Experience on such technologies gaining momentum in the research community; this study will present an overview of the current state of the art of the subjective assessment methodologies available for the Quality of Experience evaluation on Glass-free light field displays and the discussion emphasizes the special considerations, which are need during the subjective evaluation of such technology.**

***Keywords*-Quality of Experience; Light Field Display; Perceived quality; Subjective quality assessment methodologies; Experimental test conditions; Subjective rating scales**

A. Scientific Literature Review

The first standard for stereoscopic television picture[1] was proposed in the year 2000. This was followed by a standard in 2015[2], that in addition to the previously included aspects of quality, also addressed the perceptional dimensions, such as picture quality, depth quality and visual comfort.

With the rapid growth of 3D visualization technologies in the recent years resulted in standards proposed in 2016[3], [4], [5], which are mainly focusing on environmental constraints, depth quality, naturalness, visual discomfort, Quality of Experience (QoE), viewing experience and the visual fatigue symptoms during the subjective assessment of stereoscopic video content.

At the time of this paper, all the available 3D standards on subjective quality assessment address stereoscopic display technologies. Currently there is no ITU standard that addresses the subjective evaluation of autostereoscopic light field displays.

The work of Darukumalli et al.[6] introduces an experiment that involves different subjective tests performed on a HoloVizio C80 light field cinema system[7]. Three scales were used, namely an ACR scale and a 7-point pair comparison scale for level of zoom assessment, and a Single Stimulus Method for visual comfort (5-point visual comfort scale[8]). All three experiments used the same rendered stimuli, and were conducted with identical conditions, such as 2.5H viewing distance.

B. Conclusion

In this paper, we presented the current state of the art of standards and recommendations for 3D quality of Experience evaluation methodologies and a discussion on the quality assessment methodologies for subjective experiments on light field displays. The discussion emphasizes that while there are already subjective studies were done on Glass-free light field displays Quality of Experience evaluation, there is no standard of recommendation determines the proper parametrization of such experiments, while some of these conditions may fundamentally affect the subjective results. Future work will support the discovery and analysis of experimental parameters and test conditions that may influence the new glasses-free user experience.

Acknowledgment

The work in this paper was funded from the European Union's Horizon 2020 research and innovation program under the Marie Sklodowska-Curie grant agreement No 643072, Network QoE-Net. I would like to thank Peter Andras Kara, Research Associate at Kingston university for his continues support and guidance for this article.

REFERENCES

[1] ITU-T Rec., "BT.1438: Subjective assessment of stereoscopic television," 2000.
[2] ——, "BT.2021: Subjective methods for the assessment of stereoscopic 3DTV systems," 2015.
[3] ——, "P.914: Display requirements for 3D video quality assessment," 2016.
[4] ——, "P.915: Subjective assessment methods for 3D video quality ," 2016.
[5] ——, "P.916: Information and guidelines for assessing and minimizing visual discomfort and visual fatigue from 3D video," 2016.
[6] S. Darukumalli, P. A. Kara, A. Barsi, M. G. Martini, T. Balogh, and A. Chehaibi, "Performance comparison of subjective assessment methodologies for light field displays," in *IEEE International Symposium on Signal Processing and Information Technology (ISSPIT)*, 2016.
[7] Holovizio C80 light field cinema system, www.holografika.com/Documents/HoloVizio_C80.pdf (retrieved March 2017).
[8] ITU-R Rec., "BT.500-13: Methodology for the subjective assessment of the quality of television pictures," 2012.

S. DARUKUMALLI, "Subjective Assessment Methodologies for Quality of Experience Evaluation on Glasses-free Light Field Displays" in *PhD Proceedings Annual Issues of the Doctoral School, Faculty of Information Technology and Bionics, Pázmány Péter Catholic University 2017.* G. Prószéky, P. Szolgay Eds. Budapest: Pázmány University ePress, 2017, pp 37– 37.

The open research areas in distributed wireless industrial monitoring and control network

Máté Lőrincz
(Supervisor: András Oláh, Phd)
Pázmány Péter Catholic University, Faculty of Information Technology and Bionics
50/a Práter street, 1083 Budapest, Hungary
lorincz.mate@itk.ppke.hu

I. Summary

In the past two centuries there were three industrial revolutions. During the first one was the transition from hand production methods to mechanisation, during the second one, the emphasis was on the introduction of assembly lines and on mass production and during the third one, the reconfigurable, programmable controllers replaced the hard-wired, relay-based control panels.

Until the first decade of the 21th century, mostly the results of the third industrial revolution gave the guidelines for the industrial controlling. The PLC-s widespread throughout the industry and acquired the 83% of the industrial control market segment. Altough more than 40 years have passed since the first (1968) PLC-s, the basic principles have not changed too much. The early PLC-s had to be:

- flexible and easily reprogrammable, like a PC;
- easily maintainable and programmable in line with the so-called ladder logic;
- resistant to dirt, moisture, vibration, which are common in industrial environment;
- modular and easily expandable.

Today, the industrial productions and needs are more complex to handle them with the original principles of the third revolution. This was recognised by the German Federal Ministry of Education and Research when they published an article about the future of industry and the fourth industrial revolution, the so-called Industry 4.0.

Industry 4.0 (or Industrie 4.0 in German-speaking countries) is not an exact concept, more like an umbrella term with some design principles. The fallowing definition was given by Herman, Pentek and Otto in their review article:

> ”Industrie 4.0 is a collective term for technologies and concepts of value chain organization. Within the modular structured Smart Factories of Industrie 4.0, CPS [Cyber Physical Systems] monitor physical processes, create a virtual copy of the physical world and make decentralized decisions. Over the IoT [Internet of Things], CPS communicate and cooperate with each other and humans in real time. Via the IoS [Internet of Services], both internal and crossorganizational services are offered and utilized by participants of the value chain.”

The currently widespreading intelligent sensors and actuators have not enough computing capacity and durability to provide reliable industrial control, but together, they can serve as a base for a distributed controller. This distributed controller have some similarities to classical MIMD systems, but they have irregular topology and heterogeneous processing nodes.

The exact topology and members of the network can vary even during normal operation, so the developers need a toolbox and a method to design their control loops independently of the current network. In this paper, I suggest a programming method which is suitable for defining a network of independent processes which will deploy on the processing nodes considering the communication and resource needs of every process. This process network is a directed graph, where the nodes are the processes and the directed edges are the direct communication path between them.

The processes have well-defined inputs and outputs and they refresh independently. Refreshing the process means reading its inputs, calculating its outputs and sending them to the other dependent processes.

The independent refreshes saves the overhead of synchronisation but it makes the process network sensitive to the exact scheduling. The main focus of this paper is the prevention of this sensitivity to provide reliable and calculable behaviour.

The paper investigates two error possibilities:

- When the process graph has circles, the system can be described as a recursive equitation. The particular equation is depending on the scheduler, but the different equations have similar form. The paper proves that with proper initialisation of the communication lines, the process graph won't depend on the scheduler.
- When the process graph has no circles, the output will converge independently of the particular scheduler, but the speed of convergence and the synchronicity of the processes are linked. The paper shows a way to speed up the convergence.

The paper contains simulations generated by FluidControlSim and a process graph generator. The FluidControlSim can be used to simulate different fluids inside tanks and pipes and it's easy to test different kind of control loops with it. The process graph generator is a collection of classes and functions written in Python. It provides a hierarchical box model, which can be used to generate and run a process graph with different schedulers.

Currently, four different schedulers are implemented. The process Distribution Algorithm, which has to assign the generated processes to the physical nodes, is only partly covered by this paper.

M. LRINCZ, “The usage of distributed control systems on the field of industrial process control” in *PhD Proceedings Annual Issues of the Doctoral School, Faculty of Information Technology and Bionics, Pázmány Péter Catholic University 2017.* G. Prószéky, P. Szolgay Eds. Budapest: Pázmány University ePress, 2017, pp 38– 38.

Log-optimal portfolios with memory effects - 1 page abstract

Zsolt Nika
(Supervisor: Miklós Rásonyi)
Pázmány Péter Catholic University, Faculty of Information Technology and Bionics
50/a Práter street, 1083 Budapest, Hungary
nika.zsolt@itk.ppke.hu

In portfolio optimization the classical problem is to trade with assets so as to maximize some kind of utility of the investor. In our paper the problem is investigated with assets where their prices depend on their past values in such a way as to model real prices processes. Our utility function is the widespread logarithmic utility, which is broadly used by not only researchers but also by investors.

Despite the problem being a well-known one, there are few results where memory is treated in a parametric model. Our algorithm is optimal. The formulation of the model is discrete in time and optimality is demonstrated by numerical simulations.

Modern portfolio optimization started with Markowitz's theory in 1952, barely 20 years after that Kolmogorov had set the basics of probability theory , which is frequently used nowadays. In 1956 J. L. Kelly formulated a strong connection between information rate and portfolio theory – which we study here. A portfolio is a group of financial assets (like stock, bond) held by an investor whose intention is to optimise some kind of benefit from this ownership. The most important property of a portfolio is its price or its expected price in the future, but it is not evident how to take it into consideration. To maximize its expected value (consider the price as a random variable) seems an obvious idea, but this approach avoids to addressing risk: from two portfolios with the same profit we would choose the one with less risk. A practical approach is to maximise the expected logarithm of the portfolio value (this idea is originated from Daniel Bernoulli, reprinted in 1954 in). While plain expectation is a generalization of arithmetic mean, the logarithm transforms it into geometric mean which is sensitive to the fluctuations in the future value, i.e. to the risk.

To study the price's behaviour it is common to use the increments instead of the process itself (the *returns*) in order to get rid of the drift and see only the noise part (the volatility). The above mentioned systems assume that the noise does not have any time correlation but studies done in the 90s showed that correlation exists at a level that is not negligible. A very good overview about statistical properties of returns is written by R. Comte.

Let our portfolio contains a stock (random price) and a bond (deterministic price), their prices are S_t and B_t. The investors wealth is W_t:

$$W^\pi_{t+1} = W^\pi_t(1-\pi_t)\frac{B_{t+1}}{B_t} + W^\pi_t\pi_t\frac{S_{t+1}}{S_t} \quad (1)$$

$$= W^\pi_t\left[(1-\pi_t)(1+r) + \pi_t e^{H_{t+1}}\right], \quad (2)$$

where π_t is the investors decision at time t, that is the $(1-\pi_t)$ ratio of the current wealth W_t is invested in bond and the rest π_t ratio is invested in stock.

The log-return $H_t = \log(S_t/S_{t-1})$ has the following dynamics:

$$H_{t+1} = \alpha H_t + \rho e^{Y_{t+1}}\epsilon_{t+1} + \sqrt{1-\rho^2}e^{Y_t}\eta_{t+1}, \quad (3)$$

$$Y_t = \sum_{j=0}^{\infty}\beta_j\epsilon_{t-j}. \quad (4)$$

Here ϵ_t and η_t are independent Gaussian variables with $\mathcal{N}(0,1)$ distribution.

The desired optimal task is:

$$\max_\pi \liminf_{t\to\infty}\frac{1}{t}E[\log(W^{\pi^*}_t)], \quad (5)$$

i.e. to optimise the investors log-wealth in time-average on the long-run. The meaning of this utility function, is that logarithm emphasizes the order of the wealth. Typically investors care about the long-run problem and use the strategy for a very long time, for example, for several years and not until a given time T. This investment behaviour ensures that the investor to beats all other investment strategies after a very long time. Therefore the latter question is more interesting.

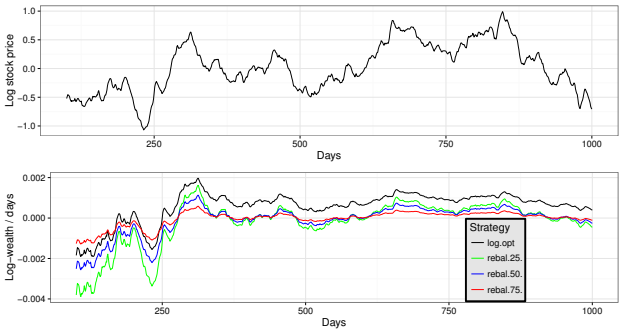

Fig. 1. Numerical simulation of a stock price with the dynamics in equation (3). The top figure shows the logarithm of the stock price, while the bottom figure shows the log-optimal solution (black) and three rebalance-strategies: 'rebal.25' always puts 25% of the total wealth into bonds (green), 'rebal.50' puts the 50% of the total wealth (blues), 'rebal.75' puts the 75% (red). The first 100 days is ignored because transient phenomena is irrelevant here. The log-optimal strategy beats all other strategies, here compared to the rebalanced portfolios.

Zs. NIKA, "Log-optimal portfolios with memory effects" in *PhD Proceedings Annual Issues of the Doctoral School, Faculty of Information Technology and Bionics, Pázmány Péter Catholic University 2017.* G. Prószéky, P. Szolgay Eds. Budapest: Pázmány University ePress, 2017, pp 39– 39.

High precision bone drilling for dental implants

Áron PAPP
(Supervisor: György CSEREY)
Pázmány Péter Catholic University, Faculty of Information Technology and Bionics
50/a Práter street, 1083 Budapest, Hungary
papp.aron@itk.ppke.hu

I. Summary

Osseointegration in clinical dentistry basically depends on the healing and reparative capacities of hard and soft tissues. The most important part of the process is the tissue response to the placement of the fixture. Former researches in the area have been set the target to find out the limits for clinical implantation procedures, allowing the bone and marrow tissues to heal fully, and avoid creation of low differentiated scar tissue with unpredictable sequelae.

Mihály Vaszilkó MD DMD Phd., assistant professor of the Department of Oro-Maxillofacial Surgery and Stomatology of the Semmelweis University presented to our work group his theory of a new method of a more precise and less time-consuming implant placement technique. According to his method, if the proposed and the final locations of the implant screw would be with tolerance of $\pm$ 0.1 mm in the same place, the manufacturing of the abutment and the tooth can be done right after the first imaging stage. The technique would allow to reduce the process into one imaging and one operation stage. As side effect, reducing the number of surgeries will also lower the risk of infection, and make the whole healing period shorter.[3]

Depending on the autonomy left to the surgeon, the guiding systems can be divided into three classes: passive, semi-active, and active. Independently of the type of the guiding system applied, the most important problem is the alignment of the drill into the surgical context. Measurements provided in [4] are proving, that using Cone Beam tomographic images and a very simple mechanism sub-mm accuracy can be achieved. A disadvantage of the system was also shown, it requires that the patient be motionless for about 70 seconds.

Although, classical ossesointegration protocol after a prescribed period of unloaded healing shows excellent long-term results, the demand was increased for early or even immediate loading of dental implants. There is available an increasing number of properly analyzed clinical reports showing that the method of connecting implants rigidly over the midline resulting a comparable survival rate to implants getting loaded just after a healing period of months.

ViSP features a large software library of elementary tasks with various visual features that can be combined together. An image processing library that allows the tracking of features at video rate, a simulator, an interface with various classical frame-grabbers - just to mention some of them. Visual servoing techniques consist of using the data provided by one or more cameras in order to control the motion of a robotic system. Depending on the sensor configuration, a set of visual features $\mathbf{s}$ must be designed from the visual measurements, allowing control of the desired degrees of freedom. The control law also must be designed so that the features $\mathbf{s}$ could reach a desired value $\mathbf{s}^*$, thus defining a correct realization of the task. A desired trajectory $\mathbf{s}^*(\mathbf{t})$ can also be tracked. The control principle is to minimize the error vector $\mathbf{s} - \mathbf{s}^*$.

In order to address the problem of 2-D geometric feature tracking, we need to consider a low level, generic framework that allows the local tracking of edges. From the set of tracked edges, it is then possible to perform a robust estimation of features parameters using an iteratively reweighted least-squares method based on robust M-estimation. The proposed tracking approach is based on the M-estimation algorithm and allows a real-time tracking of geometric features in a sequence of images.

The project is currently in the preparatory stage, that is why, we do not have any significant achievement to report. So far, we have been running different pose estimation algorithms for patterns like classical chessboard, QR-codes, symmetrical and asymmetrical circles grid, and 2×2 circles grid, with promising results, e.g. at a resolution of 800×600 pixels a notebook with Intel i7 processor, using a cheap commercial USB webcam could reach about 60 frames per seconds speed while tracking 2×2 circles grid pattern.

According to the referenced ([1], [2], [3], [4], [5]) creating a guiding system for making the installation of dental implants faster, safer and simpler is not a recent problem, so first of all, we would like to draw conclusions from former related researches. We will try to prove, that the optical pose estimation method is accurate and fast enough to provide reliable data for controlling a robotic arm to follow an object in real-time.

References

[1] Per-Ingvar Brinemark, *Osseointegration and its experimental background*, University of Göteborg and Institute for Applied Biotechnology, Göteborg, Sweden 1983.

[2] Academy of Osseointegration, *Implant Procedure*, https://osseo.org/patienting/NEWhowAreImplantsPlaced.html (Data last accessed: May-7-2017).

[3] B. Jákli, *Sensory Robotics Assisted Dental Applications*, Pázmány Péter Catholic University, Faculty of Information Technology and Bionics, Budapest, 2016

[4] Thomas Fortin, Guillaume Champleboux, Silvio Bianchi, Hervé Buatois, Jean-Loup Coudert, *Precision of transfer of preoperative planning for oral implants based on cone-beam CT-scan images through a robotic drilling machine*, Clin. Oral Impl. Res, 13, 2002; 651–656

[5] Daniel van Steenberghe, Roland Glauser, Ulf Blombäck, Matts Andersson, Filip Schutyser, Andreas Pettersson, Inger Wendelhag, *A Computed Tomographic Scan–Derived Customized Surgical Template and Fixed Prosthesis for Flapless Surgery and Immediate Loading of Implants in Fully Edentulous Maxillae: A Prospective Multicenter Study*, Department of Periodontology, Catholic University of Leuven, 2005

[6] E. Marchand, F. Spindler, François Chaumette, *ViSP for visual servoing: a generic software platform with a wide class of robot control skills*, IEEE Robotics and Automation Magazine, Institute of Electrical and Electronics Engineers, 2005, 12 (4), pp.40-52.

[7] Daniel E. Dementhon, Larry S. David, *Model-Based Object Pose in 25 Lines of Code*, Computer Vision Laboratory, Center for Automation Research, University of Maryland, College Park, 1992.

Á. PAPP, "High precision bone drilling for dental implants" in *PhD Proceedings Annual Issues of the Doctoral School, Faculty of Information Technology and Bionics, Pázmány Péter Catholic University 2017.* G. Prószéky, P. Szolgay Eds. Budapest: Pázmány University ePress, 2017, pp 40– 40.

Computational stability analysis of an uncertain Van der Pol system

Péter POLCZ
(Supervisor: Gábor SZEDERKÉNYI)
Pázmány Péter Catholic University, Faculty of Information Technology and Bionics
50/a Práter street, 1083 Budapest, Hungary
polcz.peter@itk.ppke.hu

***Abstract*—The computational stability analysis of an uncertain time inverted Van der Pol oscillator is reported in this paper using our improved optimization based method. For stability the Lyapunov function is searched in a general quadratic form composed of polynomial terms, for which the Lyapunov conditions are ensured by sufficient LMI conditions formulated using Finsler's lemma and the notion of annihilators. The stability region is estimated by determining the level set of the Lyapunov function within a suitable convex domain.**

***Keywords*-LMI; local stability; Van der Pol; Lyapunov function**

I. Introduction

Approximating the domain of attraction (DOA) is a fundamental and still an active research topic of systems and control theory. The stability properties of dynamical systems are most often studied using Lyapunov functions, accordingly, the computational construction of Lyapunov functions [5] has been addressed extensively in the literature. Furthermore, the use of linear matrix inequalities (LMI) and semidefinite optimization has become very popular due to their advantageous properties and the availability of efficient numerical tools to solve semidefinite problems.

A recent important result was published in [6], where the authors use Finsler's lemma and the notion of annihilators to compute rational Lyapunov functions. Based on this results of, we have proposed an improved method [1], [2] for estimating the domain of attraction of uncertain rational systems of the form $\dot{x} = f(x, \delta)$ (1), where the origin is locally asymptotically stable equilibrium point indifferently from the actual value of the uncertain parameter δ, which is assumed to be bounded as well as its time derivative. A Lyapunov function is search in a general quadratic form $V(x, \delta) = \pi_b^T P \pi_b$ (2) The first n coordinates of π_b are the state variables, the following p number of coordinates are (in general) rational terms of the state variables and the uncertain parameters. The Lyapunov conditions are ensured by affine parameter dependent LMI conditions because they are characterized by affine functions of the state x and the uncertain parameters δ. The DOA for the system can be estimated by the 1-level set ε_1 of the Lyapunov function, since further LMI conditions are formulated in order that ε_1 be maximal inside polytope $\mathcal{X}$, on which the Lyapunov conditions are ensured.

Using LFT and further algebraic manipulation steps, we proposed an automatic transformation of (1) to the required system representation for optimization. This technique results in a dimensionally reduced optimization problem compared to [6], since fewer rational basis are considered in the Lyapunov function. Even thought the Lyapunov function is less parameterized, the area/volume of the obtained stability regions are still adequate and comparable to known results in the literature. Furthermore, an automatic procedure is presented in [1], [2] to generate an appropriate annihilator for π_b. Using our improved method, we have successfully computed a Lyapunov function and a stability region for different Lotka-Volterra models [4] and for an uncertain continuous fermentation process with proportional and integral feedback [3].

In this work, we present the stability analysis of the time-inverted Van der Pol system with different types of uncertainty in its model equations, namely unknown constant parameter, time dependent parameter, non-rational nonlinear expression of the state variables.

II. Uncertain Van der Pol dynamics

The system $\dot{x}(t) = f(x(t), \delta(t))$

$$f(x, \delta) = \begin{pmatrix} -x_2 \\ x_1 - \delta(1 - x_1^2)x_2 \end{pmatrix}, \quad x = \begin{pmatrix} x_1 \\ x_2 \end{pmatrix} \tag{3}$$

describes the time-inverted oscillator introduced by the Dutch electrical engineer and physicist Balthasar van der Pol. This system has a locally asymptotically stable equilibrium point at the origin. Furthermore, we consider δ to be an uncertain parameter with δ_0 nominal value.

The Lyapunov function is searched in the form (2), where the set of polynomial basis to be considered in the Lyapunov function is $\pi_b^T = \begin{pmatrix} x_1 & x_2 & \delta x_2 & \delta x_1^2 x_2 & \delta x_1 x_2 \end{pmatrix}$.

III. Conclusions

We have presented the computational stability analysis for uncertain time-inverted Van der Pol system. A Lyapunov function and stability region was given for three different uncertainty models.

References

[1] P. Polcz, G. Szederkényi, and T. Péni, "An improved method for estimating the domain of attraction of uncertain rational nonlinear systems by using LMI stability conditions," Jedlik Laboratories Reports, volume III. no. 4., JLR-4/2015, pages 7–33, Pázmány University Press, Budapest, 2015.

[2] P. Polcz, G. Szederkényi, and T. Péni, "An improved method for estimating the domain of attraction of nonlinear systems containing rational functions," in *Journal of Physics: Conference Series*, vol. 659, p. 012038, IOP Publishing, 2015.

[3] P. Polcz, G. Szederkényi, and K. M. Hangos, "Computational stability analysis of an uncertain bioreactor model," in *13th International Symposium on Stability, Vibration, and Control of Machines and Structures - SVCS 2016, June 16-18, Budapest, Hungary*, pp. 1–12, 2016.

[4] P. Polcz and G. Szederkényi, "Computational stability analysis of an uncertain bioreactor model," *Hungarian Journal of Industry and Chemistry*, vol. n.a., p. (under editing), Apr/May 2017. n.a.

[5] G. Chesi, *Domain of attraction: analysis and control via SOS programming*, vol. 415. Springer Science & Business Media, 2011.

[6] A. Trofino and T. J. M. Dezuo, "LMI stability conditions for uncertain rational nonlinear systems," *International Journal of Robust and Nonlinear Control*, 2013.

P. POLCZ, "Computational stability analysis of an uncertain Van der Pol system" in *PhD Proceedings Annual Issues of the Doctoral School, Faculty of Information Technology and Bionics, Pázmány Péter Catholic University 2017.* G. Prószéky, P. Szolgay Eds. Budapest: Pázmány University ePress, 2017, pp 41– 41.

Salient object extraction methods in man-made scenes

Mihály RADVÁNYI
(Supervisor: Kristóf KARACS, Péter SZOLGAY)
Pázmány Péter Catholic University, Faculty of Information Technology and Bionics
50/a Práter street, 1083 Budapest, Hungary
radmige@itk.ppke.hu

***Abstract*—Besides modelling the human visual attention mechanism, saliency methods are widely used for extracting interesting areas of input images that are worth further processing. In this paper I present two different salient object extraction approaches, both having its own cues specific to man-made / urban environments. One method is a learning based re-specialization of a general saliency method introduced in [1], that better suits surveillance applications due to its preferred wider Field-of-View (FOV), and the other is a blob-based approach that is specifically designed to extract informative regions and signs on hand-held camera systems, typically with narrow FOVs and close-up target objects.**

***Keywords*-computer vision; learning; object detection; saliency;**

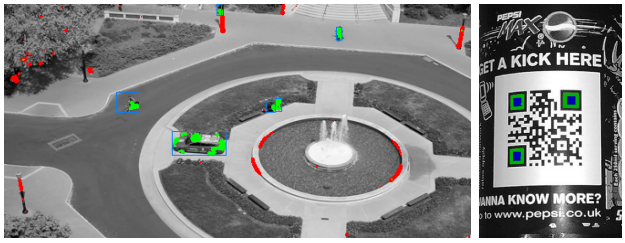

Fig. 1. Left: an example of the learning based spectral residual approach is shown. Red blobs indicate the originally salient objects, whereas green relates to salient objects after learning. Bounding boxes of target objects are also included. Right: an example of highly embedded informative regions are shown of QR codes. The colored rectangles are blobs found to be the most interesting due to their embeddedness.

I. Introduction

The large amount of data presented in each image need to be reduced to ensure real-time performance of object detection and recognition algorithms on both high resolution images or mobile, portable devices. A general problem is that each image contains way more information than it is needed for a certain task and that the processing units also have limitations on the amount of exhaustively processable image parts. A commonly used method is to generate a heat map based on image statistics, that assigns higher values to objects/regions/pixels that are more interesting than others. These heat maps are also referred as saliency maps. The core idea is that front-end algorithms which select only the most interesting parts of the image may run with less costs than back-end related classification/recognition methods. Thus it is very common to apply saliency calculations right at the front-end, and to send regions-of-interests (ROIs) to the back-end for recognition purposes.

In this paper I present two different saliency approaches, both intended to extract salient objects in man-made environments but in different viewpoints/scenarios and with different techniques. Examples are shown in Fig. 1. Once filtered data is present, recognition can be applied on smaller fragments of the input image.

II. Learnt saliency

An effective, general purpose saliency calculation was introduced in [1] that is more effective on datasets with various input images, not in real life applications. The main problem with such a general approach is that (for example) on a surveillance image sequence billboards, fountains and other *uninteresting* objects would be consistently considered as highly salient features. To overcome this issue, I re-specialized the spectral residual method by introducing a learning phase, where a short period of annotated input image sequence was used to extract frequencies that are specific to the target objects, and their impact on the spectral residual were strengthened. This way, however I turned the spectral residual method to be task specific, but meanwhile I increased the precision of the system by processing only the most relevant image regions.

III. Blob-based saliency

In hand-held computer vision systems such as smartphones the typical target objects are a man-made informative patterns or signs with a tendency of having consecutive layers of high contrast colors in order to drag visual attention. For such target objects another saliency approach is proposed that assigns saliency values to connected-components of the images by analyzing structural and regional properties of such regions. Embeddedness of regions is one of the key factors contributing in blob based saliency metrics [2].

IV. Conclusions

In this paper I presented two different saliency methods, both extracting salient objects in urban environments. By integrating a learning phase into a general purpose saliency approach, more accurate method can be applied in task dependent scenarios with wide FOVs, such as surveillance systems. On the other hand a blob-based saliency method was also discussed that assigns saliency values to connected-components, which is a more efficient way to apply recognition algorithms only on the most interesting blobs captured by hand-held devices. Both methods depend on cues specific to man-made / urban environments.

References

[1] X. Hou and L. Zhang, "Saliency detection: A spectral residual approach," in *Computer Vision and Pattern Recognition, 2007. CVPR'07. IEEE Conference on*, pp. 1–8, IEEE, 2007.

[2] M. Radvanyi and K. Karacs, "Autonomous detection of information patterns through hierarchical peeling," in *Circuit Theory and Design (ECCTD), 2013 European Conference on*, pp. 1–4, IEEE, 2013.

M. RADVÁNYI, "Salient object extraction methods in man-made scenes" in *PhD Proceedings Annual Issues of the Doctoral School, Faculty of Information Technology and Bionics, Pázmány Péter Catholic University 2017.* G. Prószéky, P. Szolgay Eds. Budapest: Pázmány University ePress, 2017, pp 42– 42.

FPGA based on-board horizon detection for UAV

LEVENTE MÁRK SÁNTHA
(Supervisor: ZOLTÁN NAGY, ÁKOS ZARÁNDY)
Pázmány Péter Catholic University, Faculty of Information Technology and Bionics
50/a Práter street, 1083 Budapest, Hungary
santha.levente.mark@itk.ppke.hu

***Abstract*—We introduce the FPGA implementation of a previously developed fast horizon detection algorithm in this paper. The algorithm is suited for visual applications in airborne environment, that is on-board a small-size unmanned aircraft. The algorithm was designed to have low complexity, because of the power consumption requirements.**

***Keywords*-UAS, UAV, Horizon, Visual, Camera, FPGA, Sense-and-Avoid**

I. FPGA IMPLEMENTATION

The theoretical basics of the horizon detection algorithm was introduced in our previous work [1]. Now I focus only on the FPGA implementation. The detected horizon is used in the SAA task to separate the ground and sky regions on the image plane. It is crucial in our case as different strategies are used at the sky and at the non-sky regions to detect the intruder [2].

We used High Level Synthesis techniques for the realization. High Level Synthesis (HLS) uses C/C++ sources to generate Hardware Description Language (HDL) sources. From these HDL files the development environment also can generate the bitstream, which can be download to the FPGA. Using High Level Synthesis has the benefit, that our previously developed C/C++ code, can be reused.

A. Pre-calculation

Figure 1 shows the block diagram of the pre-calculation submodule. Firstly we calculate the Trigonometric functions of the Euler angles provided by the Attitude Heading Reference System (AHRS) of the aeroplane. The result is written in Rot1 or Rot2 memory, which work as a ping-pong buffer. As the result is available in one of the memory, the system starts the matrix multiplication. The transformation matrix from the Body frame to the Camera frame depends only constants, thus we can calculate it offline. These transformation matrix is stored in a ROM and in the first step these matrix is the other element of the multiplication. The design is pipelined, therefor during the matrix multiplication the system calculates another trigonometric function. When the transformation matrix from the earth frame to the camera frame is calculated, the system writes it to a memory module. Than we transform the normal vector of the "pre-horizon" and one point of the "pre-horizon" line in parallel.

B. Post-calculation

Figure 2 shows the block diagram of the post-calculation sub-module. Based on the normal vector we can determine which edges, parts of the picture intersects the pre-horizon. And than we can calculate the end points of the pre-horizon. After this, the system checks, if the horizon line exits or not on the picture. If yes it calculates the base sample point and than the main cycle is started. The rotation angle values

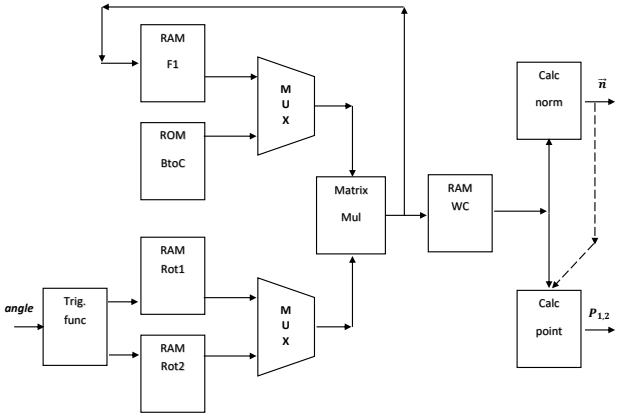

Fig. 1. Pre-calculation block diagram.

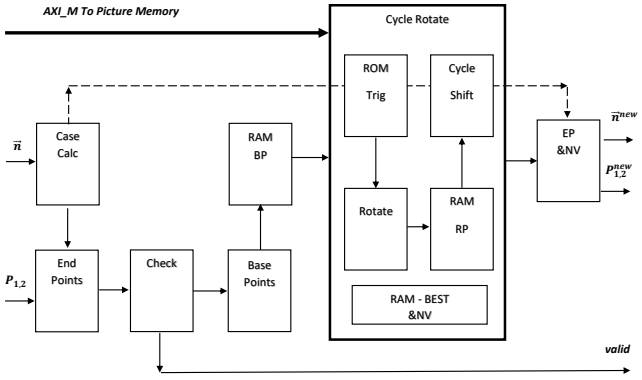

Fig. 2. Post-calculation block diagram.

are constants, therefor we can calculate they trigonometric function offline. We store these values in a ROM. The cycle is also pipelined. When we determinate the coordinates of a sample pair, pair means where we measure the intensity difference, we start to read the values of these pair from the memory, and in parallel we start to calculate the coordinates of an other sample pair. After the whole Cycle is ended, we calculate the post horizon endpoints on the picture end than we return it to the Sense and Avoid System (SAS).

REFERENCES

[1] A. Hiba, T. Zsedrovits, P. Bauer, and A. Zarandy, *Fast horizon detection for airborne visual systems*, 2016 International Conference on Unmanned Aircraft Systems (ICUAS) pp. 886–891 2016,

[2] T. Zsedrovits, P. Peter, P. Bauer, B. J. M. Pencz, A. Hiba, I. Gozse, M. Kisantal, M. Nemeth, Z. Nagy, B. Vanek, A. Zarándy, and J. Bokor, *Feature article: onboard visual sense and avoid system for small aircraft*, IEEE Aerosp. Electron. Syst. Mag., vol. 31, no. 9, pp. 18–27, Sep. 2016.

L. SÁNTHA, "FPGA based on-board horizon detection for UAV" in *PhD Proceedings Annual Issues of the Doctoral School, Faculty of Information Technology and Bionics, Pázmány Péter Catholic University 2017.* G. Prószéky, P. Szolgay Eds. Budapest: Pázmány University ePress, 2017, pp 43– 43.

Using soft-threshold in the Global Statistical and Principal Projected Edge Descriptor

Attila STUBENDEK
(Supervisor: Kristóf KARACS, Péter SZOLGAY)
Pázmány Péter Catholic University, Faculty of Information Technology and Bionics
50/a Práter street, 1083 Budapest, Hungary
stubendek.attila@itk.ppke.hu

***Abstract*—A feature-extraction is considered to be reliable if it generates the same feature on every architectures. Using hard-thresholding in feature-generation might provide distant features from near or even same inputs. In our research we investigated using soft-thresholding methods in the GSPPED feature generation. We compared results based on classification performance.**

***Keywords*-soft-thresholding; thresholding; shape recognition**

I. Introduction

The Global Statistical and Principal Projected Edge Descriptor (GSPPED) is a combined shape descriptor. [1] The GSPPED employs global statistical features and local edge characteristics by principal edge descriptors based on the PPED algorithm. [2]

Edge maps are computed in four directions, and dominant edges are extracted, then projected and concatenated to a 64-long feature vector. (see Figure 1).

II. Thresholding edge maps

Thresholding is employed with a global threshold of $g = 2$ for all the edge map values, and the principal edge value is selected by thresholding for all pixel locations as well.

$$hth_m(x) = \begin{cases} 0, & \text{if } x < m \\ x, & \text{if } x >= m \end{cases}$$

Due to its incontinuity, hard-thresholding $hth(x)$ (see Figure 2) may provide arbitrary output near the threshold value. Different architectures represent and compares floating numbers differently, resulting unambiguous results when using hard-thresholding. In our research an alternative soft-thresholding method is presented. We showed that employing soft-thresholding does not cause decrease in classification performance, but a slight increase can be achieved both in recall and in precision.

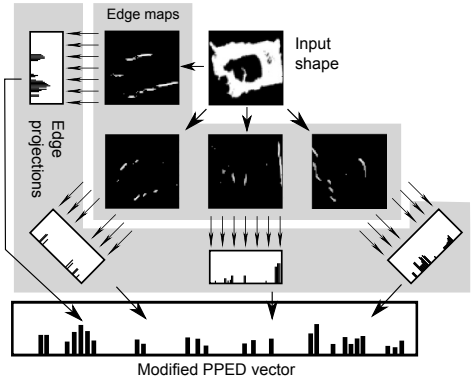

Fig. 1. The input shape is rotated, then edge maps are computed in four direction by convolution. In each coordinate the edge values are thresholded to a global threshold and to the maximum edge value in that coordinate. Finally edge values are projected and concatenated.

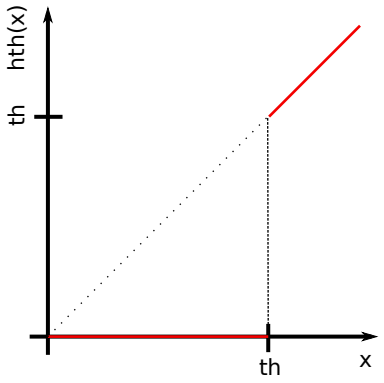

Fig. 2. The hard-threshold function

References

[1] A. Stubendek, K. Karacs, T. Roska, *Shape Description Based on Projected Edges and Global Statistical Features*, International Symposium on Nonlinear Theory and its Applications (NOLTA 2014), Luzern, Switzerland 2014.

[2] M. Yagi, T. Shibata, *An Image Representation Algorithm Compatible with Neural-Associative-Processor-Based Hardware Recognition Systems*, IEEE Trans. Neural Networks, Vol. 14, No. 5, pp. 1144-1161, 2003.

[3] D. Zhang, G. Lu, *Review of shape representation and description techniques*, Pattern Recognition 37, pp.1 – 19, 2004.

[4] S.A. Dubani, K.J. Breeding, R.B. McGhee, *Aircraft identification by moment invariants"*, IEEE Transactions on Computers, C-26:39-46, 1977.

[5] l.Gupta, M.D. Srinath, *Contour sequence moments for the classification of closed planar shapes*, Pattern Recognition, 20(3) p. 267-272, 1987.

[6] E. R. Davies, *Machine Vision: Theory, Algorithms, Practicalities*, Academic Press, New York, p. 171–191, 1997.

[7] P.J. van Otterloo, *A Contour-Oriented Approach to Shape Analysis*, Prentice-Hall International (UK) Ltd, Englewood Cliffs, NJ p. 90 –108, 1991.

[8] A.C. Evans, N.A. Thacker, J.E.W. Mayhew, *Pairwise representation of shape*, Proceedings of the 11th IAPR International Conference on Pattern Recognition, vol. 1, Hague, Netherlands, p. 133-136, 1992.

[9] H. Asada, M. Brandy, *The curvature primal sketch*, IEEE Transactions on Pattern Analysis and Machine Intelligence 8 (1), p. 2–14., 1986.

[10] G. Eichmann, et al., *Shape representation by Gabor expansion*, Hybrid Image and Signal Processing II, SPIE Vol. 1297, Orlando, Florida, USA, pp. 86 –94, 1990.

[11] Q.M. Tieng, W.W. Boles, *Recognition of 2D object contours using the wavelet transform zero-crossing representation*, IEEE Trans. Pattern Anal. Mach. Intell. 19 (8), pp. 910-916, 1997.

[12] H. Freeman, *On the encoding of arbitrary geometric configurations*, IRE Trans. Electronic Computers EC-10, p. 260–268, 1961.

[13] W.I. Groskey, R. Mehrotra, *Index-based object recognition in pictorial data management*, Computer Vision Graphics Image Process. 52, p. 416–436., 1990.

A. STUBENDEK, "Using soft-threshold in the Global Statistical andPrincipal Projected Edge Descriptor" in *PhD Proceedings Annual Issues of the Doctoral School, Faculty of Information Technology and Bionics, Pázmány Péter Catholic University 2017.* G. Prószéky, P. Szolgay Eds. Budapest: Pázmány University ePress, 2017, pp 44– 44.

PROGRAM 3
FEASIBILITY OF ELECTRONIC AND OPTICAL DEVICES, MOLECULAR AND NANOTECHNOLOGIES, NANO-ARCHITECTURES, NANOBIONIC DIAGNOSTIC AND THERAPEUTIC TOOLS

Head: Árpád CSURGAY

A Review of Skin Cancer Diagnosis

Gergely CSÁNY
(Supervisor: Miklós GYÖNGY PhD)
Pázmány Péter Catholic University, Faculty of Information Technology and Bionics
50/a Práter street, 1083 Budapest, Hungary
csany.gergely@itk.ppke.hu

***Abstract*—Skin cancer is one of the most frequent types of cancer worldwide. Melanoma maligna is responsible for the vast majority of all skin cancer deaths. Early and accurate melanoma diagnosis is a crucial problem to be solved. In this article, a short review is presented of the diagnostic methods currently used or being under investigation.**

***Keywords*-diagnosis; dermatology; melanoma; skin cancer**

I. Introduction

Skin cancer is the most common type of cancer in the United Sates [1] and the third most frequent in Hungary [2]. Melanoma (a type of skin cancer) accounts for 65% of all skin cancer deaths [3]. Prevention, early detection, adequate treatment (primarily surgical excision) and sufficient follow-up of this cancer play a crucial role in the prognosis and survival of patients [3].

II. Skin cancer Diagnosis

A. Invasive methods for skin examination

Histology is the gold standard diagnostic method currently, with advantages of diagnostic accuracy and ability to predict prognosis. Disadvantages: it is rather time-consuming, requires professional competence, is invasive (involving risk of infections) and sampling method (biopsy) also requires competence.

Whereas histopathology is an invasive and time-consuming method, non-invasive, cost- and time-efficient examination methods also appeared in the field of skin cancer diagnostics to assist diagnosis and to make it more widely accessible.

B. Non-invasive methods for skin examination

Non-invasive skin examination methods have the common goal of reducing the number of unnecessary biopsies. Some of them are also very useful for assigning the margin for excision before surgical treatment of lesions to be removed.

1) Dermoscopy: A dermoscope basically is a hand-held, lighted magnifier for skin examination. Dermoscopy improved the sensitivity and specificity of clinical melanoma diagnosis from 71% to 90% (by almost 20%) [4]. Advantages of dermatoscopy are its non-invasiveness, cost- and time-effectiveness. Drawbacks include dependence on the experience of the clinician in performance (up to about 20% difference in sensitivity), less accuracy compared to histology and loss of depth and inner structure information.

2) Confocal Laser Scanning Microscopy (CLSM): The greatest advantage of CLSM is its high resolution (good observability of morphological features and microanatomical structures [3]). Some drawbacks are small penetration depth, hazard of artefacts and a relatively long examination time.

3) Optical Coherence Tomography (OCT): OCT provides a good resolution and penetration depth. However, it is very sensitive to artefacts and to attenuation having a relatively high inter-patient variability [5].

4) Magnetic Resonance Imaging: MRI is yet only used experimentally for examination of skin diseases, providing high-quality images of the diseases, being useful in education and in determining precise lesion location for surgical planning.

5) Tape Stripping mRNA: Using an adhesive tape, mRNA sample can be collected from a lesion and genetic information can be acquired from it. A classifier examining a set of 20 genes distincted melanoma from atypical nevi with 100% sensitivity and 90.6% specificity [3].

6) Electrical Bioimpedance: Portable and cost-effective impedance-measuring device show promising results in sensitivity (92–100%) and specificity (67–80%), however, standardization of the results is still required [3].

7) Ultrasound (US): Large field of view, large penetration depth, cost-effectiveness, easy handling and low biological risk are advantages of US systems for skin examination. Drawbacks are its limited, relatively low resolution and dependence on examiner experience [6]. US *imaging* realizes examination of vertical penetration of lesions, measuring extension of lesions, examining the acoustic structure of lesions and detecting possible recurrences. *Color Doppler* is an approach to visualize tumor vasculature (being in context with prognosis).US *elastography* is a useful assisting tool in differential diagnosis, exploiting the fact of malignant lesions generally being less compressible than healthy tissue.

III. Conclusions

As presented above, a wide variety of tools and methods provide possibilities for early stage skin cancer diagnosis. Results of histology are still treated as the ”gold standard”, however, many more approaches exist to assist diagnosis, having the great advantages of being time- and cost-effective and non-invasive. These methods also help selection of lesions getting into the phase of histological examination.

References

[1] Guy GP, Thomas CC, Thompson T, Watson M, Massetti GM, Richardson LC, *Vital signs: Melanoma incidence and mortality trends and projections—United States, 1982–2030*, MMWR Morb Mortal Wkly Rep., vol. 64, no. 21, pp. 591–596, 2015.

[2] Tompa Anna, *A daganatos betegségek elöfordulása, a hazai és a nemzetközi helyzet ismertetése*, Magyar Tudomány, 2011. http://www.matud.iif.hu/2011/11/06.htm

[3] Darrell S. Rigel, Julie Russak, Robert Friedman, *The Evolution of Melanoma Diagnosis: 25 Years Beyond the ABCDs*, CA Cancer J Clin, Published Online: July 28, 2010 (10.3322/caac.20074), 2010.

[4] M. E. Vestergaard, P. Macaskill, P. E. Holt, S. W. Menzies, *Dermoscopy compared with naked eye examination for the diagnosis of primary melanoma: a meta-analysis of studies performed in clinical setting*, Br. J. Dermatol., vol. 159, pp. 669–676, 2008.

[5] C. Wassef, B. Rao, *Uses of non-invasive imaging in the diagnosis of skin cancer: an overview of the currently available modalities*, International Journal of Dermatology, vol. 52, no. 12, pp. 1481–1489, 2013.

[6] M. Koehler, S. Lange-Asschenfeldt, M. Kaatz, *Non-invasive imaging techniques in the diagnosis of skin diseases*, Expert Opinion on Medical Diagnostics, vol. 5, no. 5, pp. 425–440, 2011.

G. CSÁNY, “A Review of Skin Cancer Diagnosis” in *PhD Proceedings Annual Issues of the Doctoral School, Faculty of Information Technology and Bionics, Pázmány Péter Catholic University 2017.* G. Prószéky, P. Szolgay Eds. Budapest: Pázmány University ePress, 2017, pp 46– 46.

A review of ultrasound phantom manufacturing methods

Krisztián FÜZESI
(Supervisor: Dr. Miklós GYÖNGY)
Pázmány Péter Catholic University, Faculty of Information Technology and Bionics
50/a Práter street, 1083 Budapest, Hungary
fuzesi.krisztian@itk.ppke.hu

I. Introduction

The purpose of ultrasound phantoms are to mimic acoustic properties of tissues. They and useful tools for quality assurance of ultrasound systems, moreover also used during development of novel imaging techniques or ultrasound imaging equipment. In some applications, like the training of radiologists, it is required to mimic the structure of tissues as well.

The three most relevant acoustic properties to be achieved are longitudinal propagation speed of sound, attenuation of sound and characteristic acoustic impedance. The typically required value for these are $1540m/s, 0.3-1.1dB/cm/MHz$ and 1.62 MRayl respectively.

There are several traditionally used materials and methods available to create phantoms. Nowadays a plethora of commercial phantoms are available as well, however their disadvantage is the high price and the lack of customization.

II. Methods

Using conventional materials and methods for phantom manufacture are appropriate to mimic (some) acoustic properties of soft tissues, however construction of scatterers at arbitrary locations with desired intensity is lacking. Using thin threads of fishing line or other scattering material give limitations in the amount of scatterers, precision of placing and reproducibility, as these are usually handmade phantoms. The following techniques at subsections A and B are used to overcome these issues. Subsection A is based on our previous publication, and C is based on our abstract submitted to IEEE $IUS2017$ conference.

A. Filament deposition modelling (FDM) and Digital light processing (DLP) printing

Firstly, an FDM printer was tested using 1.75 mm round diameter filaments made of polylactic acid and acrylonitrile butadiene styrene. After acoustic characterization only PLA and ABS were used for FDM filament phantoms. A pattern of 10mm long filaments showing 'ITK' was created between two supporting wall.

DLP printing using UV-sensitive photopolymer and an UV-light emitting projector was also tested.

B. Photopolymer jetting (PPJ) printing

This type of printing is more expensive than FDM or DLP methods, however, capable of reaching resolutions below 50 microns. To print phantoms, Objet24 printer from Stratasys (Eden Prairie, MN, USA) was applied, using FC 705 as a propagation medium and VWP as scatterers.

C. 3D phantom validation of superresolution methods

The resolution of ultrasound images is limited by the bandwidth of the imaging system and the features of the propagating medium. Image restoration methods can recover out-of-bandwidth data and improve resolution. An lp-norm-regularized deconvolution for various values of p was tested. Knowledge of the scattering function allowed the comparison of the deconvolved images with the ground truth. The outer frame of scatterers was used to estimate the system PSF h and the full width half maximum (FWHM), while the inner frame was used to calculate the normalized root mean square error (RMSE) of the true scattering function estimates.

III. Results and Discussion

A. FDM and DLP printing

The measured acoustic impedance and speed of sound of the 3D printing materials are in the ranges of 2.15–2.46 MRayl and 1909.1–2244.0 m/s, respectively. For comparison, nylon, a commonly used filament scatterer in commercial phantoms, has corresponding values of 2.90–3.15 MRayl and 2600–2900 m/s.

There appears to be considerable clutter in the US images, especially between the two legs of the letter 'K'. Some of this clutter could be reduced by replacing water as propagation medium with a gel containing an attenuating substance such as aluminum oxide.

B. PPJ printing

The first and most crucial achievement was that an acoustically clear medium could be printed. Then spherical scatterers were printed to form ITK letters with a diameter of 500, 150, 100 and 50 μm to check the resolution of the printer. If placed underwater, a curvature appears on the surface of the phantoms, suggesting the presence of water absorption of the material FC705.

C. 3D phantom validation of superresolution (SR) methods

With the settings used, p=0.5 offers a higher spatial resolution gain than p=2, and also provides a higher estimation accuracy of the SF in terms of RMSE. The results show the benefits of knowing the SF during experimental testing of image restoration methods.

IV. Summary

The results show, that using 3D printing technologies cost effective and highly customizable phantoms can be manufactured. Latest results with PPJ printing shows an experimental method for evaluating the extent to which an image restoration method provides a faithful rendering of the underlying scattering structure.

K. FÜZESI, "A review of ultrasound phantom manufacturing methods" in *PhD Proceedings Annual Issues of the Doctoral School, Faculty of Information Technology and Bionics, Pázmány Péter Catholic University 2017.* G. Prószéky, P. Szolgay Eds. Budapest: Pázmány University ePress, 2017, pp 47– 47.

Applicability of computed tomography methods for tomosynthesis problems

Janka HATVANI
(Supervisor: Miklós GYÖNGY)
Pázmány Péter Catholic University, Faculty of Information Technology and Bionics
50/a Práter street, 1083 Budapest, Hungary
hatvani.janka@itk.ppke.hu

***Abstract*—In the field of X-ray 3D imaging the state of the art solution is the conventional computed tomography (CT). In this setup the detector and the source rotates at least in 180°around the object, obtaining a whole set of projections. The inverse Radon-transform makes it possible to reconstruct the volume from these projections. A solution for decreasing the radiation dose responsible for negative health effects is tomosynthesis. Projections are taken from a limited angle and/or in limited number, leading to ill-posed reconstruction problems. These cases are more sensitive to artifacts, like to noise, thus iterative methods may be used, as regularization terms are easy to incorporate into such formulas. This paper overviews the nowadays used reconstruction algorithms, focusing on the traditional back-projection, the filtered back-projection, and algebraic reconstruction techniques.**

***Keywords*-tomography; tomosynthesis; radiation dose; BP; FBP; ART; SIRT; DART; iterative methods**

I. Introduction

For lowering the damaging ionizing effects of CT a possible technique is the so called tomosynthesis. In this case less projections will be acquired compared to the custom CT imaging, so the effective dose can be decreased.

The mathematical descriptor of the imaging process is the Radon-transform. The line integral of the density function f along the line perpendicular to the projection axis equals the value at the measurement point.

II. Reconstruction algorithms

The reconstruction algorithms can be divided into two main classes: one for the analytic and the other for the algebraic methods. The first one provides an exact mathematical solution, working with continuous data. The letter group assumes fully discretised datasets and solves a system of linear equations. The strength of the iterative methods opposed to analytic techniques is their flexibility, making prior knowledge easy to be incorporated into the algorithm. Such a property can be non-negativity, thresholds on the values, predefined discrete attenuation levels or sparsity.

The basic concept of analytic or direct methods is to simply back-project (BP) the measured values onto the imaging volume. In the filtered back projection (FBP) the Ram-Lak filter is used to suppress high-frequency components.

The algebraic methods use fully discretised datasets. The transform is written in the form of a system of linear equations. The algorithms iteratively update the unknown coefficients of the unknown attenuation function by minimizing the difference between the measured and calculated detector values. Algebraic reconstruction technique (ART or ARM), simultaneous algebraic reconstruction technique (SART) and simultaneous iterative reconstruction technique (SIRT) differ in their updating frequency. ART updates after processing a single detector element, converging fast but amplifying the noise. SIRT, on the other side can over-smooth the output with slow convergence. DART constrains SIRT with predefined discrete attenuation levels.

III. Method

In this paper BP, FBP, ART, SIRT and DART (using SIRT) were studied. As ART and SIRT in their native form gave very similar results to the FBP, the iterative algorithms were enhanced with the minimum and maximum constrains.

For experimentally comparing the different reconstruction methods, ASTRA toolbox [1][2] was used in MATLAB ((MATLAB 12.b, The MathWorks Inc., Natick, MA, 2012)) framework. The algorithms were evaluated on the Shepp-Logan phantom.

The projections were simulated with parallel forward projection, using 256 detector elements. One tested parameter was the noise level (-40 dB SNR for low noise, -10 dB for high noise rate), the other was the view (-80°/+80°for high angle and -30°/+30°for limited view) with a step-size of 1°. Iterative algorithms ran with 50 loops. DART was implemented using 5 discrete levels.

IV. Results and Discussion

It has been shown, that iterative algorithms are promising because of their flexibility in terms of incorporating a priori knowledge into the model. Agreeing with the literature, even with minor assumptions, as non-negativity, better contrasted images might be acquired. The distortion artifact in the limited-view setup might be corrected with DART, where discrete levels of attenuation are preset. However, noise introduces severe reconstruction errors. In runtime BP is the fastest, FBP and SIRT are 2 orders of magnitude slower, while DART and ART are two further orders slower.

The aim of this paper was to overview the presently used main techniques, to support future researches of CT reconstruction algorithms with emphasis on sparsity-based models.

References

[1] W. van Aarle, W. J. Palenstijn, J. Cant, E. Janssens, F. Bleichrodt, D. B. J. Dabravolski, A., K. J. Batenburg, and J. Sijbers, "Fast and flexible x-ray tomography using the astra toolbox," *Optics Express*, vol. 24, no. 22, pp. 25129–25147, 2016.

[2] W. van Aarle, W. J. Palenstijn, J. De Beenhouwer, T. Altantzis, S. Bals, K. J. Batenburg, and J. Sijbers, "The astra toolbox: A platform for advanced algorithm development in electron tomography," *Ultramicroscopy*, vol. 157, pp. 35–47, 2015.

J. HATVANI, "Applicability of computed tomography methods for tomosynthesis problems" in *PhD Proceedings Annual Issues of the Doctoral School, Faculty of Information Technology and Bionics, Pázmány Péter Catholic University 2017.* G. Prószéky, P. Szolgay Eds. Budapest: Pázmány University ePress, 2017, pp 48– 48.

Design of a rapid scanning acoustic microscope platform for super-resolution research

Ákos MAKRA
(Supervisor: Miklós GYÖNGY)
Pázmány Péter Catholic University, Faculty of Information Technology and Bionics
50/a Práter street, 1083 Budapest, Hungary
makra.akos@itk.ppke.hu

Statement of originality: This report describes the work of the doctoral student during the educational years of 2015 – 2017. Parts of the work are based on the master's thesis of the doctoral student and a poster presented under the title of "Towards a Quantified Comparison of Acoustical and Optical Microscope Images" at the From Medicine to Bionics Conference, Budapest (2016).

***Abstract*—Imaging modalities of any kind have a theoretical limit on their feasible resolution. The objective of a super-resolution algorithm is to break this boundary obtaining a higher quality image with the same hardware. Scanning acoustic microscopy is a technique where high resolution volumetric images can be recorded in a non-invasive way by detecting reflected ultrasound signals. This work describes the development of such a device and its relevancy in super-resolution research.**

***Keywords*-super-resolution; SAM; microscopy**

I. Introduction

The demand to create images of higher resolution has never been greater than it is nowadays. Speaking of security cameras, satellites or professional photography the image quality becomes better and better every year. The same rule applies for medical images: the need is real for more detailed images. The more detail an images has, the more accurate diagnosis can be established based on that.

There are two different ways to enhance the image: by developing a better hardware and achieve greater resolution or by an algorithm. The algorithm can be used either real-time or as a post-processing step. The use of SR techniques provides the possibility of receiving a more detailed image at a lower cost compared to building a new hardware capable of delivering the same quality.

Scanning acoustic microscopy (SAM) is a technique where high resolution volumetric images can be acquired in a non-invasive way. By scanning the area continuously in a raster pattern a high field of view can be imaged. The higher the frequency, the smaller the penetration depth is) [1, p. 116]. The image resolution and signal-to-noise quality could be improved by SR algorithms on lower frequencies.

II. SAM system

A SAM system usually consists of the following parts: a computer, a micropositioner system (MPS), an impulse generator connected to the transducer and a device responsible for recording the back-scattered signal. The pulser is capable of generating short impulses with high energy, which will be converted into an US wave due to the inverse piezoelectric effect. The reflected wave will be detected and converted back to an electric impulse by the transducer, furthermore, recorded by the data acquisitioner, then, the transducer will be moved to the next position by the MPS and repeat this process.

III. Algorithmic Overview

Development of the data acquisition program was developed in Labview (National Instruments, 2010 SP1). All the devices can be controlled via the Labview environment. The scanning is carried out in a non-raster pattern for securing better precision. With continuous motor movement measurement points are recorded along a grid. When the endpoint is reached, the motor is homed, starting the next acquisition in the same direction.

IV. Results and discussion

A SAM system was developed which is suitable for recording volumetric data via US in a non-invasive way. A scan with a field of view of 1 cm x 1 cm (having 50 μm between data points in both directions) can be finished in approximately 30 minutes. The transducers which can be housed have a nominal central frequency of 35 MHz and 75 MHz, respectively. By the establishment of such a system, it opens the way towards being able to acquire 3D data with a high field of view. In regard to the relatively low frequencies used, a bigger penetration depth can be achieved, yielding data from bigger depths, however, at a cost of having lower resolution. By using SR algorithms to increase the resolution, the same resolution can be achieved as of higher frequencies, however, at bigger depths, which could not be achieved otherwise. Furthermore, using higher frequencies such as 1 GHz (where the inner cell structure can be seen with a resolution of approximately 1 μm) and by analyzing the images we can have a deeper understanding of what kind of assumptions should be used to be able to use SR algorithms on relatively lower frequencies (where the inner structure of the cell cannot be seen) to achieve the same resolution as of the higher frequencies.

References

[1] Thomas L. Szabo, *Diagnostic ultrasound imaging*. Elsevier Academic Press, 2004.

Á. MAKRA, "Design of a rapid scanning acoustic microscope platform for super-resolution research" in *PhD Proceedings Annual Issues of the Doctoral School, Faculty of Information Technology and Bionics, Pázmány Péter Catholic University 2017.* G. Prószéky, P. Szolgay Eds. Budapest: Pázmány University ePress, 2017, pp 49– 49.

Investigation of hippocampal dendritic signals with two-photon microscopy

Zsolt MEZRICZKY
(Supervisor: Balázs RÓZSA)
Pázmány Péter Catholic University, Faculty of Information Technology and Bionics
50/a Práter street, 1083 Budapest, Hungary
mezriczky.zsolt@itk.ppke.hu

Place cells (PCs) – with grid cells, border cells and head direction cells [1] - are the spatial navigation system of the brain. PCs were discovered by O'Keefe and Dostrovsky based on their electrophysiological work [2]. Later O'Keefe was awarded by Nobel prize with his work in this field. PCs are active in a certain point of the environment, called place field. They are located in the mammalian hippocampus CA1 pyramidal layer [2]. O'keefe later mentioned, that may the hippocampus is a cognitive map for spatial memory [3].

In early works PCs were examined with single unit recordings in vivo. Neverthless it has many disadvantage compared to the imaging for instance in characterization the genetically identified specific cells, recording the intracellular detailed particles of a neuron, distinguishing the PCs with overlapping place field or investigating the whole dendritic branch simultaneously.The optical examinations can give a high enough spatial resolution to solve the problems. Ca2+ imaging combined with two-photon (2P) laser scanning microscopy is capable to dissolve this problems [4] and also suitable for dendritic measurements [5].

With Ca2+ imaging technique we can observe the activity of cells concluded from the changed level of the intracellular Ca2+. The technique needed special Ca2+ sensors to detect difference between the active and inactive cells. Genetically encoded calcium indicators (GECIs) are the most useful for in vivo measurements [7]. It has an other advantage: with the help of the GECIs and the modern biotechnological techniques the immunologically different cell populations can be marked with a suitable sensor.

Ca2+ imaging technique combined with 2P laser scanning microscopy are useful tools to eliminate the disadvantages of the electrophysiological recordings [5]. The high resolution allows the observation the subcellular parts of the neuron as the dendrites and the belonging spines [8] or the axons and their boutons [9] in vivo. In vivo Ca2+ imaging with is widely used in this field, but needed special behaviour apparatus. The head-fixed mice can run in a linear [7] with tactile or olfactory stimuli; or spherical treadmill with virtual reality (VR) system [4].

The activity of PCs relatively easy detect in a somatic level in two dimension, but there is no evidence about the role of their dendritic activity. The questions arise, how the information integrate in dendritic level and how the dendritic activity modulate the input information in PCs in vivo. I our work we would investigate the activity of PC's dendrites in vivo. Perhaps the examinations give us the answer, how the PCs encode and modulate their input information in a dendritic level. The three-dimensional measurements allow to investigate the connections of the PCs for instance in the entorhinal cortex.

I. MATERIAL AND METHODS

Our experiment will execute on recombinant adeno-associated virus injected adult mice. The virus contains GCaMP6f calcium sensor, which is controlled under CaMKII promoter. The viral injection will perform in the pyramidal layer of hippocampal CA1 area.

Two weeks after the injection the mice will surgically implanted with a chronic imaging window and with a steel head plate. Head plate holds mice's head in a fix position during the measurements and the behavioural task. After the surgery the animals needs two or three weeks long training sessions to learn how behave in the setup. In the behaviour apparat will consist in linear or a spherical treadmill. The advantages and disadvantages are already described above.

We will use Ca2+ imaging combined with 2p laser microscopy with dual scanner heads (galvo and resonant) to the two-dimensional imaging and acousto-optic microscopy to the three-dimensional measurements to visualize the dendrites of PC. In our work we would investigate the dendritic activity of a PC in vivo in mice with 2P microscopies. Perhaps the activity of PCs is only the result of a complex regulation of their input segments and dendrites have a precise integrative and modulation role in the navigation.

REFERENCES

[1] Moser EI, Kropff E, Moser MB. Place cells, grid cells, and the brain's spatial representation system. 2008. Annu Rev Neurosci. ;31:69-89
[2] O'Keefe J, Dostrovsky J. 1971. The hippocampus as a spatial map. Preliminary evidence from unit activity in the freely-moving rat. Brain Res 34:171–175
[3] O'Keefe J, Nadel L. (1978). The Hippocampus as a Cognitive Map. Oxford University Press, Oxford, UK
[4] Dombeck DA, Harvey CD, Tian L, Looger LL, Tank DW. 2010. Functional imaging of hippocampal place cells at cellular resolution during virtual navigation. Nat Neurosci. 13(11):1433-40
[5] Grienberger C, Chen X, Konnerth A. 2015. Dendritic function in vivo. Trends Neurosci. 38(1):45-54
[6] Danielson NB, Zaremba JD, Kaifosh P, Bowler J, Ladow M, Losonczy A. Sublayer-Specific Coding Dynamics during Spatial Navigation and Learning in Hippocampal Area CA1. Neuron 91:1-14
[7] Tian L, Akerboom J, Schreiter ER, Looger LL. Neural activity imaging with genetically encoded calcium indicators. 2012. Prog Brain Res. 196:79-94
[8] Chiovini B, Turi GF, Katona G, Kaszás A, Pálfi D, Maák P, Szalay G, Szabó MF, Szabó G, Szadai Z, Káli S, Rózsa B. Dendritic spikes induce ripples in parvalbumin interneurons during hippocampal sharp waves. 2014. Neuron. 82(4):908-24
[9] Surjeet Mastwal, Yizhou Ye, Ming Ren, Dennisse V. Jimenez, Keri Martinowich, Charles R. Gerfen, and Kuan Hong Wang. Phasic Dopamine Neuron Activity Elicits Unique Mesofrontal Plasticity in Adolescence. 2014. J Neurosci. 34(29): 9484–9496.

Zs. MEZRICZKY, "Investigation of hippocampal dendritic signals with two-photon microscopy " in *PhD Proceedings Annual Issues of the Doctoral School, Faculty of Information Technology and Bionics, Pázmány Péter Catholic University 2017.* G. Prószéky, P. Szolgay Eds. Budapest: Pázmány University ePress, 2017, pp 50– 50.

PROGRAM 5
ON-BOARD ADVANCED DRIVER ASSISTANCE SYSTEMS

Head: Csaba REKECZKY

Phantom object removing using a 3D CNN approach

Balázs Nagy
(Supervisor: Csaba Benedek)
Pázmány Péter Catholic University, Faculty of Information Technology and Bionics
50/a Práter street, 1083 Budapest, Hungary
nagy.balazs@itk.ppke.hu

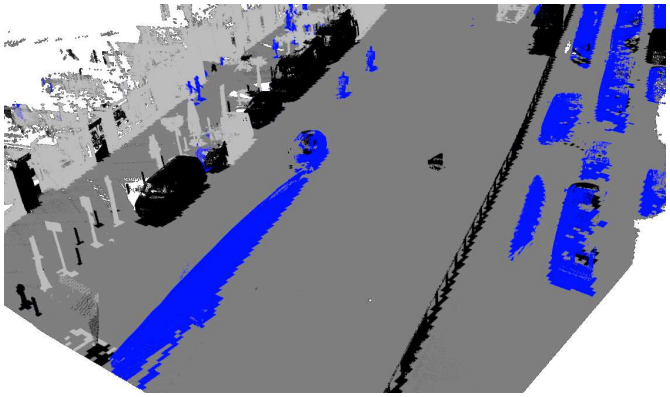

Fig. 1. Segmentation result of the 3D CNN based labeling. The color code of the predicted pillars is the following: dark grey denotes to ground, light grey marks high objects, black color is assigned to short objects and blue represents the phantom objects.

***Abstract*—In this paper we introduce a new deep learning based approach to detect and remove phantom objects from point clouds produced by mobile laser scanning (MLS) systems. The phantoms are caused by the presence of scene objects moving concurrently with the MLS platform, and appear as long, sparse but irregular point cloud segments in the measurements. We propose a new 3D CNN framework working on a voxelized column-grid to identify the phantom regions. We quantitatively evaluate the proposed model on real MLS test data, and compare it to two different reference approaches.**

***Keywords*-deep learning, 3D computer vision**

I. Introduction

Due to the sequential nature of the environment scanning process, scene objects moving concurrently with the MLS platform (such as passing vehicles and walking pedestrians) appear as phantom-like long-drawn, distorted structures in the resulting point clouds. Finding phantom regions is very challenging, since their geometric and structural properties are often very similar to real objects. Moreover, moving objects may travel at varying speed, accelerating and breaking during the observation (for example stopping in front of a traffic light), so the densities and the characteristics of the phantoms are also significantly varying.

Considering the above detailed complexity of the phantom detection task, we propose a neural network (CNN) based approach to tackle the problem.

II. 3D CNN architecture and the training process

We train our network with 3D voxelized data, thus we built a 3D CNN classifier. Applying the convolution or pooling operators the size of the output layer is reduced as a function of the size of the operator kernel. We added three 3D convolution layers to the network with $3 \times 3 \times 3$ kernels and we applied max-pooling ($2 \times 2 \times 2$ kernels) and dropout layers between the convolution layers.

To avoid overfitting, during the first dropout we drop the half of the connections, thereafter the second dropout layer eliminates the 25% of the edges. To optimize and update the network parameters we use a Stochastic Gradient Descent (SGD) algorithm, and we also decrease the learning rate from training epoch to epoch according to the following strategy: $learning\_rate = learning\_rate/number\_of\_epochs$. After each convolution layer we use ReLu activation function and the output of the network is activated with Softmax function. The CNN training step uses a k-fold cross validation ($k = 5$) based on the training data.

TABLE I
Evaluation results of the proposed 3D CNN method, featuring the precision, recall and F-measure rates w.r.t. the different classes

Class	Precision [%]	Recall [%]	F-measure [%]
Short obj.	86.5	92.6	89.5
High obj.	98.1	93.2	95.6
Phantom	90.0	88.5	89.3
Ground	99.7	98.6	99.2
Overall	91.5	91.4	91.5

III. Test and result

We tested the proposed 3D CNN framework in various MLS point cloud segments, without any overlap with the training areas. For the quantitative tests, we manually labeled 39077 pillars from the test set, which labels were used as Ground Truth during the evaluation. Quantitative detection results for the whole test set are provided in Table I.

IV. Conclusion

We proposed a new 3D CNN based approach to label the scene and find phantom regions and we showed that our approach is able to robustly detect phantom regions, meanwhile it segments the scene into four different semantic classes.

The authors would like to thank Budapest Közút Zrt (Road Management Department) for the provision of the Riegl VMX-450 MLS test data. This work was supported by the János Bolyai Research Scholarship of the Hungarian Academy of Sciences and by the National Research, Development and Innovation Fund (NKFIA K_120233).

B. NAGY, "Phantom object removing using a 3D CNN approach" in *PhD Proceedings Annual Issues of the Doctoral School, Faculty of Information Technology and Bionics, Pázmány Péter Catholic University 2017.* G. Prószéky, P. Szolgay Eds. Budapest: Pázmány University ePress, 2017, pp 52– 52.

Detection of adversarial attacks using consistency constraints

András Horváth, Csanád Egervári and Csaba Rekeczky
Faculty of Information Technology and Bionics, Pázmány Péter Catholic University

Abstract—Adversarial examples revealed and important aspect of convolutional neural networks an are getting more and more attention in machine learning. It was shown that not only small perturbations, covering the whole image can be applied but also sticker based attacks, concentrated on small regions of the image can cause misclassification. Meanwhile the first type of attack is theoretical the later can be applied in practice and lead to misclassification in image processing pipelines. In this paper we show a method how sticker based adversarial samples can be detected by estimating the measure of region based classification consistency

I. Adversarial attacks

Deep learning and the training of deep neural networks enabled the solution of problems which were not solvable before. These methods are trained in a supervised manner calculating gradients of an objective function and minimizing loss on a training set. It was shown in [1] that the exploitation of these gradients gives possibility of adversarial attacks. Since the generalization of the network is based on a dataset and the input data is extremely high dimensional there are always possible perturbations left in the system, which can be exploited and could result in misclassification by applying small changes on the original input image. The classification result of the network can be changed by small perturbations which qualitatively does not change the outlook of the image (without altering the human perception of the input), meanwhilethe quantitative output of the network is changed completely.

A. Global, low-amplitude, additive noise generation

In most cases adversarial noise and adversarial samples are generated as an additive noise which is added to the original input image and causes misclassification. This method was introduced in [1] and requires the prior knowledge of the network and the method assumes that the attacker has access to the gradients of the neural net. We can describe the network as a function: N, which had an Input image: I, as input and generates a distribution of possible output classes (noted by C):

$$C = N(I) \tag{1}$$

Adversarial noise in the sense described by Goodfellow in [1] is the generation of a special small amplitude additive noise (z) which changes the original output class to a new desired distribution:

$$C_d = N(I + z) \tag{2}$$

where C_d is the new modified output distribution, which is previously defined and different than C. The attackers goal is also to preserve the human perception and the noise cannot change the qualitative properties of the image, which means that the noise must have low amplitude: $max(z) < eps$ (eps is usually two orders smaller than the maximum intensity of the input data). The aim is to find a z tensor which minimizes the error between the actual network output and C_d. This is a similar problem as training a network for classification, but in this case our aim is to handle the noise as a variable instead of tuning the network parameters. The optimization can be done applying gradient descent algorithms, like ADAM [2]. An example of a noise which causes misclassification can be seen on Fig 1.

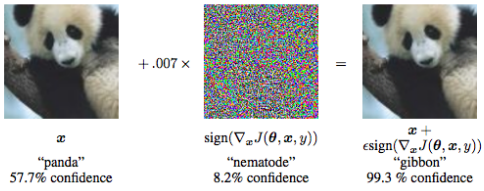

Fig. 1. A Figure demonstrating and adversarial attack, where an attacker knowing a network and selecting one input image can generate a low-amplitude additive noise, which causes the panda image to be classified as the class "gibbon". The image was taken from [1]

B. Sticker based adversarial attack

The previous method does not change the qualitative properties of the input data and affects the whole image. Fortunately this low-amplitude noise is really sensitive to additional noise, like illumination changes, perspective change and other similar alterations. These adversarial samples can be ruined by printing the image or by the noise generated by the image acquisition system (lens and sensory noise). This was already shown in [3] where applying a small random perturbation will neglect the effect of the adversarial attack and the output will usually be the original output class. Later it was shown that the generation of adversarial samples is possible by applying a concentrated structural noise on certain, small areas of the

A. HORVÁTH, Cs. EGERVÁRI, Cs. REKECZKY , "Detection of adversarial attacks using consistency constraints" in *PhD Proceedings Annual Issues of the Doctoral School, Faculty of Information Technology and Bionics, Pázmány Péter Catholic University 2017.* G. Prószéky, P. Szolgay Eds. Budapest: Pázmány University ePress, 2017, pp 53– 55.

image which is more robust to real world perturbations [4] [5]. These attacks are robust enough to cause a stable misclassification in real life applications. These methods apply dark or bright stickers and the optimization method sets the position and size of these stickers, which change the output distribution. In case of k dark stickers and l bright stickers the network output can be given as:

$$C_d = N(I + \sum_{i=1}^{k} St_i(x_i, y_i, w_i, h_i) + \sum_{j=1}^{l} St_j(x_j, y_j, w_j, h_j)) \tag{3}$$

Where a sticker value St_i could be defined as zero values in case of a dark sticker minus the image values at that position, meanwhile a bright sticker can be defined as maximum intensity values minus the image values at the stickers position. The parameters of each sticker: x and y positions and width (w), height (h) has to be optimized for every i and j. The output and result of such and adversarial attack can be seen on Figure 2.

Fig. 2. A sticker based adversarial attack using three dark and three bright stickers on the left ($k = 3$ and$l = 3$) and 2-2 stickers on the right ($k = 2$ and $l = 2$). These perturbations were tested in real life applications and can cause misclassification in various conditions resulting a threat for the application of convolutional networks. The original image was taken from [6].

II. 2. Detection of sticker based attack

Adversarial example generation was tested on the MNIST dataset [7] and the The German Traffic Sign Detection Benchmark (GTSDB) [8].The MNIST dataset is a frequently cited dataset containing 75000 handwritten numbers from 10 different classes one for each digit. The GTSDB contains 900 images of traffic signs in various classes which shows a much more practical application of adversarial attacks, since one of the most popular application of convolutional networks is in the vision system of self driving cars. Example images from these two datasets can be seen in Figure 3. First a four layered convolution network followed by a fully connected layer with 32 features and another fully connected layer for classification was trained on the training set of the MNIST dataset, which reached an accuracy of 92.8% on the independent test set and reached 89.4% on the GTSDB. We have to note that our aim was not the generation of a high accuracy network and adversarial attacks can be performed on the elements of the training set as well. Because of this, adversarial attacks does not depend heavily on network accuracy or on network structure. In the tests 10 000 images from the MNIST dataset and 300 images from the GTSDB were selected, which were all classified correctly by the network. In the test adversarial noise was trained on these images and the task was to find the appropriate additive noise parameters which will result in the misclassification of these images. The desired output class for the attack was selected randomly. Our method tried to place 4 stickers (two dark and two bright ones) to the image at different positions. This method was able to force misclassification on all images from these test sets.

Fig. 3. Example images from the MNIST database (left) and from the GTSDB (right).

Our proposal and a possible method for sticker based attack detection could be the localization of regions which can cause the misclassification of the network. We will show the main idea of this detection method on GTSBD. In case of sticker based attacks only a small region is responsible for the misclassification, while larger regions will not change in the image. Using a method which is usually used for visualization of network decision [9] one can identify which regions are responsible for the classification. Once a classification was done and the network output is known one can generate a mask containing average gray values with a small size (for example a mask of 5x5 pixels, but this size also depends on the size of the input image) and slide this mask through the input image and record a heat-map which denotes the classification probabilities at every position of the mask. If the classification probability drops significantly at a position one can infer that this region is important in the classification and the classification is mainly affected by this region. In case of a normal image the whole object will be responsible for the output class, meanwhile in case of a sticker based adversarial attack mostly the position of the stickers will be responsible for the output class. An example image about this heat-map can be seen on Figure 4.

As it can be seen on Figure 4 the background was not important in the classification process, because classification probability remained high (red values on the heat-map) when this region was masked out. The pixels of

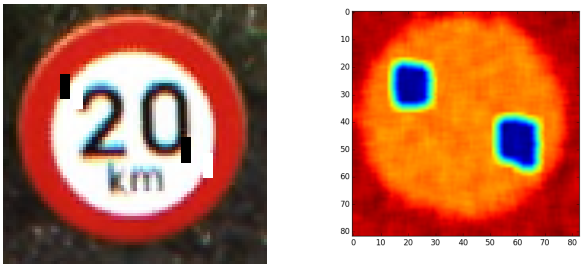

Fig. 4. A sticker based attack a heat map identifying how classification probability changes by masking out 5x5 regions in the image. The original input image can be seen on the left and the heat-map can be seen on the right.

the input image changed the output probability slightly, meanwhile masking out the region of the stickers have changed the output class drastically. Knowing the expected objects shapes and identifying small regions which drastically alter the output class, signals the possibility of an adversarial attack and alarms the applications to handle these cases carefully. Additionally, applying this method in the decision can be used to identify that the adversarial attack is coming from a small patch. Apart from that a map of decision can be made masking out the regions of the attack. Then one could see that the regions with the largest area would classify the example as a speed limit sign (instead of a misclassified stop sign). This way the method could help not only in the detection of adversarial attacks, but also in the elimination of the attacks and the identification of the original class. To test our hypothesis we have defined a simple measure which identifies how consistent a detection is. We have identified the blob with highest intensity on the detection heat-map and our aim was to find low-intensity region, "holes" in this blob, which would indicate the presence of adversarial stickers on the image. We have determined the intensity of the holes as half of the mean intensity of the blob with the highest values. Using this method we were able to identify 98% of adversarial attacks correctly (294 cases out of the 300 images). Unfortunately we are not aware any other methods which would be able to identify adversarial attacks on a trained network for comparison, since most of the methods aim the prevention of adversarial sample generation. We also have to note that the applications of stickers with large area or a high number of stickers would fool this method, because this could yield to abrupt changes on the whole image (It is true though that this cannot be really considered as an adversarial sample or attack, because it would also change our perception of the object.)

III. Conclusion

In this paper we have described two possible adversarial attacks. The additive noise based attack is not robust enough to be applied in practice and sticker based attacks, which were shown to be robust enough for possible applications. We have shown that the visualization of the decision of the network by masking out regions in the input image with a sliding window and generating a heat-map of the classification could help in the identification of these attacks, because this method will show that mainly the stickers are responsible for the classification and most of the features covering a larger portion of the image would result another output class. In this analysis we have shown that neither low-amplitude additive noise nor sticker based adversarial attacks could be applied in practical applications to fool neural networks and simple methods could be used to eliminate such attacks.

References

[1] Goodfellow, I. J., Shlens, J., and Szegedy, C. (2014). Explaining and harnessing adversarial examples. arXiv preprint arXiv:1412.6572.

[2] Kingma, D. P., and Ba, J. (2014). Adam: A method for stochastic optimization. arXiv preprint arXiv:1412.6980.

[3] Jiajun Lu, Hussein Sibai, Evan Fabry, and David Forsyth. No need to worry about adversarial examples in object detection in autonomous vehicles. 2017. URL https://arxiv.org/ abs/1707.03501.g]

[4] Eykholt, K., Evtimov, I., Fernandes, E., Li, B., Song, D., Kohno, T., ... and Tramer, F. (2017). Note on Attacking Object Detectors with Adversarial Stickers. arXiv preprint arXiv:1712.08062.

[5] Evtimov, I., Eykholt, K., Fernandes, E., Kohno, T., Li, B., Prakash, A., ... and Song, D. (2017). Robust physical-world attacks on machine learning models. arXiv preprint arXiv:1707.08945.]

[6] Yuan, X., He, P., Zhu, Q., Bhat, R. R., and Li, X. (2017). Adversarial Examples: Attacks and Defenses for Deep Learning. arXiv preprint arXiv:1712.07107.

[7] Lecun, Y., Cortes, C., and Christopher, B. (2016). JC,"The MNIST database of handwritten digits.".yann.lecun.com/exdb/mnist/

[8] Sebastian Houben and Johannes Stallkamp and Jan Salmen and Marc Schlipsing and Christian Ige: German Traffic Sign Benchmarks (2014) benchmark.ini.rub.de/

[9] Zeiler, M. D., and Fergus, R. (2014, September). Visualizing and understanding convolutional networks. In European conference on computer vision (pp. 818-833). Springer, Cham.

APPENDIX

PROGRAM 1: Bionics, Bio-inspired Wave Computers, Neuromorphic Models	
Name	**Supervisor**
Flóra BÁLINT	Zsolt LIPOSITS MD DSc, Imre FARKAS MD PhD
Virág BOKODI	Dániel FABÓ MD PhD
Luca Anna BORS	Franciska ERD PhD
Áron CSERKASZKY	Péter SZOLGAY DSc
Dániel DUDOLA	Zoltán GÁSPÁRI PhD
Bálint FILE	István ULBERT MD DSc
András GELENCSÉR	Péter SZOLGAY DSc
Márton Áron GODA	Ferenc KOVÁCS PhD
Máté HANDBAUER	Zoltán GÁSPÁRI PhD
Zita HARMAT	Zoltán GÁSPÁRI PhD
Márton HARTDÉGEN	Kristóf IVÁN PhD
Anett HINSENKAMP	Zoltán GÁSPÁRI PhD
János JUHÁSZ	Sándor PONGOR MHAS
Ágnes KANDRÁCS	Lucia WITTNER PhD
Annamária KISS-TÓTH	Zoltán GÁSPÁRI PhD
Bertalan KOVÁCS	Zoltán GÁSPÁRI PhD
Domokos MESZÉNA	István ULBERT MD DSc
Vivien MICZÁN	István KATONA DSc, András HORVÁTH PhD
György Miklós PERCZEL	László GERENCSÉR PhD, Loránd ERSS MD PhD
Sára SÁRAY	Tamás FREUND MHAS, Szabolcs KÁLI PhD
Beáta Tünde SZABÓ	István ULBERT MD DSc, István WINKLER DSc
Csilla SZABÓ	Lucia WITTNER PhD
Réka SZALKAI-DÉNES	Zsolt RÓNAI MD PhD, Zoltán GÁSPÁRI PhD
Balázs SZÉKY	Sarolta KÁRPÁTI MD DSc, Miklós GYÖNGY PhD
Ádám György SZÉLIG	Kristóf IVÁN PhD

PROGRAM 2: Computer Technology Based on Many-core Processor Chips, Virtual Cellular Computers, Sensory and Motoric Analog Computers	
Name	**Supervisor**
Subbareddy DARUKUMALLI	Péter SZOLGAY DSc
Máté LRINCZ	András OLÁH PhD
Zsolt NIKA	Péter SZOLGAY DSc, Miklós RÁSONYI PhD
Áron PAPP	György CSEREY PhD
Péter POLCZ	Gábor SZEDERKÉNYI DSc
Mihály Gergely RADVÁNYI	Péter SZOLGAY DSc, Kristóf KARACS PhD
Levente Márk SÁNTHA	Ákos ZARÁNDY DSc, Zoltán NAGY PhD
Attila STUBENDEK	Péter SZOLGAY DSc, Kristóf KARACS PhD

PROGRAM 3: Feasibility of Electronic and Optical Devices, Molecular and Nanotechnologies, Nano-architectures, Nanobionic Diagnostic and Therapeutic Tools	
Name	**Supervisor**
Gergely CSÁNY	Miklós GYÖNGY PhD
Krisztián FÜZESI	Miklós GYÖNGY PhD
Janka HATVANI	Miklós GYÖNGY PhD
Ákos MAKRA	Miklós GYÖNGY PhD
Zsolt MEZRICZKY	Balázs RÓZSA PhD

PROGRAM 5: On-board Advanced Driver Assistance Systems	
Name	**Supervisor**
Balázs NAGY	Csaba BENEDEK PhD